Phosphatome RNAi Screen Identifies Eya1 as a Positive Regulator of Hedgehog Signal Transduction

Phosphatome RNAi Screen Identifies Eya1 as a Positive Regulator of Hedgehog Signal Transduction

A dissertation presented
by
Adriana Eisner

to

The Division of Medical Sciences

in partial fulfillment of the requirements

for the degree of

Doctor of Philosophy

in the subject of

Neurobiology

Harvard University

Cambridge, Massachusetts

June 2013

Dissertation Advisor: Dr. Rosalind Segal Adriana Eisner

Phosphatome RNAi Screen Identifies Eya1 as a Positive Regulator of Hedgehog Signal Transduction

Abstract

The Hedgehog (Hh) signaling pathway is vital for vertebrate embryogenesis and aberrant activation of the pathway can cause tumorigenesis in humans. In this study, we used a phosphatome RNAi screen for regulators of Hh signaling to identify a member of the Eyes Absent protein family, Eya1, as a positive regulator of Hh signal transduction. Eya1 is both a phosphatase and transcriptional regulator. Eya family members have been implicated in tumor biology, and Eya1 is highly expressed in a particular subtype of medulloblastoma (MB). Here we show that RNAi-mediated knock-down of Eya1, as well as knock-down of its co-factor, Six1, blocks Hh signaling as assessed by induction of Hh response genes. Utilizing small molecule agonists, RNAi, and protein over-expression methods, we place the influence of Eya1 and Six1 within the Hh signaling pathway downstream of Smoothened (Smo) and at or above the level of Suppressor of Fused (Sufu). Interestingly, Eya1 appears to be specifically required for Hh-responsive gene activation mediated by Gli transcriptional activators but not for Hh-mediated transcriptional de-repression mediated by the inhibition of Gli transcriptional repressors. Furthermore, we find that Eya1 and Six1 regulate the expression of Neuropilin1 (Nrp1)

and Neuropilin2 (Nrp2), known positive regulators of Hh signaling, providing a mechanism by which Eya1 and Six1 exert their effects.

Based on these data, we investigated a role of Eya1 in Hh signaling *in vivo*. We obtained *Eya1*$^{-/-}$ mice and focused our attention on the developing cerebellum, where Sonic Hedgehog (Shh) is a major factor promoting neural precursor proliferation. In the *Eya1*$^{-/-}$ cerebellum, we find a striking reduction in neural precursor proliferation. In addition, we surveyed several other locations where Shh and/or Eya1 are known to be important for development. These include the embryonic otic vesicle, neural tube, and lung. In the developing inner ear we find *Eya1*$^{-/-}$ mice display reduced Hh signaling *in vivo* and a genetic interaction between Eya1 and Hh signaling. In lung tissue, *Eya1*$^{-/-}$ mice have reduced levels of *Nrp* expression. Together, these data further our understanding of the Hh signaling pathway and provide evidence for a role of Eya1 in Hh signal transduction.

Table of Contents

List of Tables

List of Abbreviations

Hedgehog (Hh)
Medulloblastoma (MB)
Smoothened (Smo)
Fused/Suppressor of Fused (Sufu)
Neuropilin1 (Nrp1)
Neuropilin2 (Nrp2)
Sonic Hedgehog (Shh)
Drosophila melanogaster (*Drosophila*)
Indian Hedgehog (Ihh)
Desert Hedgehog (Dhh)
Skinny hedgehog (Ski/Skn)
Dispatched (Disp/Displ1)
Patched (Ptc/Ptch1)
β-arrestin2 (β-Arr)
Protein kinase A (PKA)
Casein kinase I alpha (CK1α)
G-protein coupled receptor kinase 2 (GRK2)
Ci/Gli repressor (CiR/GliR)
Ci/Gli activator (CiA/GliA)
Glycogen synthase kinase 3 (GSK3)
Costal2 (Cos2)
Fused (Fu)
Intraflagellar transport (IFT)
Basal cell carcinoma (BCC)
Retinal determination gene network (RDGN)
Branchio-oto-renal (BOR)
Branchio-oto (BO)
Haloacid dehalogenase (HAD)
Embryonic day (E)
RNA interference (RNAi)
Small interferring RNA (siRNA)
Messenger RNA (mRNA)
Short-hairpin RNA (shRNA)
ShhLightII cells (SL2 cells)
Firefly luciferase (F luciferase)
Renilla luciferase (R luciferase)
Sodium Orthovanadate (Na_3VO_4)
Vehicle (veh)
Class III Semaphorin (Sema3)
Vascular endothelial growth factor (VEGF)
Placental growth factor (PlGF)
Quantitative real-time PCR (qRT-PCR)
GAIP interacting protein, C terminus (GIPC)
Granule cell precursors (GCPs

Acknowledgements

This project would not have been possible were it not for the collaborations provided by colleagues from the Segal lab and the greater scientific community.

Beginning my graduate studies in the Segal lab, my technical abilities were limited at best. First and foremost, I would like to thank Dr. Rosalind Segal and every past and present member of the Segal lab for their technical advice, patient instruction, and continued scientific mentoring.

Specifically, I would like to acknowledge Dr. Srividya Balasubramanian who initiated our RNAi screen project and conducted initial protocol optimizations. Dr. Pencheng Zhou and Maria Pazyra Murphy contribute data to this dissertation. Dr. Xuesong Zhao and Dr. Tatyana Ponomaryov generously shared reagents they developed. Jennifer Kalscheuer, Jose Alfaro, and Emily Chadwick skillfully assisted with managing mice used in my studies. I would also like to thank my "bay-mates", Dr. Rochelle Witt and Dr. Xuesong Zhao, who, in turn, expertly, patiently, and thoughtfully fielded my many spur-of-the-moment technical questions, providing much helpful advice. In small group meetings, Dr. Xuesong Zhao, Dr. Pencheng Zhou, Dr. David Yang, Jose Alfaro, Emily Chadwick, and Dr. Rosalind Segal reviewed my data, assisted with data interpretation, and provided assistance designing future experiments. In lab meeting, the entire Segal lab reviewed my data, assisted with data interpretation, and provided assistance designing future experiments. I would like to thank Dr. Rosalind Segal, Maria Pazyra Murphy, and Kat Cosker for their comments on this manuscript.

In addition, I would like to acknowledge the Broad Institute RNAi Consortium, Dr. So Young Kim, Leslie Wardwell, Dr. Anna Schinzel, Dr. William C. Hahn, Dr.

Alexandra Smolyanskaya, Dr. Pin-Xian Xu, Allison Nishitani, Dr. Lisa Goodrich, and Dr. Clifford Tabin for their contributions to my project in the form of providing reagents, advice, and/or technical assistance.

I would like to thank Dr. Davie Van Vactor, Dr. Tom Schwarz, Dr. Chenghua Gu, and Dr. Rosalind Segal for allowing me to rotate in their labs as a beginning graduate student. I would like to thank the following people from the Program in Neuroscience at Harvard Medical School for their advice, guidance, administrative support, and moral support: Dr. Gary Yellen, Dr. Rosalind Segal, Dr. Rick Born, Dr. Rachel Wilson, Gina Conquest, and Karen Harmin. I would like to thank my Dissertation Advisory Committee, Dr. Josh Sanes, Dr. Xi He, and Dr. Connie Cepko for their insightful perspectives and critical advice as my dissertation project evolved and developed over the years.

In pursuing and completing my Ph.D., I have deep gratitude to my advisor, Dr. Rosalind Segal. As a mentor, Roz is a truly motivational force. Her optimism, excitement, and enthusiasm for the projects in our lab are encouraging and her passion for science is inspiring. She is brilliant and dedicated both as a scientist and as a teacher. I thank Roz for the time, patience, and support she has shown me over the last several years. I've had a wonderful experience in her lab and will be forever grateful for the lessons I've learned under her guidance.

In addition to the many scientific contributions above, this project would not have been possible were it not for the friendship and support I received from colleagues, friends, and family.

Again, first and foremost, I would like to thank the members of the Segal lab. The lab was not only a place where I came conduct experiments but a place where I found camaraderie and true friendship. I was also blessed to enter graduate school with a cohort of talented and fun classmates whose company I've greatly enjoyed and with whom I look forward to sharing life-long friendships. I would like to thank Eric Miles, Brian Diesel, and Ulysses Lateiner for their companionship and support during my time in graduate school.

I would like to thank my late paternal grandparents, Oscar and Marie Eisner, my parents, Wayne and Marianna Eisner, my sister, Alexa Eisner, and my best friend in the entire world, Rachel Lale for their unwavering love and confidence in my ability to succeed. Finally, my deepest gratitude is to my late maternal grandparents, John and Milena Milovich, who were always my greatest cheerleaders.

CHAPTER 1: INTRODUCTION

Hh Signaling: In Flies and Mice

Hh was first identified in the fruit fly *Drosophila melanogaster* (*Drosophila*) and was named for its role in embryonic patterning, as mutants exhibit a pattern of larval denticles that resemble the bristles of a hedgehog (Nusslein-Volhard & Wieschaus, 1980). In *Drosophila*, Hh signaling is important for embryonic segmental identity and for the development of imaginal discs that give rise to adult structures such as the wing and eye imaginal discs (reviewed in Hooper et al. 2005). Subsequently, three mammalian homologs have been identified, Indian Hedgehog (Ihh), Desert Hedgehog (Dhh), and Shh (reviewed in Ingham & McMahon 2001). Ihh functions primarily in bone development, Dhh is present in the peripheral nervous system and is involved in reproductive organ development, while Shh is a key regulator in many areas of development including the development of the nervous system (Chiang et al. 1996), limb (Chiang et al. 2001; Bénazet & Zeller 2009), lung (Pepicelli et al. 1998), and kidney (Yu et al. 2002). In these tissues, Shh acts as a mitogen and/or morphogen. Additionally, dysregulated Shh signaling can result in a wide variety of devastating birth defects (reviewed in Cohen 2010) and the development of cancers (reviewed in Barakat et al. 2010). This chapter will discuss Hh signal transduction in *Drosophila* and vertebrates.

The basic principles of Hh signal transduction as initially characterized in *Drosophila* are largely evolutionarily conserved. Many of the underlying molecular mechanisms, however, have diverged from flies to mice, including the appearance of the primary cilia in vertebrate Hh signaling (reviewed in Robbins et al. 2012; Ingham et al. 2011; Wilson & Chuang 2010).

Hh Ligand Production

In *Drosophila* and vertebrates, Hh is a signaling molecule secreted into extracellular space, able to signal to cells near and far. It is synthesized as a precursor and undergoes multiple post-translational modifications before release. The 45kDa Hh precursor peptide is targeted to the endoplasmic reticulum and the Golgi apparatus, where it undergoes autoproteolytic cleavage, generating two fragments, a 19kDa N-terminal fragment with a cholesterol attached to its C-terminus and a 25kDa C-terminal fragment, (Lee et al. 1994; Bumcrot et al. 1995; Porter et al. 1996). The N-terminal fragment then receives a palmitate to its N-terminus via the acyltransferase Skinny hedgehog (Ski/Skn), generating a signaling molecule with two permanent lipid attachments (Chamoun et al. 2001; Pepinsky et al. 1998). The dually-lipidated N-fragment (referred to as "Hh" from here on) forms multimers, is packaged into lipoprotein particles, and is released into extracellular space with the help of Dispatched (Disp/Displ1), a 12-pass transmembrane protein (Zeng et al. 2001; Burke et al. 1999; Caspary et al. 2002; Kawakami et al. 2002). Hh's dual modifications are important for high-level Hh signaling, multimerization and/or packaging (Zeng et al. 2001; Chen et al. 2004a), movement in extracellular space, and gradient distribution (Li et al. 2006).

Hh Ligand Reception

In both *Drosophila* and mammalian Hh-responding cells, Hh signaling is transduced as described below (see Figure 1.1a-b for a representation of mammalian Hh signal transduction).

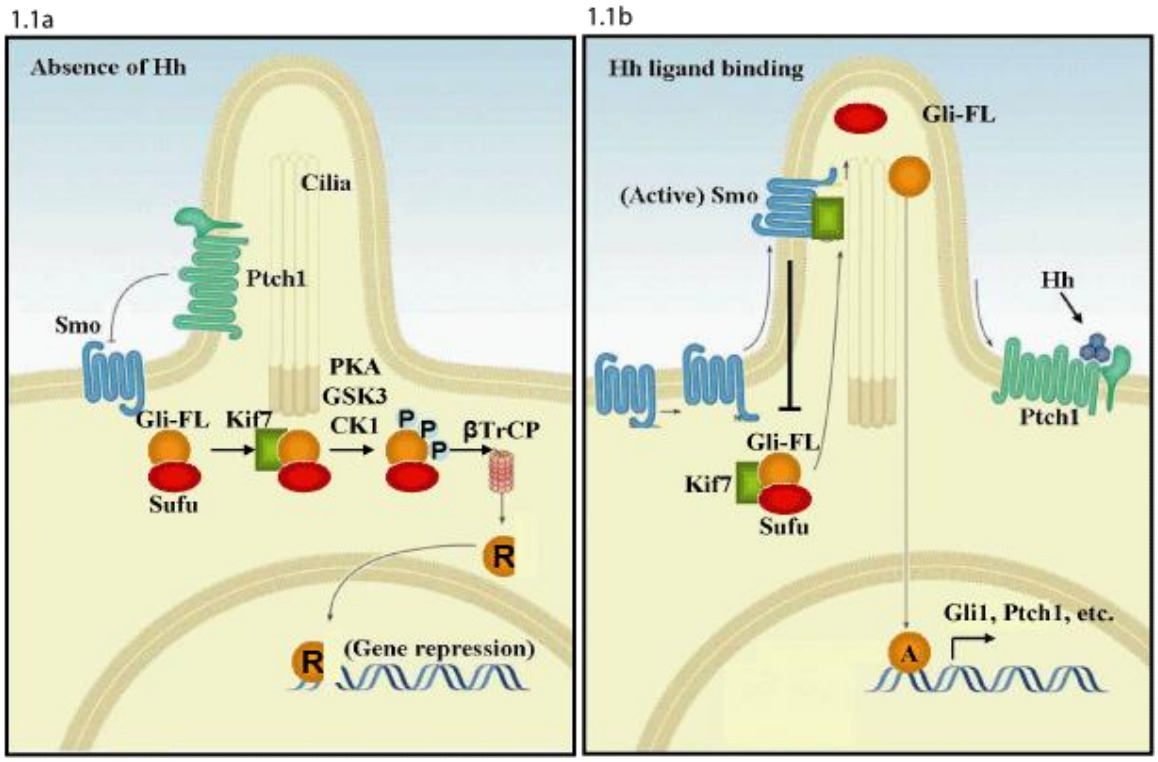

Figure 1.1 Vertebrate Hh signal transduction. A) In the absence of Hh ligand, Ptch1 localizes to the primary cilia and inhibits Smo activation. Full-length Gli complexes with Sufu in the cytoplasm. Sufu and Kif7 promote the phosphorylation of Gli by PKA, GSK3β, and CK1α. Phosphorylated Gli is recognized by the E3 ubiquitin ligase βTrCP, resulting in ubiquitination and proteasomal degradation to generate an N-terminal Gli repressor, GliR. **B)** In the presence of Hh ligand, Ptch1 exits the cilia allowing Smo transport into the cilia. Active Smo promotes the ciliary localization and the disassembly of Sufu, Gli, and Kif7. Full-length Gli is shuttled from the cilia into the nucleus where it activates Hh target genes. Adapted from (Ryan & Chiang 2012).

Hh binds its receptor Patched (Ptc/Ptch1), a twelve-pass transmembrane protein and negative regulator of pathway activity. In the absence of Hh ligand binding, Ptch1 inhibits the activity of Smo, a seven-pass transmembrane protein and potent pathway activator. The mechanism by which Ptch1 inhibits Smo is an open question. Given sequence similarities between Ptch1 and the RND family of bacterial transporter proteins, it is thought Ptch1 represses Smo by regulating the transport and/or synthesis of an unidentified small molecule (Taipale et al. 2002). Upon Hh binding, Ptch1 repression of Smo is relieved and Smo is activated.

Hh binding to Ptch1 is affected by the presence of other Hh-binding proteins at the cell surface (Figure 1.1b). Positive regulators of Hh reception include the co-receptors Ihog/Cdo, Boi/Boc, and the vertebrate specific Gas1 (reviewed in Beachy et al. 2012). A second vertebrate specific Hh-binding protein, Hhip, acts as a negative regulator of Shh signaling, likely by competing with Ptch1 for available Hh ligands (Chuang & McMahon 1999). Interestingly, these Hh-binding proteins are transcriptionally regulated by Hh signaling, thereby introducing a number of negative feedback loops that function to attenuate signaling. Positive co-receptors (i.e., Ihog/Cdo, Boi/Boc, and Gas1) are transcriptionally repressed while the expression of negative co-factors (i.e., Ptch1 and Hhip) is up-regulated following pathway activation. These complex negative feedback loops may function to sensitize and/or desensitize cells to Hh signaling and is crucial for cells to properly interpret the duration and graded level of Shh Signaling they receive (reviewed in Ribes & Briscoe 2009).

In both *Drosophila* and mammalian Hh signaling, the reciprocal trafficking and subcellular localization of Ptch1 and Smo are important. In both systems, Ptch1 and Smo

are found in opposite locations. The manner in which the proteins are localized and regulated, however, is a point of divergence between the two systems. In *Drosophila,* inactivated Smo is retained intracellularly in endosomes and vesicles. Ptc is present at the plasma membrane and in intracellular compartments and prevents Smo localization at cell surface. Upon Hh binding, Ptc and Hh form complexes which are internalized and degraded, allowing Smo movement to the cell surface where it is active (Denef et al. 2000; Zhu et al. 2003).

In the mammalian system, the trafficking of Ptch1 and Smo involves the primary cilia, a microtubule-based organelle present on nearly all mammalian cells (Figure 1.1a-b). In the absence of Hh binding, Ptch1 is localized to the cilia and Smo is not; upon Hh binding, Ptch1 moves from the cilia and Smo translocates to the cilia (Corbit et al. 2005; Rohatgi et al. 2007). Smo translocation to the cilia is dependent on Kif3a and β-arrestin2 (β-Arr; Chen et al. 2004b; Kovacs et al. 2008).

Although the details are yet to be fully elucidated, the biochemical activation of Smo diverges from flies to mice. In *Drosophila*, Smo is hyperphosphorylated at its C-terminal tail by protein kinase A (PKA) and casein kinase I (CK1α), translocates to the cell membrane, and undergoes conformational changes (reviewed in Chen & Jiang 2013). The phosphorylation of Smo is critical for its activation; the extent of phosphorylation corresponds to its activity level and to the amount of Smo accumulated at the cell surface (Jia et al. 2004; Zhang et al. 2004a). The C-terminus of mammalian Smo does not contain PKA phosphorylation sites although phosphorylation may still be an important regulatory mechanism (Chen et al. 2011b). Mammalian Smo is phosphorylated in response to Hh signaling by G-protein coupled receptor kinase 2 (GRK2) and CK1α,

inducing a conformational change and transport into the primary cilia (Chen et al. 2011b).

Gli Transcription Factors

The Gli family transcription factors (Ci/Gli) are conserved as the effectors of Hh signaling. Ci/Gli can serve as transcriptional repressors (CiR/GliR) or activators (CiA/GliA) and thereby mediate Hh signaling (Méthot & Basler, 2001). Hh signaling induces gene transcription by two mechanisms: de-repression of transcription by blocking CiR/GliR function and direct transcriptional activation through promoting CiA/GliA function (reviewed in Hui & Angers 2011). Low levels of Hh signaling block CiR/GliR, while higher levels of Hh are needed to activate CiA/GliA (Méthot & Basler 2000). In accordance with this model, graded Hh signaling triggers the expression of different sets of response genes by shifting the balance of GliR relative to GliA (reviewed in Hui & Angers 2011; Ribes & Briscoe 2009)

The repressor and activator functions of Ci have been distributed among three vertebrate homologs, Gli1-3. Gli3 serves as the primary transcriptional repressor of the pathway, Gli2 is primarily a transcriptional activator, and Gli1 exists only as a transcriptional activator. Gli1 is a Shh response gene, acting as positive feedback to strengthen GliA activity and serves as a readout of pathway activation. For Ci/Gli2/3, the Hh-induced switch between repressor and activator functions is regulated through phosphorylation.

In the absence of Hh signaling, full-length Ci/Gli proteins are constitutively phosphorylated at multiple phosphorylation sites by PKA, CK1α, and glycogen synthase kinase 3 (GSK3; Figure 1.1a; Chen et al. 1998; Price & Kalderon 1999; Price & Kalderon

2002; Jia et al. 2002; Pan et al. 2006; Pan et al. 2009; Tempé et al. 2006). The newly hyperphosphorylated Ci/Gli is recognized by Slimb/βTrCP, a substrate-specific receptor of an E3 ubiquitin ligase, ubiquitinated and targeted for proteosomal processing (Jiang & Struhl 1998; Tempé et al. 2006; Pan et al. 2006; Wang & Li 2006). The resulting truncated peptide acts as a transcriptional repressor. Full-length Gli2 and full-length Gli3 are both phosphorylated but Gli3 is processed more efficiently and proteolyzed to form Gli3R while the majority of Gli2 remains full-length. Gli2 that is phosphorylated and processed is degraded by the proteosome (Pan & Wang 2007; Pan et al. 2006). The preferential formation of Gli3R over Gli2R may be due to a difference in the C-terminal domains of proteins (Pan & Wang 2007; Pan et al. 2006).

Upon Smo activation, Ci/Gli proteolysis is inhibited. Simultaneously, the activator function of full-length Ci/Gli proteins is promoted (see below). It is unclear why Gli2 preferentially acts as an activator. One hypothesis is that full-length Gli3 is more efficiently degraded than Gli2 in the nucleus via the Cullin-3-based ubiquitin ligase adaptor HIB/Spop (Chen et al. 2009; Wen et al. 2010). Gli1 is not degraded by Spop (Chen et al. 2009; Wen et al. 2010).

In addition to PKA, CK1α, and GSK3 phosphorylation control of Gli processing, other kinases influence the activity of Gli proteins in mammalian cells. Dual-specificity tyrosine phosphorylation-regulated kinase 1A (DYRK1A) phosphorylates Gli1 promoting nuclear localization and transcriptional activity of GFP-tagged Gli1 (Mao et al. 2002). DYRK1B acts as a negative regulator of transcriptional output by inhibiting Gli2A (Lauth et al. 2010). In addition, DYRK2 phosphorylates Gli2 and promotes

proteosomal degradation of Gli2-3 (Varjosalo et al. 2008). MAP3K10 affects Gli2 indirectly by modulating the activity of DYRK2 and GSK3 (Varjosalo et al. 2008).

Hh Signal Transduction

The composition, formation, and assembly of intracellular signaling complexes controlling Ci/Gli activity exhibit great evolutionary divergence. In *Drosophila*, Ci is found in a complex with Costal2 (Cos2), Fused (Fu), and Sufu proteins (reviewed in Wilson & Chuang 2010; Hooper & Scott 2005). In the absence of Hh, Cos2 functions primarily as a negative regulator of signaling. Cos2 associates with microtubules and serves as a scaffold for PKA, CKI and GSK3 to promote the efficient phosphorylation of Ci and subsequent formation off CiR. Upon activation, Smo binds Cos2 and Fu phosphorylates Cos2 leading to the dissociation of complex and blunting of CiR production. Sufu may serve as a negative regulator of the pathway by associating with Ci to keep it from going into the nucleus and becoming an activator. Sufu's primary role in the *Drosophila* Hh pathway, however, seems to be regulating Ci stability by blocking HIB/Spop-mediated degradation (Chen et al. 2009).

Targeted knockout studies in mice have shown a conserved role for the Cos2 homolog, Kif7, where it may play an analogous scaffolding role localizing components of the pathway to the primary cilia (Cheung et al. 2009; Endoh-Yamagami et al. 2009; Liem et al. 2009). Kif7 localizes at the base of the cilia near the basal body and interacts with Gli proteins (Figure 1.1a). *Kif7*$^{-/-}$ have spinal cord and limb phenotypes consistent with loss of Gli3R function showing Kif7 is needed for the formation of GliR. When crossed onto *Gli2*$^{-/-}$ and *Ptch1*$^{-/-}$ backgrounds, *Kif7*$^{-/-}$ double-mutant phenotypes suggest Kif7 also

has a positive regulatory role, perhaps by regulating Gli2 localization (Cheung et al. 2009; Endoh-Yamagami et al. 2009; Liem et al. 2009).

In contrast, the targeted knockout of the mouse Fu homolog has no Hh-related phenotypes, suggesting the role of this kinase is not conserved (Merchant et al. 2005; Chen et al. 2005). In vertebrate Hh signaling, Sufu plays new and more significant roles. In mammalian Hh signaling, Sufu regulates Glis at several distinct steps, serving as a potent inhibitor of the pathway. *Sufu* knock-down in NIH3T3 cells and *Sufu*$^{-/-}$ mouse embryonic fibroblasts display ligand-independent pathway activation (Svärd et al. 2006; Cooper et al. 2005; Varjosalo et al. 2006). *Sufu*$^{-/-}$ embryos die by embryonic day 9.5 (E9.5) resembling the gain-of-function phenotype found in *Ptch1*$^{-/-}$ embryos (Svärd et al. 2006; Cooper et al. 2005).

Sufu directly interacts with all three Gli proteins in the absence of Hh signaling and sequesters full length Gli in the cytoplasm (Figure 1.1a). This sequestration has two effects: it promotes the phosphorylation of full-length Gli and thus GliR formation (Humke et al. 2010) while preventing nuclear translocation and inappropriate pathway activation (Ding et al. 1999; Kogerman et al. 1999). Cytoplasmic Sufu and Gli dissociate upon Hh binding (Figure 1.1b; see below). As in *Drosophila*, mammalian Sufu stabilizes full-length Gli2 and Gli3 by protecting them from proteosomal degradation mediated by Spop/Cul3 in the nucleus (Wang et al. 2010). In this role, Sufu functions as a positive regulator in Hh signaling transduction. Sufu phosphorylation by Cdc2l1 modulates Sufu-Gli binding and relieves Sufu inhibition of Gli-dependent transcription (Evangelista et al. 2008). Sufu function can also be modulated by phosphorylation. PKA- and GSK3-

mediated phosphorylation promotes Sufu ciliary localization and thereby negatively regulates Shh signaling (Chen et al. 2011a).

Primary Cilia

The primary cilia functions as a signaling center to facilitate Hh signal detection and pathway activation. Many of the core components of the vertebrate Hh pathway localize to cilia and pathway activation requires the primary cilia. The primary cilia is a microtubule-based structure consisting of an axoneme, nine peripheral double tubules arranged around a core (reviewed in Goetz & Anderson 2010). The assembly, disassembly, and maintenance of the cilia depend on intraflagellar transport (IFT) proteins and their associated kinesin and dynein motors. Mice lacking cilia due to mutations in critical IFT genes display a loss of GliR and GliA function, demonstrating a requirement of cilia for proper Hh signal transduction and Gli processing (Houde et al. 2006; Huangfu et al. 2003; Liu et al. 2005; May et al. 2005; Tran et al. 2008).

Many critical core components of Hh signaling localize to the cilia in a Hh-dependent manner, including Ptch1, Smo (Rohatgi et al. 2007), Kif7 (Endoh-Yamagami et al. 2009), and Gli proteins. Upon pathway activation, Sufu-Gli complexes move into the cilia and dissociate, allowing Gli to accumulate at the distal tip of the cilia and also translocate to the nucleus and activate gene transcription (Figure 1.1b; Humke et al. 2010; Tukachinsky et al. 2010; Chen et al. 2009; Wen et al. 2010; Kim et al. 2009). The activation of endogenous GliA correlates with ciliary accumulation; prompting the hypothesis that GliA formation is regulated via transport or accumulation in the cilia (Wen et al. 2010; Qin et al. 2011; Tran et al. 2008).

Hh Activation in Tumorigenesis

Many human cancers have active Shh signaling as indicated by GIL1 and PTCH1 expression, including MB, basal cell carcinoma (BCC), glioma, gastrointestinal cancer, leukemia, breast cancer, and prostate cancer (reviewed in Marini et al. 2011). The identification of PTCH1 mutations in Gorlin syndrome patients, who develop multiple BCCs and have increased risk of MB, provided the first clues that activation of the canonical Hh signaling pathway is sufficient to initiate tumorigenesis (Hahn et al. 1996; Johnson et al. 1996). The ability of Hh signaling to cause cancer has subsequently been confirmed in mouse models and inhibition of the pathway provides a novel successful treatment for some cancers (see below).

MB is a highly malignant brain tumor of cerebellar origin and is the most common malignant brain tumor in children. Current treatments for MB include surgery, craniospinal radiation and chemotherapy, which can result in severe long-term side-effects in young patients (reviewed in Leary & Olson 2012). Thus, developing targeted drug therapies limiting the dose of radiation therapy is of great interest.

There are multiple subtypes of MB defined by distinctive gene expression profiles and tumor histologies. About 25% of MBs belong to the "Shh-subtype", which is characterized by aberrant expression of Shh pathway components and increased Shh pathway activation (reviewed in Northcott et al. 2012). The ability of Hh signaling to initiate MB is consistent the role of Shh as a mitogen in cerebellar development (reviewed in Manoranjan et al. 2012). Aberrant activation of the Hh pathway has been shown to generate MB via any one of multiple mechanisms: by loss-of-function of

negative pathway regulators *Ptch1* and *Sufu*, and over-active mutations of *Smo* or *Gli2* (Lee et al. 2009; Hatton et al. 2008).

BCC, the most common cancer in humans, is a skin cancer thought to arise from the abnormal proliferation of cells that normally form the hair follicle (reviewed in Barakat et al. 2010; Epstein et al. 2008). Most sporadic BCCs have activated Hh signaling (Reifenberger et al. 2005). Specifically, 90% of sporadic BCC patients have mutations in at least one PTCH1 allele and an additional 10% have SMO activating mutations, with less frequent SUFU mutations. In mice, loss of *Ptch1*, loss of *Sufu*, active *Smo*, or active *Gli* can result in BCC (reviewed in Barakat et al. 2010).

Several promising small molecule inhibitors of the Smo have been developed and are in clinical trial to treat BCC and MB (reviewed in Cohen et al. 2012). Vismodegib (GDC-0449; Curis/Genentech), recently became the first FDA approved Hh pathway inhibitor, approved for the treatment of BCC; clinical trials for the treatment of other cancers with active Hh signaling are underway.

Studies in the past twenty years have provided many insights into the mechanisms of Hh pathway signaling, including the importance of subcellular localization and protein phosphorylation as regulatory mechanisms. Future studies to identify additional Hh pathway targets and inhibitors will be important to treat tumors which are caused by mutations downstream of Smo and to treat patients who develop resistance to Smo inhibitors through acquired SMO mutations (Rudin et al. 2009; Yauch et al. 2009). Two low-molecular-weight compounds inhibiting Gli function, GANT58 and GANT61, have been identified (Lauth et al. 2007). A more detailed understanding of Hh pathway

components downstream of Smo and of the mechanisms that regulate these components could offer further therapeutic targets and expand the treatable patient population.

The Retinal Determination Gene Network (RDGN)

In *Drosophila*, eye development is controlled by members of the RDGN, Ey, Toy, Eya, So, and Dac (Figure 1.2; reviewed in Rebay et al. 2005; Pappu & Mardon 2004). These transcription factors and co-factors form protein complexes to control gene expression. Members of the RDGN are necessary for eye development and, with the exception of *So*, their overexpression is sufficient to induce ectopic eye development in *Drosophila*. The RDGN is hierarchical with Ey and Toy inducing the expression of *So* and *Eya*.

1.2

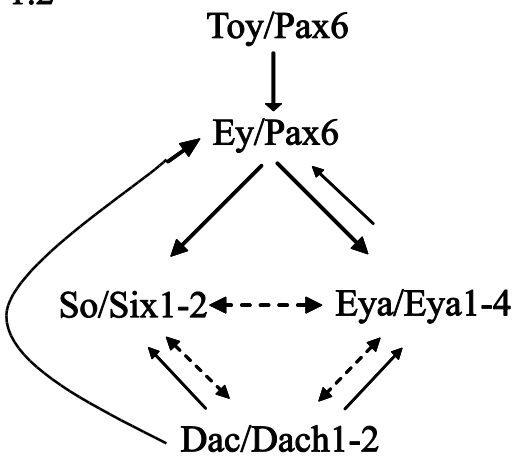

Figure 1.2 The RDGN. In *Drosophila* eye development, the RDGN is expressed in a transcriptional hierarchy in which Toy/Pax6 promotes Ey/Pax6 expression, which leads to the expression of So/Six1-2 and Eya/Eya1-4. In *Drosophila* eye development, So/Six1-2 and Eya/Eya1-4 interact with Dac/Dach1-2. Feedback loops maintain Ey/Pax6 expression. This network is adapted to vertebrate development. Solid arrows represent known transcriptional relationships; dotted-arrows represent known protein-protein interactions. *Drosophila* gene names are on the left, vertebrate homologs are on the right. Adapted from (Jemc & Rebay 2007).

RDGN members are conserved in mammals: Pax6 is a homolog of Ey and Toy, Eya1-4 are Eya homologs, Six1-2 are So homologs, and there are two vertebrate Dac proteins, Dach1-2. In mammalian development, this network plays roles in the development of multiple organs including the eye, muscle, ears, lungs, and craniofacial skeleton (reviewed in Tadjuidje & Hegde 2012).

Six family proteins are homeodomain-containing factors characterized by a highly conserved Six domain. There are three subgroups within this family: So/Six1-2, dSix4/Six4-5, and Optix/Six3/6 (Jean et al. 1999; Seo et al 1999). Six transcription factors are repressors or weak activators. However, co-transcriptional binding partners can result in repressor or activator functions. For example, Six1-2 bind Groucho family co-repressors (Lopez-Rios et al. 2003; Kobayashi et al. 2001) while binding to Eya converts Six1-2 and Six4-5 into strong transcriptional activators (Ohto et al. 1999; Li et al. 2003). Unlike Six1-2 and Six4-5, Six3/6 have not been shown to interact with Eya.

Eya1

The human EYA1 gene was first identified in patients with branchio-oto-renal (BOR) or branchio-oto (BO) syndromes (Abdelhak et al. 1997). BOR patients are born with ear, kidney, and lung defects (reviewed in Kochhar et al. 2007). 93% of affected individuals are deaf and BOR accounts for 2% of profoundly deaf children (Abdelhak et al. 1997). Mutations in EYA1 account for 40% of BOR patients; SIX1 and SIX5 mutations are also found in BOR patients (Ruf et al. 2004; Hoskins et al. 2007). In mice, *Eya1* null mutations result in lethality at birth, failure of inner ear development, dysmorphic or absent kidneys, lung abnormalities, craniofacial and skeletal defects, as well as thymus, parathyroid, and thyroid defects (Xu et al. 1999; Xu et al. 2002; El-

Hashash et al. 2011b). While EYA1 mutations have been identified in human patients with congenital cataracts and other ocular abnormalities (Azuma et al. 2000), *Eya1*$^{-/-}$ mice do not have an eye phenotype, suggesting the crucial role of Eya in eye development is not conserved from flies to vertebrates. However, multiple *Eya* genes are expressed in the murine eye, leaving open the possibility that there is functional redundancy among multiple Eya family members in the developing eye (Xu et al. 1999).

Eya as a Transcription Factor

As a member of the RDGN, Eya proteins are co-transcriptional activators. Eya does not have the ability to bind DNA directly and activates gene transcription through protein-protein interactions with Six or Dach transcription factors (reviewed in Tadjuidje & Hegde 2012; Jemc & Rebay 2007). Eya proteins have a highly conserved C-terminal domain called the Eya domain (ED) and an N-terminal domain that is less well conserved. The ED domain is necessary for Eya to bind Six or Dach proteins (Ohto et al. 1999; Li et al. 2003) and the N-terminal domain contains a proline/serine/threonine rich region required for transactivation (Xu et al. 1997; Silver et al. 2003). *In vitro*, overexpressed Eya is cytoplasmic. When co-transfected with *Six1-2* or *Six4-5*, Eya and Six proteins form complexes and translocate to the nucleus (Ohto et al. 1999; Zhang et al. 2004b). Eya and Dac are thought to bind directly in *Drosophila* eye development but a direct interaction between vertebrate Eya and Dach proteins is less well established. Eya is not known to have a Six- or Dach-independent ability to activate gene transcription.

Eya as a Phosphatase

Eya1 is a rare example of a transcription co-factor that is also a phosphatase (Rebay et al. 2005). The ED domain contains sequence motifs that match haloacid

dehalogenase (HAD) class of enzymes and has active tyrosine phosphatase activity (Li et al. 2003; Tootle et al. 2003; Rayapureddi et al. 2003). In addition, the N-terminal domain appears to have activity as a threonine phosphatase (Okabe et al. 2009, Sano & Nagata 2011). Eya is not considered a dual specificity phosphatase, however, because its phosphatase activities are in different catalytic domains and there is no evidence that Eya can dephosphorylate tyrosine and threonine residues of the same substrate.

The dual activities of Eya, as a transcription co-factor and as a phosphatase, raise the question as to whether and how these functions are linked. The discovery that Eya dephosphorylates the histone H2A variant H2AX in the nucleus following double-stranded DNA breakage suggests that Eya acts as a phosphatase independently of its role as a co-transcriptional factor (Cook et al. 2009; Krishnan et al. 2009). Eya also interacts with cytoplasmic Abelson (Abl) tyrosine kinase in the *Drosophila* larval visual system (Xiong et al. 2009). Abl phosphorylates Eya which recruits Eya to the cell membrane where Eya function requires phosphatase activity. These data suggest Eya has cytoplasmic roles as a phosphatase in development that are independent of its nuclear functions (Xiong et al. 2009).

It is possible that Eya phosphatase activity is also important for its role as a transcriptional co-factor. Missense mutations that ablate Eya tyrosine phosphatase activity without impairing Eya protein-protein interactions show reduced transactivation activity, compromise the ability of full-length Eya to rescue the eyeless phenotype in *Drosophila,* and do not induce eye formation as effectively *in vivo* in *Drosophila* (Rayapureddi et al. 2003; Tootle et al. 2003). These data demonstrate that Eya phosphatase activity is not required for but contributes to Eya transcriptional activity.

Human BOR mutations appear to disrupt both the phosphatase activity and transactivation functions of Eya without affecting the ability of Eya to translocate to the nucleus with Six (Buller et al. 2001). Similarly, *in vitro* studies in cultured *Drosophila* cells indicate that Eya-Six interactions are not compromised with HAD- or BOR-type mutations (Mutsuddi et al. 2005). Together, these studies suggest phosphatase-dead Eya binds to Six but the complex is impaired in their ability to activate transcription. How, exactly, Eya phosphatase activity influences transcriptional regulation remains unclear.

Cellular Functions of Eya

H2AX is a physiologically relevant Eya substrate (Krishnan et al. 2009; Cook et al. 2009). Following double-stranded DNA breaks, H2AX is phosphorylated at Ser139 near the breakage to produce a modified form, termed γH2AX (reviewed in Stucki 2009). γH2AX is recognized by MDC1, a large protein which coordinates the assembly of DNA damage response proteins. H2AX is constitutively phosphorylated at Tyr142 and, in contrast to Ser139, this residue is dephosphorylated following double-stranded breaks in a manner that is dependent on Eya1 or Eya3 (Cook et al. 2009). Eya1 and Eya3 interact with γH2AX and loss of Eya1 or Eya3 results in increased cell death *in vivo*. It seems MDC1 more stably associates with γH2AX after Tyr142 dephosphorylation (Cook et al. 2009; Xiao et al. 2009). In this way, Eya-mediated dephosphorylation of H2AX Ty142 promotes DNA repair and cell survival over apoptosis (Figure 1.3; Stucki 2009).

1.3

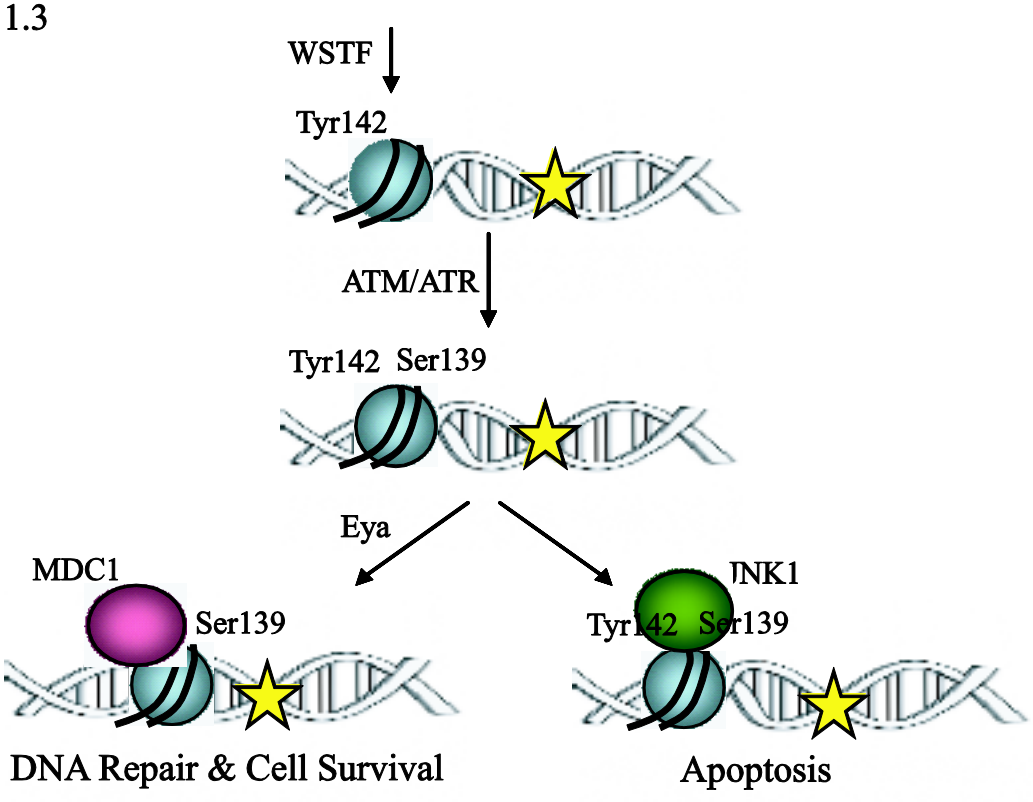

Figure 1.3 Eya promotes cell survival following DNA double-stranded breakage. H2AX (blue circle) is constitutively phosphorylated at Tyr142 by WSTF (Williams–Beuren syndrome transcription factor, also known as BAZ1B). Upon double-stranded DNA breakage (indicated by a yellow star), H2AX is phosphorylated at Ser139 by the ATM (ataxia-telangiectasia mutated) and ATR (ataxia telangiectasia and Rad3-related protein) kinases. Eya dephosphorylates H2AX Tyr142, facilitating the recruitment of MDC1 (mediator of DNA damage checkpoint 1) and cell survival. If H2AX remains dually-phosphorylated, JNK1 (c-Jun N-terminal protein kinase 1) is recruited, leading to apoptosis.

In addition to the better characterized roles of Eya described above, Eya has been implicated in a variety of other cellular functions. In both *Drosophila* (Bai & Montell 2002) and vertebrates Eya plays a role regulating tissue polarity (El-Hashash et al. 2011a). In vertebrates Eya1 is involved in controlling mitotic spindle orientation in lung epithelium through dephosphorylation of aPKC-zeta and Numb (El-Hashash et al. 2011a). In addition, Eya4 has been implicated in regulating the innate immune response to nuclei acids *in vitro* via interactions with IPS-1, Sting, Nlrx1 (Okabe et al. 2009). This response requires Eya4 N-terminal threonine phosphatase activity (Okabe et al. 2009). Eya1 has been shown to interact with Sox2 by immunoprecipitation and may have a role in sensory cell development of the inner ear (Zou et al. 2008). Eya2 appears to bind Gαz and Gαi subunits which recruit Eya to the cell membrane and prevent Six-mediated nuclear translocation (Embry et al. 2004; Fan et al. 2000). Finally, Eyas are implicated in cell migration, a function fundamental to developmental biology with important implications for cancer biology. Overexpression of *Eyas* in breast epithelial cell lines increases cell migration (Stucki 2009; Tadjuidje et al. 2012) while RNAi targeting *Eya3* or *Eya4* reduce migration in endothelial cells or malignant peripheral nerve sheath tumor cells, respectively (Tadjuidje et al. 2012; Miller et al. 2010).

Eyas are unusual proteins as they contain both phosphatase and transactivation functions. Eyas are required for the normal development of many organs and *Eya* mutations result in multiple disorders. Future studies identifying mechanisms regulating Eya activity, additional Eya substrates, and additional Eya binding partners will be of great interest.

In the following study, we conduct an RNAi screen with the aim of identifying novel phosphatases regulating the Hh signaling pathway. We apply a phosphatome library of shRNAs to Hh-responsive cells and identify Eya1 as a factor needed for maximal hedgehog signaling in Hh-responsive cells. We find evidence that Eya1 is working in concert with its co-factor Six1 to regulate gene expression necessary for Hh signaling transduction. Specifically, we find Eya1 and Six1 regulate *Nrp* expression, a known regulator of Hh signaling (Hillman et al. 2011), thus providing a mechanism underlying the requirement of Shh signaling for Eya1 and Six1. Furthermore, we present data in the developing mouse demonstrating *in vivo* significance for this interaction.

CHAPTER 2: IDENTIFICATION OF NOVEL PHOSPHATASES IN THE HH SIGNALING PATHWAY BY RNAi SCREENING

Introduction

The history of Hh signaling is closely tied to screening in that Hh itself was identified in a *Drosophila* mutagenesis screen as an important determinant of segmental patterning in larva (Nusslein-Volhard & Wieschaus 1980). Subsequent screening has proven successful in identifying novel signaling components of the Hh pathway via mutagenesis screens, RNA interference (RNAi) screens, and protein overexpression screens in *Drosophila* and mammalian Hh signaling pathways (Nusslein-Volhard & Wieschaus 1980; Lum et al. 2003; Nybakken et al. 2005; Varjosalo et al. 2008; Evangelista et al. 2008; Hillman et al. 2011; Jacob et al. 2011). Non-overlapping sets of hits between screens to identify components of the Hh pathway, however, suggest that little can be conclusively said for genes that are not selected as hits in a study and that these screens were not saturated and are complementary (Evangelista et al. 2008; Varjosalo et al. 2008). Given the success of previously published screens and the fact that much remains to be discovered about this important pathway, we were motivated to further screen for novel regulators of Hh signaling by RNAi.

In contrast to hypothesis testing, unbiased screening allows investigators to look beyond the current understanding of biology and releases scientists from the constraint of preconceived ideas. Over decades, screens have yielded seminal discoveries and opened new areas of study. In addition to classical *in vivo* mutagenesis screens, the discovery of RNAi has provided an additional approach to screening whereby an investigator is able to

selectively deplete particular gene products. Unlike *in vivo* mutagenesis screens, by screening with an RNAi library (i.e., genome-wide RNAi or RNAi targeting each of a specific class of gene products), an investigator can systematically test the significance of individual genes within a biological system. This approach also allows an investigator to examine the effect of acutely depleting a gene product and avoids costly and time consuming gene mapping. In addition, this approach is free from limitations of selectivity imposed by mutagenesis methods.

There are multiple methods to achieve RNAi-mediated knock-down of a specific gene product (reviewed in Campeau & Gobeil 2011; Echeverri & Perrimon 2006), many of which have been utilized in RNAi screens designed to identify components of Hh signaling (Lum et al. 2003; Nybakken et al. 2005; Jacob et al. 2011; Hillman et al. 2011; Evangelista et al. 2008). *Drosophila* cells can be treated with double-stranded RNA (dsRNA), which are processed by Dicer into small interfering RNAs (siRNA). siRNAs range from 19 to 27 nucleotides and are incorporated into the RISC silencing complex, resulting in sequence-specific degradation of messenger RNAs (mRNAs). In mammalian cells, siRNAs may be generated by treating long dsRNA with recombinant Dicer enzyme *in vitro* to generate diced RNAi pools or they may be synthesized and introduced by lipid-based transient transfection. Vector-expressed short hairpin RNAs (shRNAs) can be introduced via viral particles and are stably incorporated into the cell's genome. shRNAs are about 65 nucleotides long and are cleaved by the Dicer complex to generate siRNAs.

Differences in sets of hits could be due to different experimental RNAi screening setups and/or methods of statistical analyses and hit criteria (Campeau & Gobeil 2011).

Potential sources of discrepancy from reported screens of the Hh pathway might include screening modality, cell culture system, RNAi library utilized, method of pathway stimulation, and the criteria applied to determine which candidates qualify as hits (Table 2.1). Each of these potential sources of discrepancy is discussed below.

Table 2.1 Comparison of published RNAi screens identifying components of the Hh signaling pathway. Published RNAi screens vary in their methodology by features such as RNAi modality, cell culture system assayed, screening library applied, the stimulation and read-out protocol, and by the analysis and hit criteria set to identify hits. These methodological differences may account for differences in reported findings. (F) = F luciferase, (R) = R luciferase.

Table 2.1 (continued):

Author	RNAi Modality	Cell Culture System	Screening Library	Stimulation and Read-Out	Analysis and Hit Criteria
Lum et al. 2003	co-transfect dsRNA	*Drosophila* clone 8 wing imaginal disc cell line co-transfect ptc-luciferase (F) and copia-Renilla	*Drosophila* kinome and phospha-tome; (generated within lab)	~30hr after transfection, stimulate with media containing Hh-N for 24hr. Dual-Luciferase Assay Kit (Promega)	Normalize (F)/(R). Basal luciferase activity (-Hh): > 5 SD. Fold induction (+Hh/-Hh): <-1.75 SD.
Nybakken et al. 2005	co-transfect dsRNA	*Drosophila* clone 8 wing imaginal disc cell line co-transfect ptc-luciferase (F) and pol-III Renilla co-transfect construct expressing full-length Hh (pAc5C-Hh)	Genome-wide 21,000 dsRNAs; (*Drosoph-ila* RNAi Screening Center)	Assay 5 days after transfection. Dual-Glo Assay Kit (Promega)	Normalize (F)/(R). Normalize to within-plate, internal-well negative control. Average z-scores from replicate plates. z score <-2 or >3.
Evangelista et al. 2009	transfect single siRNA	S12 (derivative of C3H10T1/2 fibroblasts), stable Gli-luc (F) no non-responsive reporter for normalization	Kinome 812 unique Kinases; (Dharma-con)	64hr after transfection, stimulate with Octyl-modified Shh for 24hr. Steady Lite Reagent (Perkin Elmer)	Log-transform (F). Normalize to noncoding within-plate control. Average triplicates. Subtract -Hh condition value from +Hh condition. <-1.5 SD from mean. >=2 siRNAs/gene.

Table 2.1 (continued):

Author	RNAi Modality	Cell Culture System	Screening Library	Stimulation and Read-Out	Analysis and Hit Criteria
Hillman et al. 2011	transfect dsRNA pools	SL2 (derivative of NIH3T3 cells), stable Gli-Luc (F), stable renilla luciferase (R)	Regulators of signal trans-duction; 816 siRNA pools	24hrs after transfection, stimulate with media containing Shh for 24-30hr. Dual-Glo Assay Kit (Promega)	Normalize (F)/(R) Normalize to within-plate control. Remove siRNA pools with (R)<30% compared to negative control well. z score <-1.5
Eisner (un-published)	lentivirus infection; shRNA	SL2 (derivative of NIH3T3 cells), stable Gli-Luc (F), stable renilla luciferase (R)	Phospha-tome 320 gene products (Broad Broad Institute RNAi Consort-ium)	72hrs after infection, stimulate with media containing Shh or SAG for 72hrs. Dual-Luciferase Assay Kit (Promega)	Normalize (F)/(R). Remove shRNAs with (R)=0 in either stimulation. condition Average replicate (F)/(R)values. Log-transform (F)/(R). Robust z score <-1.5 or >1.5. >=2 shRNA/gene

While siRNAs and shRNAs both deplete targeted gene products, the difference in the route of administration (i.e., transient lipid-based transfection or electroporation vs. virally-mediated stable genome incorporation) may result in differences in the duration of knock-down, as well as in the efficiency of RNAi, particularly if the cell type is not easily transfected. It is possible these differences may alter the observed phenotype following knock-down.

While many principals of Hh signaling are conserved between *Drosophila* and mammals (reviewed in Robbins et al. 2012; Ingham et al. 2011; Wilson & Chuang 2010), *Drosophila*-specific aspects of Hh signaling would not be detected in a mammalian culture system and vice versa, justifying the need for screening in both cell culture systems.

The RNAi library utilized for screening can also affect the results of the screen. By design, the library determines which gene products will be tested for a role in the signaling pathway under observation. For example, a library containing only kinases would only provide the opportunity to identify relevant kinases in a pathway and not relevant phosphatases. In addition, an RNAi library may not be fully verified resulting in false negatives due to poor knock-down or off-target effects. In a screen for disease-associated genes common to Hh and Wnt signaling, Jacob et al. (2011), screened two libraries in parallel, one from Dharmacon and one from Qiagen. Of 535 genes of interest identified as hits by either library, only five genes were identified as hits in both libraries (Jacob et al. 2011). This suggests that the results of an RNAi screen depend heavily on the high-throughput screening platform and/or library used.

The method and timing of Hh pathway stimulation may be another factor affecting the relative importance of a gene product in the pathway. Hh signaling involves many complicated feedback loops (reviewed in Ribes & Briscoe 2009) and it is conceivable that the importance of a protein in the pathway would vary at different time-points post-stimulation. For this reason, it is possible that stimulating cells with an exogenous Hh ligand may yield different results than constitutively expressing Hh in the cell system. Similarly, a 24-hour stimulation protocol may produce different results than a 48-hour stimulation protocol.

After an RNAi screen has been conducted and raw primary data have been collected, the method of data analysis, exclusion criteria, and hit criteria applied determine which candidates quality as hits. Without standardized analysis methods, this may further explain variation among the hits identified in published Hh screens.

Motivation for a Phosphatome RNAi Screen

Protein phosphorylation and consequent de-phosphorylation underlie an enormous spectrum of physiological functions. The phosphorylation state of a substrate can modulate its activity, cellular localization, and/or binding to other proteins. Aberrant phosphorylation is associated with many cancers; kinases, which catalyze phosphorylation, serve as therapeutic targets (reviewed in Cohen 2002; Blume-Jensen & Hunter 2001). Thus, understanding the regulation of phosphorylation is crucial for understanding cellular biology in healthy and diseased states.

While two mammalian screens have been conducted specifically to identify novel kinases in the Hh signaling pathway (Evangelista et al. 2008; Varjosalo et al. 2008), none have been conducted to specifically examine the role of phosphatases, which catalyze the

removal of phosphate groups. Additionally, very few phosphatases have been identified as regulators of Hh signal transduction in broader or genome-wide RNAi screens (Hillman et al. 2011; Jacob et al. 2011; Nybakken et al. 2005).

Just as the phosphorylation of substrates is important to transduce a signal, dephosphorylation may be an equally important regulatory mechanism. For this reason, in collaboration with the Broad Institute RNAi Consortium, we conducted a screen for novel phosphatases acting in the Hh pathway. It is our hope that these studies will advance our understanding of Hh biology while providing potential therapeutic targets for Shh-related cancers such as MB.

Results

Phosphatase Inhibitors Alter Hh Pathway Activation

Before conducting our RNAi screen to identify novel phosphatases in the Hh signaling pathway, we first verified that phosphatase activity is important for Hh pathway activation and that the impact of phosphatases on Hh pathway activity can be measured. We applied phosphatase inhibitors to Hh-responsive cells shortly before stimulating the pathway and measured the ability of cells to respond to stimulation.

We measured pathway activation using ShhLightII (SL2) cells which are derived from NIH3T3 cells stably expressing a Gli-dependent firefly luciferase (F luciferase) reporter and constitutive pRL-TK Renilla luciferase (R luciferase; Taipale et al. 2000). Accordingly, SL2 cells produce F luciferase in response to Hh pathway stimulation and continually produce R luciferase. The amount of F luciferase and R luciferase produced by cells are independently measured using commercially available luciferase assay reagents that generate quantifiable light reactions. The F luciferase value serves as a readout for Hh pathway activation while the R luciferase value allows for normalization to cell number and/or potential differences global transcriptional activity. In these experiments we measure pathway activation as F luciferase normalized to R luciferase (F/R luciferase).

To test whether phosphatase activity regulates the Hh signaling pathway, we applied phosphatase inhibitors to SL2 and measured the impact of the inhibitors on the ability of cells to respond to stimulation by SAG, a small molecule Smo agonist (Chen et al. 2002). We tested Okadaic Acid, a protein serine/threonine phosphatase inhibitor, and Sodium Orthovanadate (Na_3VO_4), a protein tyrosine phosphatase and alkaline

phosphatase inhibitor. F/R luciferase values for SAG-stimulated cells treated with Okadaic Acid showed a very strong trend towards a reduced response to SAG compared to uninhibited cells treated with a vehicle (veh) control (Figure 2.1a). Interestingly, application of Na_3VO_4 had a potent and dose-dependent effect increasing the F/R luciferase value regardless of pathway stimulation by SAG (Figure 2.1b). These data are striking because they demonstrate an ability of Na_3VO_4 to activate the pathway in a ligand-independent manner. It is important to note that the effects of Okadaic Acid and Na_3VO_4 on F/R luciferase values are largely the result of changes in F luciferase; R luciferase values were not dramatically altered by phosphatase inhibitors (data not shown).

These data provide evidence that phosphatases are involved in the Hh signaling pathway. Furthermore, these data suggest that phosphatases could be acting as potent positive and as negative regulators of Hh signal transduction. As pharmacological phosphatase inhibitors have multiple targets, we next conducted an RNAi screen to identify individual phosphatases that regulate Hh signaling.

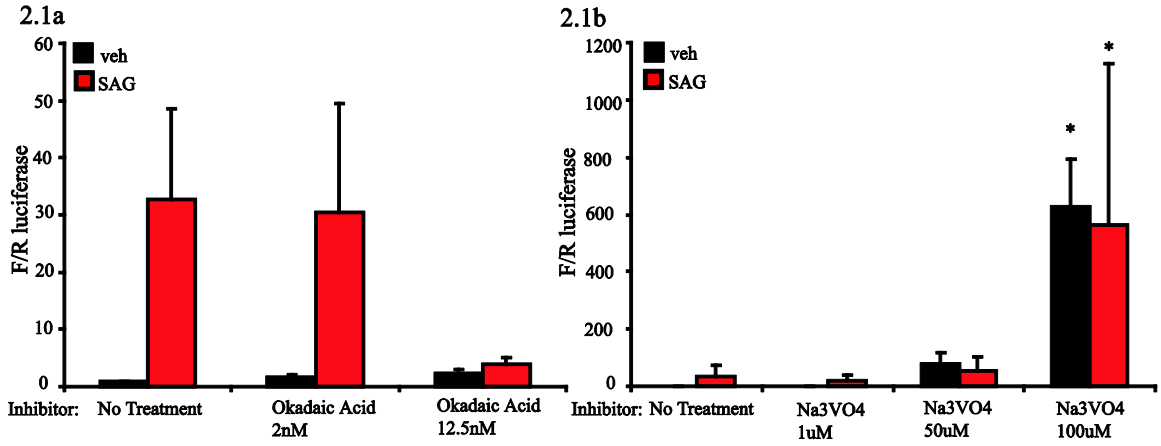

Figure 2.1 Phosphatase inhibitors alter Hh pathway activation. F/R luciferase values following stimulation with veh or SAG (300nM) were altered following the application of phosphatase inhibitors for 45 minutes prior to stimulation. **A)** Okadaic Acid trends towards a reduction in pathway stimulation at 12.5nM, normalized to untreated (veh, No Treatment) condition (N=7). **B)** Na_3VO_4 increases pathway activation at 100uM in both veh and SAG, normalized to untreated (veh, No Treatment) condition (N=9). Paired Student's t-test with Bonferroni correction, *$p<0.05$; error bars = SEM.

Primary Screen Results

RNAi was achieved using pLKO.1 lentiviral shRNA constructs generated by the Broad Institute RNAi Consortium against the mouse phosphatome. This library was composed of 320 genes, with four or five unique shRNAs targeting each gene product. The screen included a plate of "negative control" shRNAs which targeted genes not present in these cells (e.g., *GFP*, *RFP*, *β-galactosidase* [*LacZ*]). In addition, negative control shRNAs were added to each screening plate. Two shRNAs targeting *Smo* were included on each screening plate as positive controls. The screen was conducted in four "batches", with replicates run in parallel.

Before conducting the RNAi screen we optimized our screening assay for several parameters including cell density for seeding, the concentration of virus containing shRNA, time-course of adding reagents, and the luciferase reporter kit used to measure luciferase levels (data not shown). We also confirmed that we had achieved high viral infection efficiency in SL2 cells by showing R luciferase values of infected cells are similar with and without puromycin selection (Figure 2.2a). The pLKO.1 lentiviral shRNA constructs used in our experiments convey puromycin resistance. Similar R luciferase values with and without puromycin selection suggest similar numbers of cells are present, indicating that the majority of cells are puromycin resistant and therefore infected with high efficiency. Uninfected cells appear dead by light microscopy after puromycin treatment and have an R luciferase value equal to zero, confirming puromycin sensitivity in uninfected SL2 cells and a correlation between the R luciferase value and cell number (Figure 2.2b).

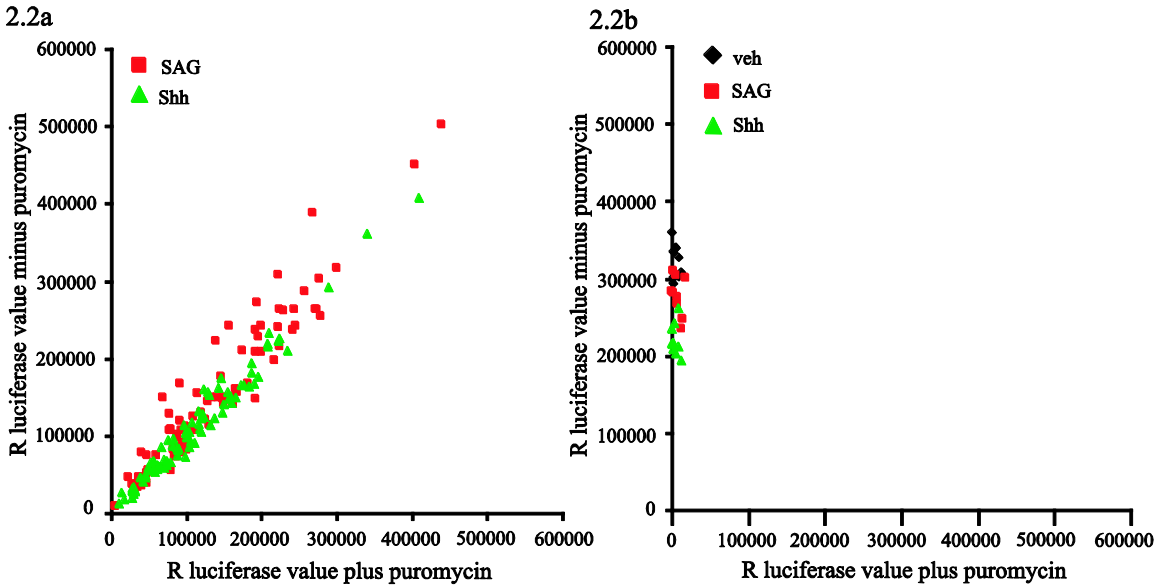

Figure 2.2 SL2 cells have high infection efficiency. A) R luciferase values of SL2 cells infected with negative control shRNA are similar with or without puromycin selection (R^2 = 0.81 in the SAG stimulation condition; R^2 = 0.86 in the Shh stimulation condition). **B)** R luciferase values of uninfected SL2 cells equal zero confirming that uninfected cells are puromycin sensitive.

The screen was conducted as follows: 24 hours after SL2 cells were plated, virus encoding a single shRNA was added to each well. The next day, cells were selected for successful infection with puromycin. After two days of selection, cells had grown to confluency and the Hh pathway was stimulated using either Shh-conditioned media, SAG, or veh. 72 hours post-stimulation, cells were lysed and assayed for luciferase levels (Figure 2.3).

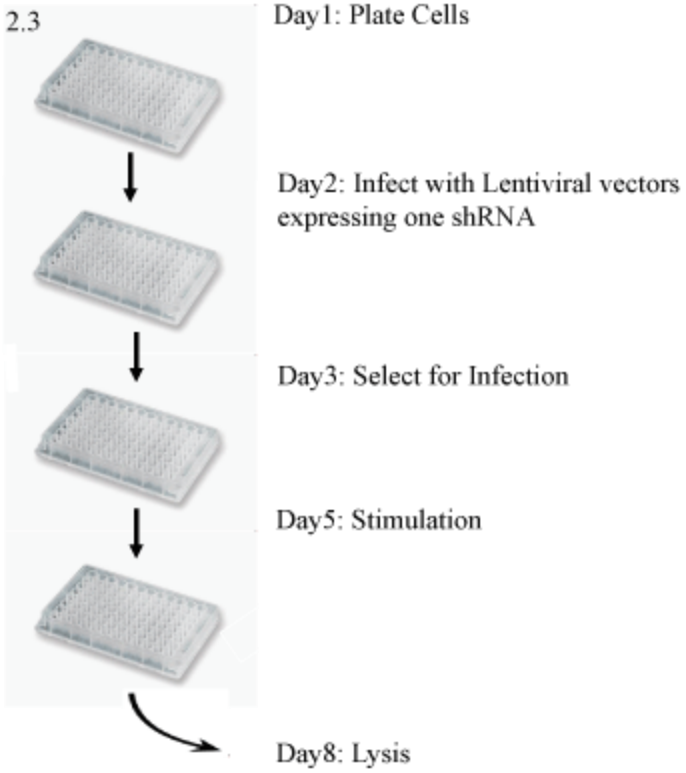

Figure 2.3 RNAi screen schematic. **A)** Cells were plated in 96-well plates. **B)** 24 hours after plating, cells were infected with virus encoding a single shRNA targeting a phosphatase gene product. **C)** After 24 hours of infection, media was removed and cells were selected for successful infection with 4ug/ml puromycin. **D)** After 48 hours of selection, media was removed and cells were stimulated with Shh-conditioned media, SAG, or veh in low-serum media. **E)** 72 hours after stimulation, cells were lysed and assayed for luciferase levels.

Before analyzing the screen, we first ensured successful stimulation of the Hh pathway. Average F/R luciferase data for each stimulation condition from the screen show that Shh and SAG successfully stimulated the pathway relative to the unstimulated veh condition (Figure 2.4a).

To begin the primary screen analysis, we first excluded wells with low cell survival. When the R luciferase value for either replicate was equal to zero, that shRNA was eliminated from analysis in that stimulation condition because this indicated that the cells were dead, possibly due to poor infection efficiency followed by puromycin selection or because the phosphatase targeted was necessary for cell viability. We then normalized F luciferase to R luciferase and substituted all F/R luciferase values equal to zero for a value of $1x^{10-6}$; this value is lower than any measured F/R luciferase ratio. We did this to avoid taking the natural log of zero in subsequent steps of the analysis (see below). We next averaged the F/R luciferase ratios for the two replicates because the replicates were close (Figure 2.4b).

Figure 2.4 Primary screen results. A) Average F/R luciferase values for each stimulation condition of the primary screen confirm that SAG and Shh stimulation activated the Hh pathway (N=1720 wells/stimulation condition), error bars = SEM. **B)** Replicate plates of SAG-stimulated cells infected with shRNA show similar F/R luciferase values (R^2=0.7). **C)** Replicate F/R luciferase values were averaged for each shRNA in each stimulation condition and then converted to their natural log value. Rank-ordered natural log values show a range of responses to Shh and SAG stimulation. **D)** Scatter plot of primary screen robust z-score results. Natural log values were assigned a robust z-score. Genes with two or more hairpins with a robust z-score less than -1.5 (below the lower black line) or grater than 1.5 (above the top black line) were considered hits for further analysis. shRNAs with an average F/R luciferase value equal to zero are not shown in D).

Figure 2.4 (continued):

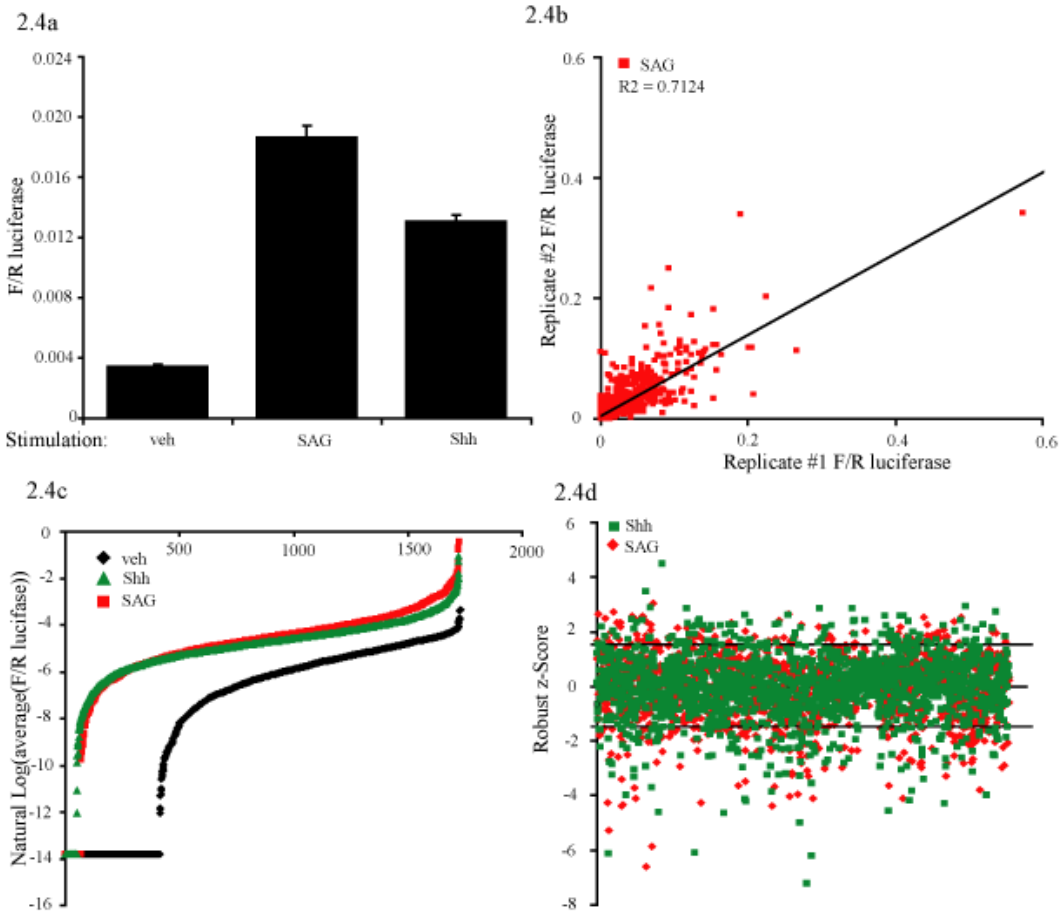

To identify which shRNAs were hits, we converted the averaged F/R luciferase ratios to natural log values (Figure 2.4c) and assigned each shRNA a robust z-score based on all the values collected in that batch for that stimulation condition (Figure 2.4d). A z-score describes the number of standard deviations a sample is from the mean. A robust z-score differs from a z-score by using the median instead of the mean and the median absolute deviation rather than the standard deviation when assigning values (Birmingham et al. 2009). This desensitizes the analysis to outliers and makes our substitution of $1x^{10-6}$ for F/R luciferase values equal to zero irrelevant. Genes with two or more targeting shRNAs with a robust z-score less than -1.5 and genes with two or more targeting shRNAs with a robust z-score greater than 1.5 were considered hits. Genes were considered hits if targeting shRNAs met the z-score criteria in the Shh and/or SAG stimulation conditions (e.g., a gene with two targeting shRNAs that had z-scores less than -1.5 in the SAG stimulation condition but not have any qualifying shRNAs in the Shh stimulation condition would be considered a hit as would a gene with one qualifying shRNA in the Shh stimulation condition and one qualifying shRNA in the SAG stimulation condition).

Of 320 gene products screened, 73 were identified as positive regulators of the pathway (i.e., shRNAs targeting these genes inhibited the ability of the cells to respond to Shh, resulting in a lower F/R luciferase value; Table 2.2) and 22 gene products were identified as negative regulators of the pathway (i.e., shRNAs targeting these genes increased the response of cells to pathway stimulation as indicated by an increased F/R luciferase value; Table 2.3). Six gene products met criteria as both positive and negative regulators because a subset of shRNAs targeting those genes resulted in reduced F/R luciferase values while other shRNAs targeting those same genes resulted in increased F/R luciferase values (Table 2.4). This result could be due to shRNA off-target effects. Alternatively, the shRNAs may target different splice variants of the phosphatase where one splice variant acts as a positive regulator and another functions as a negative regulator.

Among many novel phosphatases, our screen also confirmed several phosphatases identified by previous RNAi screens for members of the Hh pathway including catalytic and regulatory subunits of *Pp2a* as well as *Acp1*, *Dusp13*, *Pten*, *Ptp4a3*, and *Ptprn2* (Nybakken et al. 2005; Hillman et al. 2011; Tables 2.2, 2.3, 2.4). That *Pp2a*-encoding genes were identified as hits validates the ability of our screen to identify regulators of the pathway.

Table 2.2 Positive regulators of Hh signaling identified in the primary screen. Genes identified as positive regulators in the primary screen listed by gene symbol, RefSeq number, and NCBI Gene ID. A subset of genes identified as positive regulators of Hh signaling in the primary screen were re-screened using an adapted screen setup (Rescreened). A subset of genes re-screened were further identified as negative or positive regulators of Hh signaling (Re-Screen Hit; *italics* indicate genes identified as negative regulators in the re-screen). A subset of the genes identified in our primary screen have been implicated in Hh signaling in prior Hh RNAi screens (Previously Identified).

Table 2.2 (continued):

Symbol	RefSeq	NCBI Gene ID	Rescreened	Re-Screen Hit	Previously Identified
Acp1	NM_021330	11431	Acp1	Acp1	Hilman et al. 2011
Acp5	NM_007388	11433			
Acpl2	NM_153420	235534	Acpl2		
Akp-ps1	XM_136795	208256	Akp-ps1		
Alpi	XM_129951	76768	Alpi	Alpi	
Alpl	NM_007431	11647	Alpl		
Arid1a	NM_033566	93760	Arid1a	Arid1a	
BC005764	NM_181681	216152	BC005764		
Brd7	NM_012047	26992			
Cant1	NM_029502	76025	Cant1	Cant1	
Dusp11	NM_028099	72102	Dusp11		
Dusp21	XM_135794	73547	Dusp21		
Dusp26	NM_025869	66959	Dusp26	Dusp26	
Dusp28	NM_175118	67446	Dusp28	Dusp28	
Dusp8	NM_008748	18218			
Ebf2	NM_010095	13592	Ebf2		
Entpd4	NM_02617	67464	Entpd4		
Epb4.1l4a	NM_013512	13824	Epb4.1l4a		
Eya1	NM_010164	14048	Eya1	Eya1	
Eya2	NM_010165	14049	Eya2	Eya2	
Fam48a	NM_019995	56790	Fam48a		
Fbp1	NM_019395	14121	Fbp1		
G3bp1	NM_013716	27041			
G6pc2	NM_021331	14378	G6pc2		
Gfi1b	NM_008114	14582	Gfi1b	*Gfi1b*	
Gm5601	XM_485994	434233	Gm5601		
Impa2	NM_053261	114663	Impa2		
Inpp5d	NM_010566	16331	Inpp5d	*Inpp5d*	
Mfn1	NM_024200	67414			
Mtm1	NM_019926	17772	Mtm1		
Mtmr4	NM_133215	170749	Mtmr4		
Olfr1231	NM_146454	258446			
Olfr1265	NM_146343	258340			
GA_x5J8B 7W2BV0-3116-4045	NM_146263	257663			
Olfr140	NM_020515	57272	Olfr140		
Olfr1506	NM_146265	257665	Olfr1506	*Olfr1506*	
Pdxp	NM_020271	57028			
Pfkfb4	NM_173019	270198			
Phlpp1	XM_129968	98432	Phlpp1		

Table 2.2 (continued):

Phlpp2	XM_146511	244650	Phlpp2		
Pou2f2	NM_011138	18987	Pou2f2		
Ppm1a	NM_008910	19042			
Ppm1k	NM_175523	243382	Ppm1k		
Ppp1cb	NM_172707	19046	Ppp1cb	*Ppp1cb*	
Ppp2r3a	XM_135153	235542	Ppp2r3a		Nybakken et al. 2005
Ppp2r5a	NM_144880	226849	Ppp2r5a		Nybakken et al. 2005
Ppp5c	NM_011155	19060			
Ppp6c	NM_024209	67857			
Psph	NM_133900	100678			
Pten	NM_008960	19211			Hilman et al. 2011
Ptp4a2	NM_008974	19244	Ptp4a2		
Ptp4a3	NM_008975	19245	Ptp4a3		Hilman et al. 2011
Ptpn14	NM_008976	19250			
Ptpn22	NM_008979	19260	Ptpn22	*Ptpn22*	
Ptprc	NM_011210	19264			
Ptprg	NM_008981	19270	Ptprg	*Ptprg*	
Ptprj	NM_008982	19271			
Ptprn	NM_008985	19275			
Ptprq	XM_137234	237523	Ptprq		
Ptprs	NM_011218	19280			
Ptprt	NM_021464	19281			
R3hdm2	NM_027900	71750	R3hdm2	*R3hdm2*	
Rngtt	NM_011884	24018			
Sgpp2	NM_001004173	433323			
Sh2d1b1	NM_012009	26904			
LOC436244	XM_488395	436244	LOC381574		
LOC381574	XM_485481	381574			
Smarca4	NM_011417	20586			
Smarcc1	NM_009211	20588			
Ssh2	NM_177710	237860			
Stat3	NM_011486	20848			
Styxl1	NM_029659	76571			
Synj2	NM_011523	20975			

Table 2.3 Negative regulators of Hh signaling identified in the primary screen. Genes identified as negative regulators in the primary screen listed by gene symbol, RefSeq number and, NCBI Gene ID. A subset of genes identified as negative regulators of Hh signaling in the primary screen were re-screened using an adapted screen setup (Rescreened). A subset of genes re-screened were further identified as negative or positive regulators of Hh signaling (Re-Screen Hit; *italics* indicate genes identified as negative regulators in the re-screen). A subset of the genes identified in our primary screen have been implicated in Hh signaling in prior Hh RNAi screens (Previously Identified).

Symbol	RefSeq	NCBI Gene ID	Rescreened	Re-Screen Hit	Previously Identified
Acaca		107476			
Atp6v0e	NM_025272	11974	Atp6v0e	*Atp6v0e*	
C79127	NM_177691	232941			
Dupd1	XM_487320	435391	Dupd1	*Dupd1*	
Dusp13	NM_013849	27389			Hilman et al. 2011
Dusp18	NM_173745	75219			
Enoph1	NM_026421	67870	Enoph1		
Mtmr6	NM_144843	219135	Mtmr6		
Nt5e	NM_011851	23959			
Olfr1199	NM_146458	258450	Olfr1199		
Ppap2c	NM_015817	50784			
Ppp2ca	NM_019411	19052	Ppp2ca	*Ppp2ca*	Nybakken et al. 2005
Ppp2r5b	NM_198168	225849	Ppp2r5b	*Ppp2r5b*	Nybakken et al. 2005
Ppp3cc	NM_008915	19057			
Ppp3r1	NM_024459	19058			
Ptpn1	NM_011201	19246			
Ptpn3	XM_355486	19257			
Ptprf	NM_011213	19268			
Ptprn2	NM_011215	19276			Hilman et al. 2011
Ptpru	NM_011214	19273	Ptpru	*Ptpru*	
Ptprv	NM_007955	13924	Ptprv	*Ptprv*	
Sirpa	NM_007547	19261			

Table 2.4 Genes identified as positive and negative regulators of Hh signaling in the primary screen. Genes identified as negative and positive regulators in the primary screen listed by gene symbol, RefSeq number, and NCBI Gene ID. These genes were re-screened using an adapted screen setup (Rescreened). A subset of genes re-screened were further identified as negative or positive regulators of Hh signaling (Re-Screen Hit; *italics* indicate genes identified as negative regulators in the re-screen). None of these genes have previously implicated in Hh signaling in prior Hh RNAi screens (Previously Identified).

Symbol	RefSeq	NCBI Gene ID	Rescreened	Re-Screen Hit	Previously Identified
Arpp21	NM_033264	74100	Arpp21		
Dusp19	NM_024438	68082	Dusp19		
Dusp4	NM_176933	319520	Dusp4		
Impa1	NM_018864	55980	Impa1	*Impa1*	
Nudt6	NM_153561	229228	Nudt6	Nudt6	
Ppapdc1a	XM_355946	381925	Ppapdc3		

Primary Screen Validation

To confirm our primary screen results, we re-screened 57 of our hits using the same screen setup with two minor technical improvements (see methods; Tables 2.2, 2.3, 2.4). Because these shRNAs were selected for their effect on the pathway from the first screen, analyzing the second screen with a robust z-score may have skewed our results. Therefore, to evaluate the effect of shRNAs on Hh pathway induction in the second screen, we compared the F/R luciferase value of each shRNA to the F/R luciferase value measured from cells treated with negative control virus. We screened a 96-well plate of cells treated with unique negative control shRNAs and recorded the median F/R luciferase value following stimulation with Shh, SAG or veh. We reasoned this median negative control F/R luciferase value was representative of an unperturbed Hh pathway response to stimulation and looked for shRNAs targeting phosphatases which blocked the ability of the cells to respond to stimulation or sensitized the response relative to this value. To determine which primary screen hits were considered hits in the second screen, we set a criteria whereby shRNAs with an F/R luciferase value less than 25% of the median negative control F/R luciferase value were identified as positive regulators of the pathway (Figure 2.5c-d); shRNAs with an F/R luciferase value greater than four-fold the median negative control F/R luciferase value were identified as negative regulators of the pathway (Figure 2.5a-b). We only considered genes for which 25% or more of shRNAs targeting that gene met the above F/R luciferase value criteria.

Figure 2.5 Re-screen results. A subset of hits from the primary screen were re-screened. Pink squares indicate values corresponding to shRNAs targeting *Eya1* or *Smo*. F/R luciferase values are normalized to the median F/R luciferase value of negative control shRNAs. **A)** F/R luciferase values rank-ordered show a range of responses to Shh and SAG stimulation. **B)** F/R luciferase values as a scatter plot show a range of responses to Shh and SAG stimulation. Values greater than four-fold the F/R luciferase value of negative control shRNAs (above the black line in A and B) are considered hits. **C)** Magnified portion of the rank-order graph in A. **D)** Magnified portion of the scatter plot in B. Values less than 25% the F/R luciferase value of negative control shRNAs (below the block line in C and D) are considered hits.

Figure 2.5 (continued):

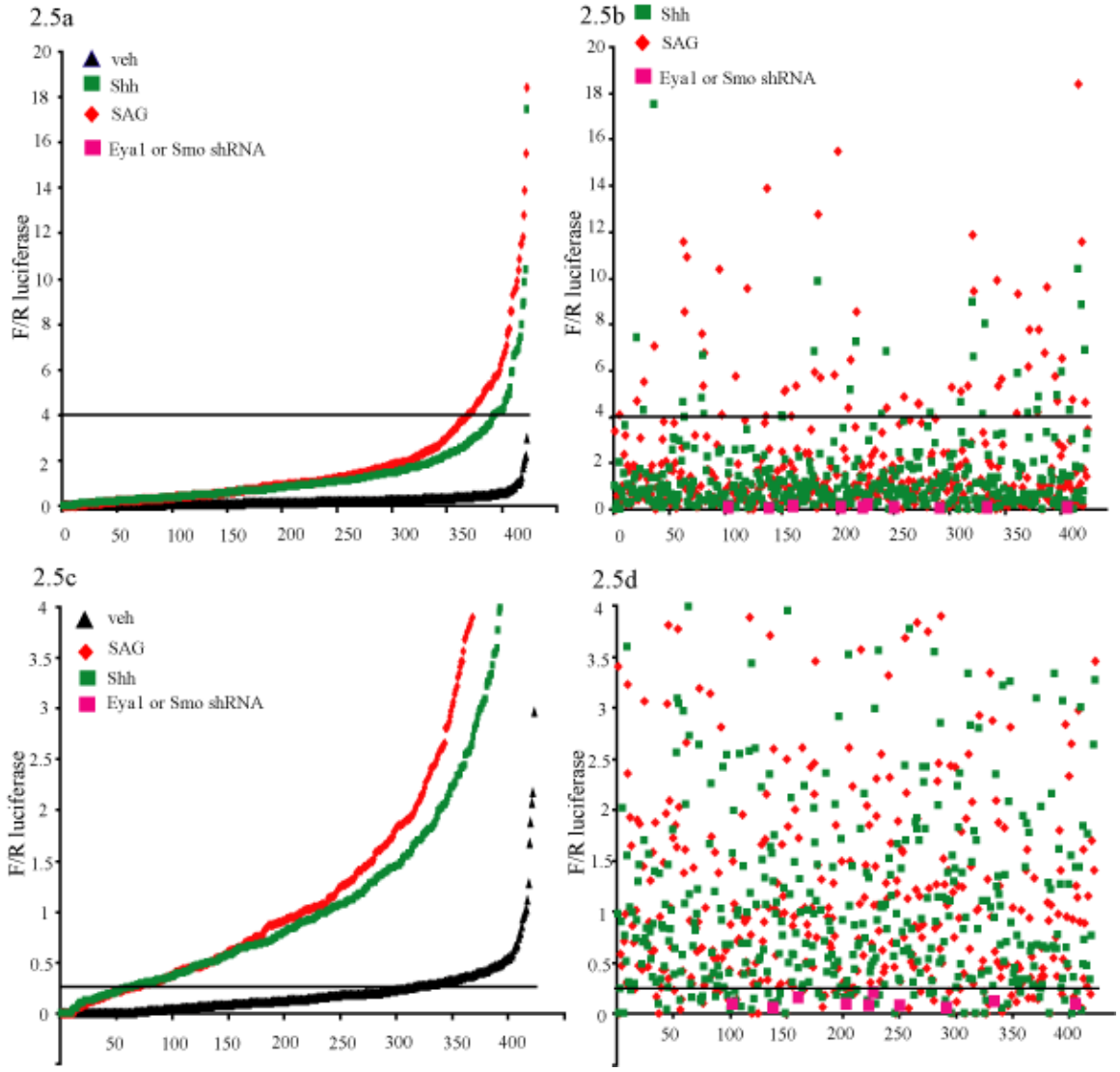

Of 57 genes re-screened, 14 came out as positive regulators of the pathway and nine were identified as negative regulators of the pathway (Tables 2.2, 2.3, 2.4). Again, shRNAs targeting *Smo* and known phosphatases came out as hits in the screen including *Pp2* catalytic and regulatory subunits.

Phosphatases Likely Important for Shh-Dependent MB

To select which hits to pursue for further study, we looked for phosphatases more likely to be involved in Shh-dependent MB. There are multiple subtypes of MB defined by distinctive gene expression profiles; the "Shh-subtype" of MB is characterized by aberrant expression of Hh pathway components and increased Hh pathway activation (reviewed in Northcott et al. 2012). Utilizing three previously published sets of MB gene expression data (Kool et al. 2008; Northcott et al. 2011; Thompson et al. 2006), we asked if any of our hits are also up- or down-regulated in the Shh-subtype of MB relative to other MB subtypes. Of the 39 hits from our primary screen that were not re-screened, 10 showed specific up- or down-regulation in the Shh-subtype of MB relative to other MB subtypes in one or more data-sets; one gene (*Ppm1a*) was identified in two published data sets (Table 2.5). Of the 23 hits identified following re-screening, nine showed specific up- or down-regulation in Shh-subtype MB relative to other MB subtypes. Of these, three genes (*Cant1*, *Eya1*, *Eya2*) were noted in two or more data sets (Table 2.6).

Table 2.5 Genes identified in the primary screen that were not re-screened have been reported to be up- or down-regulated in Shh-dependent MB. Of the 39 hits from our primary screen identified as positive or negative regulators of Hh signal transduction that were not re-screened, 10 (Symbol) have specific up- or down-regulation in the Shh-subtype of MB relative to other MB subtypes as reported in one or more of three published gene expression studies (Kool et al. 2008; Thompson et al. 2009; Northcott et al. 2010).

Symbol	Direction of Regulation Screen	Kool et al. 2008 direction of regulation in MB	Thompson et al. 2009 direction of regulation in MB	Northcott et al. 2010 direction of regulation in MB
Acaca	Negative			down
Mfn1	Positive			up
Nt5e	Negative			up
Pdxp	Positive	down		
Ppm1a	Positive	down	down	down
Ppp6c	Positive			down
Psph	Positive	down		
Ptprt	Positive		down	
Smarca4	Positive			down
Smarcc1	Positive		up	

Table 2.6 Genes identified in the primary screen that were re-screened have been reported to be up- or down-regulated in Shh-dependent MB. Of the 23 hits identified as hits following re-screening, nine (Symbol) have specific up- or down-regulation in the Shh-subtype of MB relative to other MB subtypes as reported in one or more of three published gene expression studies (Kool et al. 2008; Thompson et al. 2009; Northcott et al. 2010).

Symbol	Direction of Regulation Screen	Kool et al. 2008 direction of regulation in MB	Thompson et al. 2009 direction of regulation in MB	Northcott et al. 2010 direction of regulation in MB
Arid1a	Positive			down
Cant1	Positive	down		down
Dusp26	Positive			up
Eya1	Positive		up	up
Eya2	Positive	down	down	down
Impa1	Negative	down		
Inpp5d	Negative			up
Ppp2ca	Negative		down	
Ptpru	Negative			down

From the list of genes that appeared in two or more MB databases as being up- or down-regulated in Shh-subtype MB relative to other MB subtypes (i.e., *Ppm1a*, *Cant1*, *Eya1*, *Eya2*), we choose to pursue the role of *Eya1* because the effect on Hh pathway activation of knocking-down this gene in SL2 cells is consistent with the direction of deregulation in Shh-subtype MB. In the SL2 cells, knocking-down *Eya1* blocked the ability of the cells to respond to stimulation, suggesting Eya1 is a positive regulator of the pathway. In MB cells, where the pathway is known to be overly active, *Eya1* is up-regulated, also consistent with the idea that Eya1 is a positive regulator of the pathway. In contrast, the other three hits identified in our screen and found to be specifically regulated in Shh-subtype MB (*Ppm1a*, *Cant1*, and *Eya2*) were identified as positive regulators of Hh signal transduction by our RNAi screen in SL2 cells but were found to be down-regulated in Shh-dependent MB cells.

In addition, we also chose to pursue the role of Eya1 in Hh signaling given overlapping roles of Eya1 and Shh signaling in disease and development to be discussed in the following chapter.

Discussion

In this study, we conducted an RNAi screen identifying novel phosphatases in the Hh signaling pathway. In addition, several phosphatases previously implicated in Hh signaling were identified in our screen, validating our system. Phosphatases identified in our screen contribute to our understanding of this important signaling pathway and may serve as future therapeutic targets in treating Shh-dependent cancers.

Phosphatase Inhibitors

For a preliminary look at the potential necessity of phosphatases for Hh signaling, we measured the ability of SL2 cells to respond to SAG following treatment by a serine/threonine protein phosphatase inhibitor or an inhibitor to tyrosine phosphatases and alkaline phosphatases. Our findings confirmed that dephosphorylation may be an important regulatory mechanism in Hh signaling.

Okadaic Acid strongly inhibits Pp1, Pp2A, and Pp2B. 1-2nM concentrations of Okadaic Acid will result in a 50% reduction in enzymatic activity (ID_{50}) of Pp2A; Pp1 has an ID_{50} ~300nM and Pp2B has an ID_{50} of 4-5uM concentrations of Okadaic Acid (Bialojan & Takai 1988). Our finding that 12.5nM Okadaic Acid blocks the ability of cells to respond to SAG is consistent with previous reports implicating Pp2A in the Hh pathway (Jia et al. 2009; Jin et al. 2011; Krauss et al. 2008) as well as with our own primary screen data identifying *Pp2A* encoding genes as hits.

Na_3VO_4 is an inhibitor of protein tyrosine phosphatases, alkaline phosphatases, and ATPases and is used at mM concentrations (Kim et al. 1999). Our preliminary finding that Na_3VO_4 activates the Hh pathway at 50uM concentrations is very intriguing. Therefore, this class of phosphatase was of particular interest to us in conducting our

phosphatome RNAi screen. Of 101 primary screen hits, at least 21 are potential Na_3VO_4 targets (see discussion below).

RNAi Screen Design and Analysis

In any experiment, an investigator must carefully design his or her study to minimize false positive and false negative results. This is especially true in designing and analyzing a screen which returns a graded and continuous range of results (e.g., a continuous range of z-scores). As such, determining criteria for which gene candidates qualify as hits is subjective and different criteria will produce a different set of hits.

In analyzing our screen, we took steps to minimize false positive and false negative results. We assigned robust z-scores by batch to account for potential batch-to-batch variation from slight differences in plating, stimulation, cell lysis, or other technical aspects of the screening protocol. To minimize the number of false positive hits, we made our z-score criteria sufficiently stringent to exclude all negative control shRNAs as hits (i.e., multiple shRNAs targeting *RFP*, *GFP*, and *LacZ*). These negative control shRNAs were selected because the genes they target are not expressed in this cell system and therefore the shRNAs should not alter the ability of cells to respond to Hh pathway stimulation. To reduce the chance that an effect on Hh pathway stimulation was due to off-target effects of shRNA, we set a minimum criterion of two targeting shRNAs per gene. To ensure our analysis detected negative regulators of the pathway, we also designed z-score criteria to be sufficiently generous to identify our positive controls (shRNAs targeting *Smo* and *Luciferase*).

Despite our considerations, there remain several potential sources of false positive and false negative results. As SL2 cells are maximally Shh-responsive when confluent

(data not shown), a potential source of false positive hits may include genes targeted by shRNA in virus with low infection efficiency. After puromycin selection, wells treated with low-efficiency virus may not reach confluency and may therefore be less responsive to Shh and SAG, resulting in a low F/R luciferase ratio. A potential source of false negative hits in our screen includes shRNA constructs which successfully entered cells and conveyed puromycin resistance but failed to sufficiently knock-down their target. In addition, the timing of our assay may not have been optimal to detect phenotypes from knocking-down some phosphatases that impinge upon the pathway.

RNAi Screen Results

Interestingly, in the primary screen, we found evidence of many kinds of phosphatases influencing Hh pathway activation including protein phosphatases, protein tyrosine phosphatases, alkaline phosphatases, dual-specificity phosphatases, lipid phosphatases, and sugar phosphatases. Among these, phosphatases encoded by *Pp2*, *Acp1*, *Dusp13*, *Pten*, *Ptp4a3*, and *Ptprn2* may be promising candidates to pursue in future studies as targeting these genes altered Shh-responsiveness in our screen as well as in previous RNAi screens (Hillman et al. 2011; Nybakken et al. 2005). Stat3 may be an additional interesting candidate to pursue as it has been previously implicated in hedgehog signaling (Yang et al. 2012).

While knocking-down a direct regulator of Hh signaling would alter the response of SL2 cells to Shh or SAG, hits likely also include phosphatases acting indirectly on the pathway. For example, knocking-down a phosphatase needed to regulate a factor involved in trafficking Smo to the primary cilia might also affect the ability of cells to respond without being a core member of the pathway. Further studies examining the

activity, cellular localization, and potential substrates of a candidate phosphatase would need to be carried out to understand how a candidate is functioning to regulate Hh signal transduction.

In our experimental design, we included three stimulation conditions, Shh, SAG, and veh. We included Shh, which activates the pathway through binding Ptch1, as well as SAG, which activates the pathway through direct Smo activation, with the hope of identifying phosphatases acting in the Hh pathway between Ptch1 and Smo as very little is known about the mechanisms mediating Ptch1 inhibition of Smo. Unfortunately, however, we did not identify any hits which had an effect in the Shh stimulation condition while having no effect in the SAG stimulation condition. While disappointing, this result is consistent with previous screening attempts (Evangelista et al. 2008).

Encouraged by results that Na_3VO_4 has the ability to induce F luciferase in SL2 cells, the veh stimulation in our screen condition provided an opportunity to identify strong negative regulators of Hh signaling in SL2 cells (i.e., phosphatases that, when knocked-down, result in ligand-independent pathway activation). Unfortunately, of nearly 1,800 shRNAs screened, only eight had a robust z-score greater than 1.5 in the veh condition and these shRNAs targeted eight unique phosphatases, failing to meet our criteria requiring a gene have two qualifying targeting shRNAs to be considered a hit. However, two of the eight activating shRNAs targeted protein tyrosine phosphatases, *Ptplad1* and *Ptprm*, which are potential targets of Na_3VO_4. It is possible that knock-down of a single gene product was unable to induce extraordinary high F luciferase values in veh-treated cells because the large effect observed by Na_3VO_4 application is the result of inhibiting multiple phosphatase targets simultaneously while our screen

examined the effect of knocking done single genes. Additionally, around 40% of our veh samples had at least one replicate F luciferase equal to zero, suggesting SL2 cells have very low basal levels of Hh pathway activation. Additionally, this observation suggests that the basal activity in SL2 cells is often below the level of detection by our assay. Perhaps by having so many samples with a zero reading, our median F/R luciferase value was artificially high in the veh condition, making it difficult to identify shRNAs which had modest activating affects on the pathway.

We also looked for negative regulators of the pathway in the Shh and SAG stimulation conditions (i.e., shRNAs that enhanced the cells' response to Hh pathway stimulation). Of 22 phosphatases identified as having two or more targeting shRNAs with a robust z-score greater than 1.5, six were protein tyrosine phosphatases and potential targets of Na_3VO_4. We also noticed that there were more than three times as many positive regulators of the pathway identified as hits than negative regulators. One potential explanation for this could be that we were maximally stimulating the cells, leaving little room for enhanced pathway activation. More sensitive experiments to identify positive pathway regulators might involve stimulating the pathway with SAG concentrations around 10-50nM (i.e., 6-30x less concentrated than was applied in our screen).

The phosphatases identified in our screen contribute to our knowledge of the Hh signaling pathway. By focusing on phosphatases more likely to be important in Shh-dependent MB, it is our hope that this information may contribute to the development of cancer therapies. Specifically, we chose to focus our studies on *Eya1* which was the only hit to be shown by two independent studies to be significantly differentially regulated in

Shh-subtype MB while showing consistent effects on pathway activation by RNAi-mediated knock-down. In the next chapter we will pursue the role of Eya1 in Hh signaling.

Methods

SL2 Cell Stimulation

Shh-conditioned media: 293FT cells (derived from human embryonic kidney cells transformed with the SV40 large T antigen) were transfected with full-length Shh in a pcDNA3 vector using Lipofectamine 2000 (Life Technologies Catalog #11668019) following manufacturer's instructions. Media was changed the next day (~18 hours after transfection), 24 hours later media was changed a second time, 24 hours later media was collected and concentrated using Amicon Ultra centrifugal filter units (Millipore). The presence of Shh ligand was verified by western blot (antibody: N-Shh19, Santa Cruz). Smo agonist, SAG (Enzo Life Sciences) was reconstituted in equal parts water and DMSO and stored at -20°C. Veh treated samples were stimulated using equal parts water and DMSO. When applying a phosphatase inhibitor before pathway stimulation, media was removed from each well and the inhibitor was added to the well in a volume of 30ul (at 1.7x concentration) for 45 minutes, after which 20ul of stimulation media (at 2.5x concentration) was added to the wells for a final volume of 50ul.

SL2 Luciferase Assay

For all SL2 luciferase assays, SL2 cells (ATCC Catalog # CRL-2795) were plated in 96-well opaque tissue culture dishes (Falcon Catalog #353296) and maintained in growth media (DMEM, 10% calf serum, 1unit/ml penicillin, 1ug/ml streptomycin, 0.4mg/ml G418, and 0.15mg/ml zeocin). In all SL2 stimulation experiments, growth media was removed and cells were stimulated with 300ng/ml SAG or the same volume of veh in low serum conditions (DMEM, 0.5% calf serum, 5mM HEPES). To assay

pathway stimulation, media was removed and cells were lysed at room temperature for 15 minutes on a rotator using Passive Lysis Buffer from the Dual Luciferase Reagent (DLR; Promega #E1960) kit. Plates were stored at -20°C or assayed immediately for luciferase activity, following manufacturer's instructions with the modification that we added 30ul Passive Lysis Buffer and 60ul of Luciferase Assay Reagent and 60ul of Stop & Glo to each well.

RNAi Screen

Lentiviral infections for the screen were performed using pLKO.1 lentiviral shRNA constructs generated the Broad Institute RNAi Consortium and arrayed in 96-well plates. SL2 cells were plated using a microfill cell dispensing machine. 24 hours later, polybrene (final concentration of 8ug/ml) and 10ul of virus containing a single shRNA were added to screening plates using an automated cell culture robot. Plates were spun in a centrifuge at 2500rpm for 20 min at room temperature to enhance infection efficiency. Each plate was prepared in duplicate. Four hand-spiked shRNAs targeting *RFP*, *GFP*, or *LacZ* plus two shRNAs targeting *Smo* were included on each plate as negative and positive controls, respectively. In addition, a plate of negative control shRNAs prepared in parallel with the phosphatome library was included in the screening set. 24 hours after plating, media was removed and cells were selected for infection by adding growth media containing 4ug/ml puromycin. 48 hours following selection, media was removed, cells were rinsed twice with low-serum media, and cells were stimulated using Shh-condition media, SAG, or veh in low-serum media. 72 hours following stimulation, stimulation media was removed and cells were lysed. For the re-screen, cells

were plated in virus and polybrene, shortening the screening protocol by 24 hours. For the re-screen cells were rinsed with PBS before lysis.

RNAi Screen Analysis

shRNAs with an R luciferase value for either replicate equal to zero were eliminated from analysis in that stimulation condition. We next averaged the F/R luciferase ratios and F/R luciferase ratios equal to zero were given a value of F/R luciferase equal to $1x^{10-6}$. We then took the natural log of the average F/R luciferase value. We assigned each shRNA a robust z score [(x-median)/(median absolute deviation); median absolute deviation = median(abs(x- median))*1.4826] based on all the values collected in that batch. For the primary screen, genes with two or more shRNAs targeting that gene with a robust z score less than -1.5 or greater than 1.5 in either the Shh or SAG stimulation conditions were considered hits.

For the re-screen, we identified hits as having an F/R luciferase value less than 25% or greater than four-fold the median F/R luciferase value from a plate of negative control shRNAs. Genes with 25% or more of shRNAs targeting that gene were hits.

Screen analysis was preliminarily conducted in Microsoft Excel and secondarily re-analyzed in Matlab.

Author Contribution:

Dr. Srividya Balasubramanian initiated our RNAi screen project and conducted initial protocol optimizations. We conducted additional optimizations together and I also conducted optimizations independently. The primary and second screens were conducted and analyzed in collaboration with Dr. So Young Kim, Leslie Wardwell, Dr. Anna

Schinzel, and Dr. William C. Hahn. Dr. Alexandra Smolyanskaya assisted with the re-analysis of screen data in Matlab.

CHAPTER 3: EYA1 IS A POSITIVE REGUALTOR OF HH SIGNAL TRANSDUCTION

Introduction

Rationale for Pursuing Eya1 in Hh Signaling

In selecting which hits from our RNAi screen to pursue as potentially important regulators of Hh signaling, we focused on genes specifically up- or down-regulated in human Shh-dependent MB as compared to other MB subtypes. We made this decision for three reasons. Firstly, the Hh signaling pathway is over-active in Shh-dependent MB and many Hh pathway components are up-regulated in those tumors; a difference in expression of a gene in Shh-dependent MB could indicate a role for the protein product encoded by that gene in the Hh signaling pathway. Secondly, a greater understanding of MB biology could yield future therapeutic targets. In addition, a phosphatase implicated in Hh signaling in these two very different contexts, human MB and murine embryonic fibroblasts, demonstrates a potentially generalizable function of that phosphatase in regulating Hh signal transduction.

We identified *Eya1* as a positive regulator of Hh signal transduction in our primary screen and *Eya1* is also specifically up-regulated in Shh-dependent MB (Kool et al. 2008; Northcott et al. 2011; Thompson et al. 2006). We additionally chose to pursue the role of Eya1 in Hh signaling because Eya1 and Hh signaling have overlapping roles in development from *Drosophila* to mammals. In *Drosophila*, Hh and Eya are both crucial for eye development. In vertebrate development, Eya1 and Shh overlap in the development of the otic vesicle, lung, and kidney.

Eya1 and Hh in *Drosophila* Eya Development

Eya gets its name from its role in *Drosophila* eye development as a member of the RDGN (reviewed in Pappu & Mardon 2004; Silver & Rebay 2005). The *Drosophila* visual system is comprised of two compound eyes and three ocelli. The compound eyes contain ommatidia, structures comprised of photoreceptors and accessory cells; ocelli are simple light-sensitive organs at the top of the adult head. Hh signaling is necessary for both compound eye and ocelli organ systems, and interacts genetically with the RDGN (Aguilar-Hidalgo et al. 2013; Blanco et al. 2009; Pappu et al. 2003).

In the compound eye Eya and its co-factor, So, are required for the initiation and progression of photoreceptor differentiation. In this developmental context, the role of Hh is to relieve CiR-mediated repression of *Eya* expression (Pappu et al. 2003). In the absence of Hh signaling, CiR represses *Eya* expression, preventing the initiation and progression of photoreceptor differentiation. Hh signaling inhibits the formation of CiR, allowing *Eya* induction. The removal of CiR is sufficient to induce *Eya* expression while loss-of-function studies show that full-length CiA plays little or no role in photoreceptor development (Pappu et al. 2003).

Hh signaling regulates *Eya* expression in the developing ocelli as well. In contrast to the mechanism of transcriptional regulation in the compound eye, in ocellar precursor cells, CiA is responsible for *Eya* gene activation (Blanco et al. 2009). In *Smo* mutant clones without Hh signaling, *Eya* is not expressed whereas in *Ptc* mutants clones with active Hh signaling, *Eya* expression is induced (Blanco et al. 2009). While Hh signaling regulates *Eya* expression in *Drosophila* eye development, So regulates *Hh*

expression, creating a complex network intricately linking RDGN and Hh signaling in this context (Pauli et al. 2005).

Much of the Hh signaling pathway described in *Drosophila* is conserved in mammalian Hh signaling (reviewed in Robbins et al. 2012; Ingham et al. 2011; Wilson & Chuang 2010). Similarly, the RDGN as characterized in *Drosophila* has also been adapted to mammalian development (reviewed in Silver & Rebay 2005). This precedent for Hh and RDGN pathway conservation from *Drosophila* to vertebrates and these examples of a genetic interaction between Hh and Eya in *Drosophila* eye development helped motivate our decision to pursue Eya1 in the context of mammalian Hh signaling.

Nrp Biology

Nrps are transmembrane proteins, functioning as co-receptors with roles in axon guidance and angiogenesis (reviewed in Pellet-Many et al. 2008; Parker et al. 2012). There are two mammalian *Nrp* genes, *Nrp1* and *Nrp2*, which share the same domain structure and 44% amino acid homology (Giger et al. 1998). Nrps have five external domains, a single transmembrane alpha helix, and a short intracellular domain. The extracellular domains consist of two tandem complement/Uegf/Bmp1 (CUB) domains, two tandem Factor V/VIII homology domains, and one Meprin/A5-antigen/ptp-Mu (MAM) domain. The external domains bind ligands, including class III Semaphorin (Sema3) family members and vascular endothelial growth factor (VEGF) family members. Nrp1 and Nrp2 bind distinct yet overlapping members of the Sema3 and VEGF families (reviewed in Neufeld & Kessler 2008).

Nrps bind Sema3s and function in axon guidance as co-receptors with Plexin proteins (He & Tessier-Lavigne 1997; Kolodkin et al. 1997; Takahashi et al. 1999).

Sema3s are secreted guidance factors, repelling axons during axonal path finding. Within the Nrp-Plexin-Sema3 complex, Nrps bind Sema3s with high-affinity while Plexins transduce an intracellular signal resulting in the collapse of the actin cytoskeleton in the growth cone. Nrps serve as obligate co-receptors in some, but not all, contexts of Sema3 signaling (Gu et al. 2005).

A second well-characterized function of Nrp is to bind VEGF as a co-receptor with VEGF receptors in angiogenesis (Soker et al. 1998; Gluzman-Poltorak et al. 2001). VEGF binds both a VEGF receptor and Nrp, perhaps bridging the two transmembrane proteins. Nrps can serve to enhance VEGF binding to its receptor and strengthen VEGF receptor-mediated intracellular signaling (Soker et al. 2002).

In addition to serving as a co-receptor in complexes where its partner transduces the lion's share of intracellular signaling, Nrp may have independent intracellular signaling capabilities. The Nrp intracellular domain contains three critical C-terminal amino acids that constitute a PDZ domain-binding motif, allowing Nrps to bind to PDZ domain proteins such as GAIP interacting protein, C terminus (GIPC; Cai & Reed 1999). This PDZ domain-binding motif may provide a mechanism for Nrp to directly transduce intracellular signaling.

Consistent with roles of Nrps in axon guidance and angiogenesis, *Nrp1* mutant mice die by E12.5-E13.5 with severe abnormalities in axon path finding and vascular defects (Kawasaki et al. 1999). *Nrp2* mutants survive to adulthood with less severe axon pathfinding and vascular phenotypes (Giger et al. 2000; Chen et al. 2000; Yuan et al. 2002). It is worth noting that *Nrp1* and *Nrp2* mutants display axon guidance defects in an overlapping but distinct set of nerves. *Nrp1/2* double-mutants die earlier than either

single mutant at E8.5, with a more severe abnormal vascular phenotype than either single knock-out mouse (Takashima et al. 2002). Consistent with the characterization of *Nrp* mutant mice, the expression patterns of *Nrp1* and *Nrp2* are overlapping yet distinct in the developing embryo (Chen et al. 1997). Together, these observations suggest Nrp1 and Nrp2 protein function is partially redundant in mammalian development.

Nrp and Hh Signaling in Development and Disease

Nrp1 and Nrp2 have been identified as positive regulators of Hh signal transduction in an RNAi screen (Hillman et al. 2011). Hillman and colleagues (2011) show siRNA targeting *Nrp1* and *Nrp2* block the ability of SL2 cells to respond to Shh ligand or SAG as measured by multiple readouts for pathway activation. *Nrp1* and *Nrp2* are only partially redundant in this context as targeting both genes simultaneously provides the greatest inhibition of pathway stimulation. In addition, Hillman et al. (2011) report that two non-overlapping morpholinos targeting *nrp1a*, a Zebrafish *Nrp* homolog, result in Zebrafish phenotype consistent with Hh loss of function. This provides *in vivo* evidence for conserved role of Nrp in Hh signaling from bony fish to mammals.

A role for Nrps in Hh signaling is consistent with *Nrp* expression patterns in areas where Hh signaling is important during mouse embryonic development. These locations include the spinal cord, limb bud, and yolk sac. *Nrps* are expressed in the ventral spinal cord at E10.5, a time when the ventral spinal cord cells are responsive to Shh ligand. In addition to its role as a morphogen in the developing spinal cord, Shh also has a role in axon guidance as a chemoattractant for commissural neurons projecting to the floor plate (Charron et al. 2003). After exposure to Shh ligands and having crossed the ventral midline, axons then become sensitive to Sema3 ligands, which bind Nrp2;

Sema3/Nrp2/Plexin signaling repels the axons, preventing them from doubling back into the floor plate or recrossing the midline (Zou et al. 2000). Shh signaling from the floor plate activates the responsiveness of crossing axons to Sema3s so they become newly sensitive to Sema3 repulsion after crossing (Parra & Zou 2010). This sequential sensitivity to Shh and Sema3 ligands may indicate cross-talk between the two signaling pathways.

Nrps are expressed in the developing limb bud where Shh signaling is vital for digit patterning (Kitsukawa et al. 1995; Chen et al. 1997). In its role in patterning digits, Shh signaling is needed to inhibit the formation of Gli3R (reviewed in Bastida & Ros 2008). In Shh-deficient limb buds, Gli3R gene repression results in a loss of digits; $Gli3^{-/-}$ limbs are polydactyllous (Hui & Joyner 1993; Chiang et al. 1996; Litingtung et al. 2002). Interestingly, chimera mice constitutively overexpressing exogenous *Nrp1* also display extra digits (Kitsukawa et al. 1995). The overlap of expression patterns and similarity of phenotypes suggest that Shh and Nrp signaling could interact in digit formation.

The murine embryonic visceral yolk sac is a third location of active Hh signaling where *Nrps* are expressed and play a role in embryonic development (Hillman et al. 2011). *Ihh* and *Ptch1* expression patterns and yolk sac phenotypes from $Ihh^{-/-}$ and $Smo^{-/-}$ embryos demonstrate a role for Hh signaling in yolk sac vessel remodeling (Farrington et al. 1997; Maye et al. 2000; Byrd et al. 2002). *Nrp1/2* double-mutants also display errors in yolk sac vasculogenesis (Takashima et al. 2002).

Finally, a recent paper has linked Nrp1 and Shh in MB (Snuderl et al. 2013). Placental Growth Factor (PGIF), a member of the VEGF family, promotes growth and

survival of tumor cells through Nrp1 signaling. Snuderl and colleagues (2013) report that placental growth factor (PlGF) is expressed by tumor and stromal cells and that PlGF in the stroma is produced in response to Shh ligand secreted from the tumor. While the exact role of PlGF in tumor growth is unclear, these studies suggest combined Shh and PlGF inhibition might represent a new target therapy for MB.

In this chapter, we show Eya1 is a positive regulator of Hh signal transduction. Motivated by our RNAi screen results and previous studies linking Eya and Hh in disease and development, we investigate the effect of Eya1 knock-down on the ability of SL2 cells to respond to Hh pathway stimulation. We show that knock-down of *Eya1*, as well as knock-down of its co-factor and fellow RDGN-member, *Six1*, block the induction of Hh response genes. Furthermore, we provide evidence that Eya1 and Six1 act on the Hh pathway by regulating the transcription of *Nrp1* and *Nrp2*. Furthermore, we show that Eya1 and Six1 act within the Hh signaling pathway downstream of Smo and at or above the level of Sufu.

Results

Eya1 Blocks Hh Pathway Stimulation

To pursue Eya1 as an important regulator of Hh signaling, we first verified that *Eya1* shRNAs efficiently knock-down their target and block the ability of SL2 cells to respond to Hh pathway activation.

We confirmed that *Eya1* and *Smo* shRNAs knock-down their target mRNAs by quantitative real-time PCR (qRT-PCR; Figure 3.1a-b). In these experiments we use shRNA targeting *LacZ* as a negative control because SL2 cells do not express *LacZ*; we use shRNA targeting *Smo* as a positive control because Smo is a potent positive regulator of Hh signaling.

Unfortunately, Eya1 antibodies are unable to detect endogenous Eya1 protein (data not shown). Therefore, to ensure shRNAs targeting *Eya1* reduce Eya1 at the protein level, we tested the ability of shRNAs to reduce levels of overexpressed Eya1 protein. Co-expression of a full-length *Eya1* construct with an shRNA targeting *Eya1* results in reduced levels of Eya1 protein in SL2 cells. Co-expression of an shRNA targeting *Eya2* has no effect on Eya1 protein in these cells (Figure 3.1c). Similarly, co-expression of an HA-tagged recombinant *Eya1*construct with either of two additional shRNAs targeting *Eya1* reduces levels of HA-tagged Eya1 (Figure 3.1d). These data show that shRNAs targeting *Eya1* mRNA successfully reduce Eya1 protein levels.

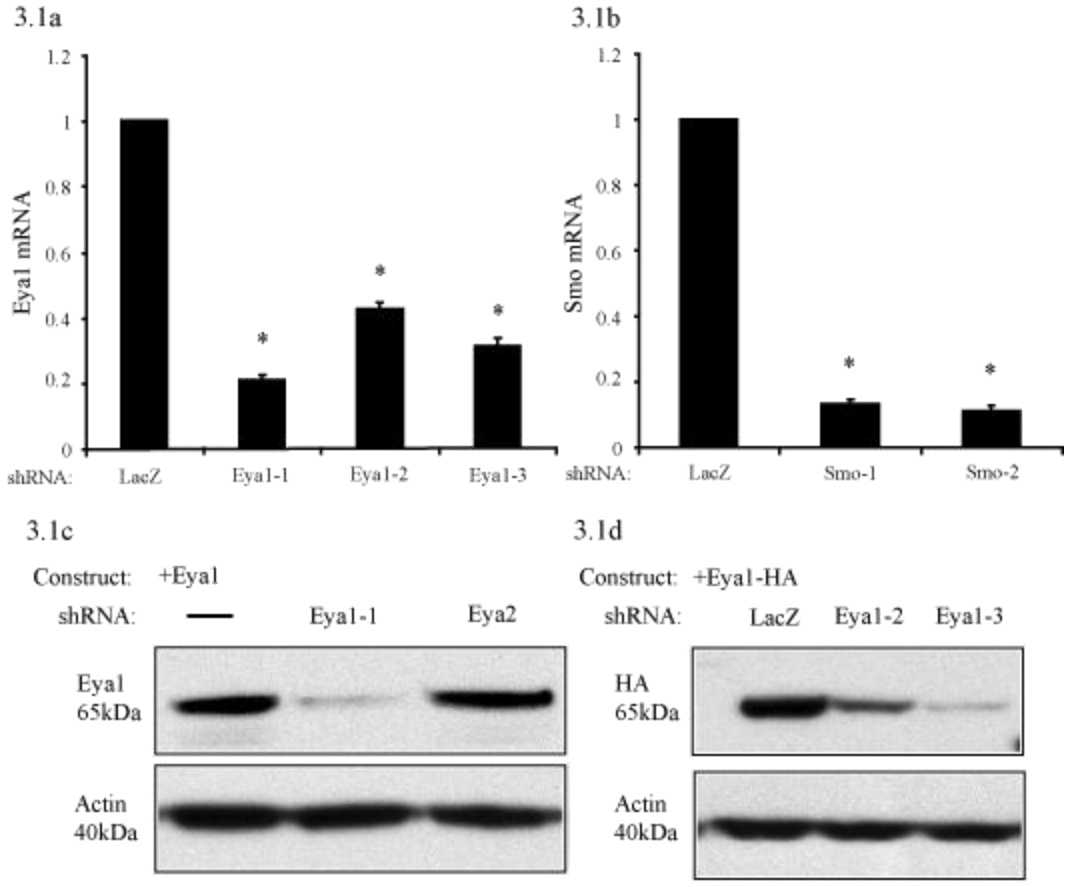

Figure 3.1 *Eya1* and *Smo* shRNAs successfully knock-down their targets. A) Three shRNAs targeting *Eya1* (Eya1-1, Eya1-2, Eya1-3) successfully knock-down *Eya1* in SL2 cells, normalized to GAPD levels and an shRNA targeting *LacZ* (N=7-10). **B)** Two shRNAs targeting *Smo* (Smo-1, Smo-2) successfully knock-down *Smo* in Sl2 cells normalized to GAPD levels and an shRNA targeting *LacZ* (N=2-4). Z-test; *p<0.01; error bars = SEM. **C)** shRNA targeting *Eya1* (Eya1-1) reduces levels of overexpressed Eya1 when co-transfected in 293T cells; an shRNA targeting *Eya2* (Eya2) does not lower levels of Eya1 protein. **D)** Two additional shRNAs targeting *Eya1* (Eya1-2, Eya1-3) reduce levels of recombinant HA-tagged Eya1 when co-transfected in 293T cells.

Having verified *Eya1* shRNAs knock-down their target, we confirmed our preliminary RNAi screen results using lentivirus generated in our lab. We measured the effect of shRNAs targeting *Eya1* in SL2 cells after stimulation with SAG using multiple read-outs for Hh pathway activation.

In agreement with our screening results, we found *Eya1* shRNAs have the ability to block SAG induction of Gli-responsive F luciferase in SL2 cells normalized to R luciferase (Figure 3.2a). Because the F/R luciferase signal is an artificial reporter of Hh pathway activation, we next looked at the induction of endogenous *Gli1* gene expression in SL2 cells following *Smo* or *Eya1* knock-down at the mRNA and protein levels. We found the induction of SAG-induced *Gli1* gene expression is blocked by shRNAs targeting *Eya1* as measured by qRT-PCR and by western blot (Figure 3.2b-d). The induction of a second Hh-response gene, *Ptch1* (Goodrich et al. 1996), is also blocked by *Smo* and *Eya1* shRNAs (Figure 3.2e). Importantly, the induction of *c-fos* in SL2 cells by serum following a period of serum starvation (Johansen & Prywes 1994) is not blocked by shRNAs targeting *Eya1* (Figure 3.2f). Therefore, *Eya1* shRNAs do not impair transcriptional activation generally; the effect of *Eya1* shRNAs on Hh-responsive gene induction is specific.

Figure 3.2 *Eya1* knock-down blocks Hh-responsive gene induction. Fold stimulation by SAG (SAG/veh). **A)** shRNAs targeting *Eya1* block induction of F/R luciferase in response to SAG, normalized to an shRNA targeting *LacZ* (N=2-4). **B)** shRNAs targeting *Eya1* block SAG-mediated induction of endogenous *Gli1* mRNA by qRT-PCR, normalized to GAPD levels and an shRNA targeting *LacZ* (N=5). **C)** SAG-induced increases in endogenous Gli1 protein are blocked by shRNAs targeting *Eya1*. **D)** Quantification of western blots showing a decrease in Gli1 protein induction, normalized to actin levels and an shRNA targeting *LacZ* (N=7-8). **E)** shRNAs targeting *Eya1* block SAG-mediated induction of endogenous *Ptch1* mRNA by qRT-PCR, normalized to GAPD levels and an shRNA targeting *LacZ* (N=5). **F)** *c-fos* gene expression is induced by serum stimulation following a period of serum starvation. shRNAs targeting *Eya1* do not block induction of *c-fos* mRNA following serum stimulation by qRT-PCR, normalized to GAPD levels and an shRNA targeting *LacZ* (N=5). This demonstrates Eya1 is not required for general transcriptional activation in SL2 cells. Z-test, *$p<0.01$; error bars = SEM.

Figure 3.2 (continued):

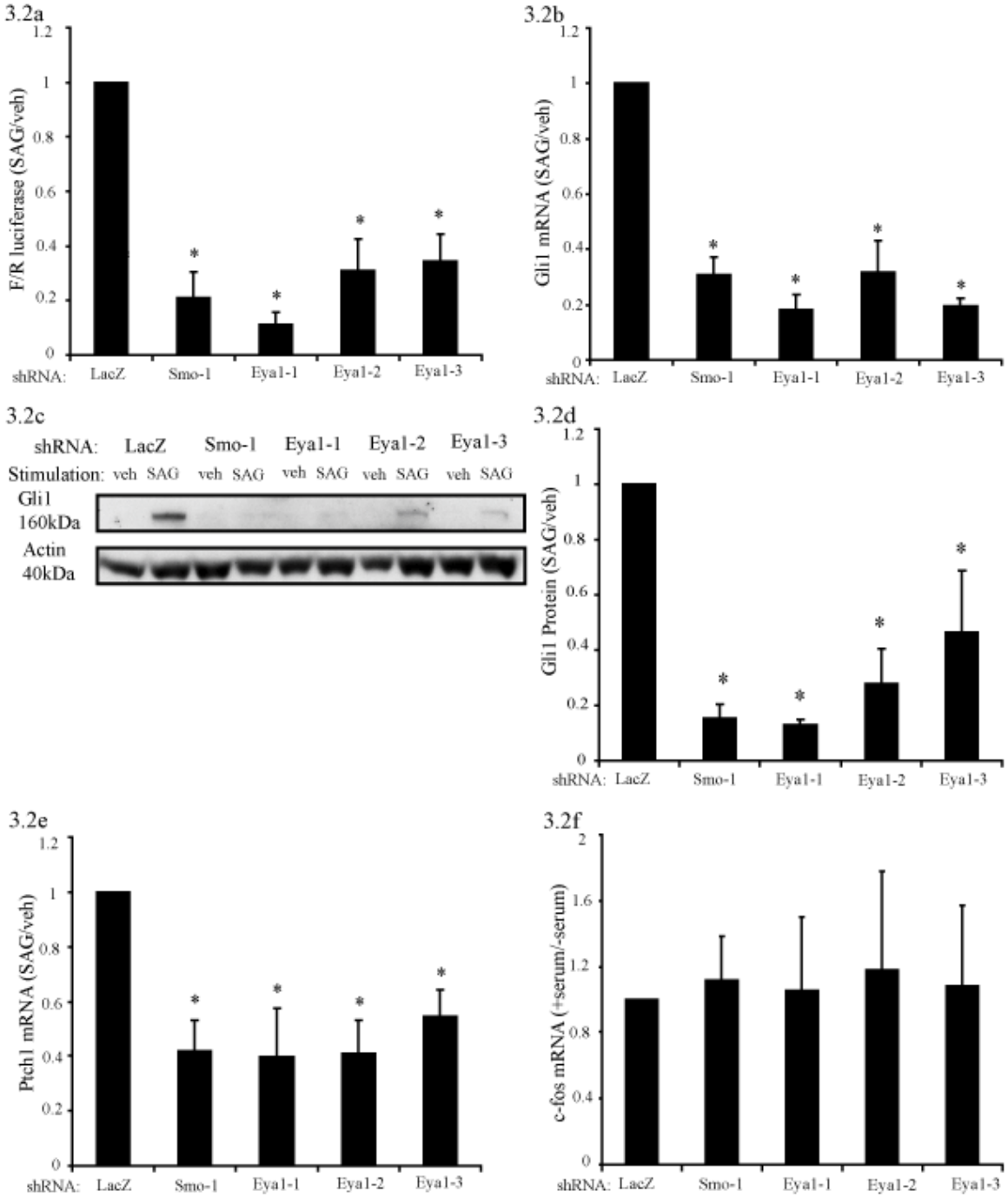

Eya1 Does Not Influence Hh Pathway Activation through H2AX Dephosphorylation

Eya1 is a tyrosine phosphatase and serves as a co-transcriptional factor with other members of the RDGN. To investigate the mechanism by which Eya1 regulates Hh signal transduction, we considered the possibilities that Eya1 modulates the pathway as a phosphatase and/or in concert with members of the RDGN as a co-transcription factor.

One hypothesis explaining the requirement of Eya1 for Hh pathway stimulation is that Eya1 dephosphorylates a substrate in the pathway required for pathway activation. To test this hypothesis, we began by looking broadly for potential Eya1 substrates in SL2 cells by assaying for proteins with a change in tyrosine phosphorylation status following *Eya1* knock-down. We applied shRNAs targeting *Eya1* to SL2 cells and probed protein lysate with 4G10, an antibody that detects protein tyrosine phosphorylation. We then looked for a difference in the pattern of phosphorylation by western blot to identify changes in protein phosphorylation status. We observed increased phosphorylation of a protein around 15kDa following *Eya1* knock-down (Figure 3.3a). We hypothesized that this band represented the tyrosine phosphorylation H2AX a protein of that size and a reported Eya substrate (Krishnan et al. 2009).

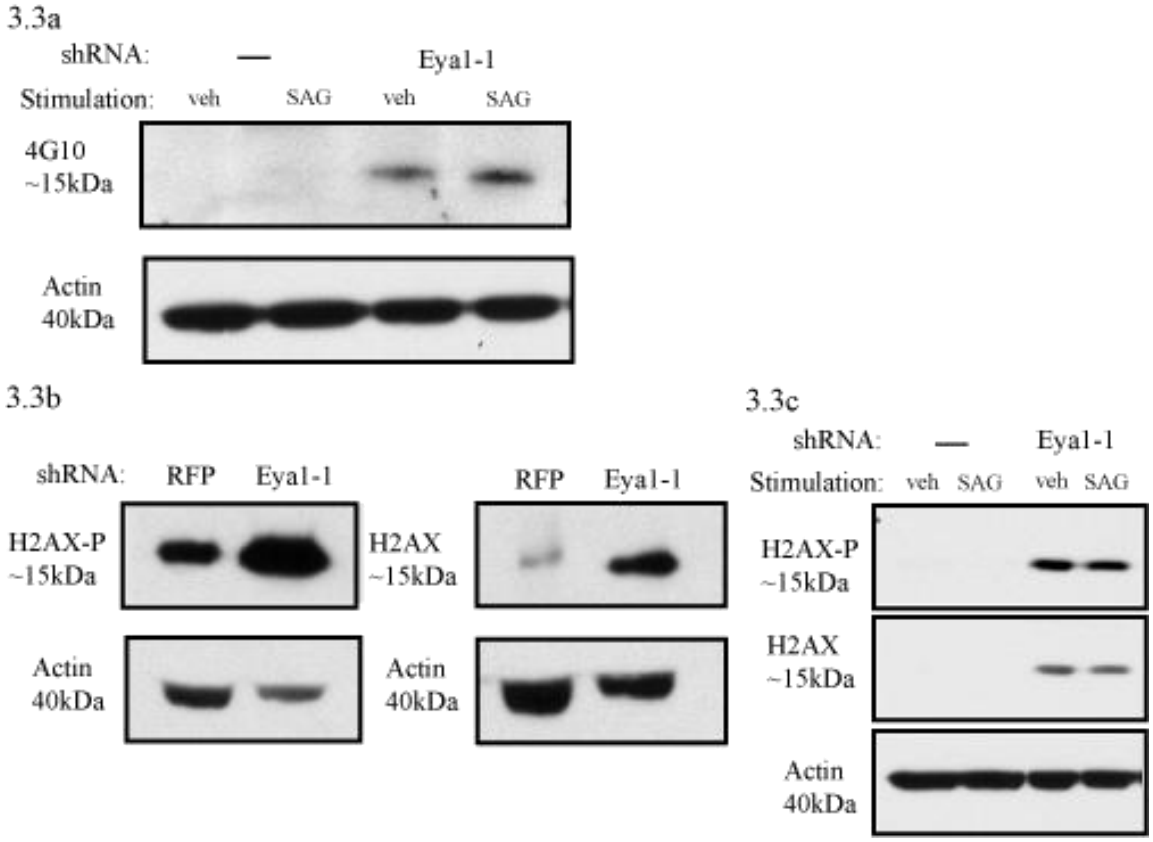

Figure 3.3 Eya1 dephosphorylates H2AX independently of its role regulating Hh signal transduction. **A)** A ~15kDa protein is phosphorylated following *Eya1* knock-down as indicated by 4G10, an antibody which recognizes protein tyrosine phosphorylation. **B)** *Eya1* knock-down results in higher levels of phosphorylated H2AX and higher levels of total H2AX protein in SL2 cell lysate as compared to H2AX levels in cells treated with a negative control shRNA targeting *RFP*; RFP is not expressed in SL2 cells. **C)** H2AX dephosphorylation and total protein levels are not modulated by Shh pathway stimulation by SAG.

H2AX is phosphorylated in response to DNA double-stranded breaks at Ser-139, then referred to as γ-H2AX. γ-H2AX recruits DNA repair machinery to the double-stranded break to promote cell survival. H2AX is constitutively phosphorylated at a tyrosine residue which is dephosphorylated by Eya1/3; dephosphorylation of this tyrosine residue by Eya1/3 following DNA double-stranded breaks promotes the DNA repair response and cell survival (reviewed in Dickey et al. 2008). Using an antibody recognizing H2AX phosphorylation at either or both phosphorylation sites, we found direct evidence that knock-down of *Eya1* increases H2AX phosphorylation, consistent with our 4G10 data and published roles of Eya1 in H2AX dephosphorylation (Figure 3.3b). Interestingly, an antibody recognizing total H2AX independent of phosphorylation or ubiquitination status indicates that Eya1 may also regulate total H2AX protein levels, which is, to our knowledge, a novel function of Eya1 (Figure 3.3b). By qRT-PCR, *Eya1* shRNAs did not alter H2AX expression, indicating decreased H2AX protein is the consequence of post-transcriptional protein regulation (data not shown).

While interesting, the role of Eya1 in H2AX dephosphorylation appears to be independent of its role as a regulator of Hh signaling. Pathway stimulation by SAG did not affect the phosphorylation status of H2AX or alter the effect of *Eya1* knock-down on H2AX phosphorylation (Figure 3.3c). We also did not find evidence that Hh pathway stimulation or *Eya1* knock-down alters the ubiquitination status of H2AX (data not shown). These results suggest Eya1 is not regulating the Hh signaling pathway via H2AX.

We next investigated a second hypothesis that Eya1 impinges upon the Hh pathway by regulating gene transcription as a transcriptional co-factor, potentially in concert with other members of the RDGN.

Six1, an Eya1 Co-factor, Regulates Hh Signal Transduction

To investigate whether other members of the RDGN are required for Hh signaling, we obtained shRNAs targeting *Six1, Six2, Six4, Six5,* and *Dach2* provided by the Broad Institute RNAi Consortium. When co-transfected with *Six1-2* or *Six4-5*, Eya and Six proteins form complexes and translocate to the nucleus to activate gene transcription (Ohto et al. 1999; Zhang et al. 2004b). Eya and Dac are thought to bind directly in *Drosophila* eye development and activate gene transcription. We did not include shRNAs targeting *Six3* or *Six6* because these members of the Six protein family are not known to bind Eya proteins and serve as transcriptional co-factors.

Before testing the effect of these shRNAs on Hh pathway activation, we first measured the efficiency of target knock-down by qRT- PCR. Two shRNAs targeting *Six1* and three shRNAs targeting *Six4* showed significant knock-down of their targets (Figure 3.4a). We also verified *Six1* knock-down by *Six1* shRNAs at the protein level (Figure 3.4c-d). We were unable to detect *Six2* expression in SL2 cells (data not shown). Given these results, we tested the effects of *Six1* and *Six4* shRNAs on Hh pathway stimulation in SL2 cells using F/R luciferase values as a readout for pathway activation. *Six1* shRNAs, but not *Six4* shRNAs, block Hh pathway induction (Figure 3.4b). These results raise the possibility that Eya1 may be working with Six1 to regulate Hh signal transduction.

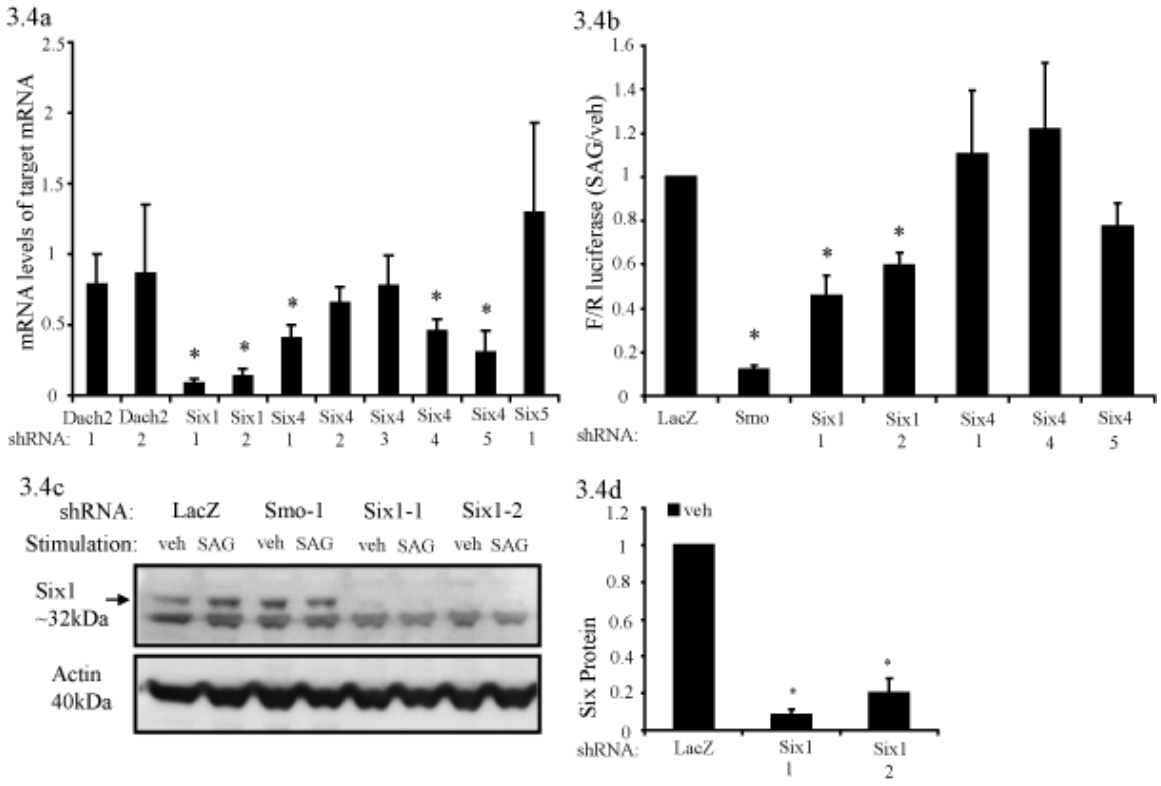

Figure 3.4 Six1, an Eya1 co-factor and RDGN member blocks Hh pathway activation. A) shRNAs targeting *Dach2* (Dach2-1, Dach2-2), *Six1* (Six1-1, Six1-2), *Six4* (Six4-1, Six4-2, Six4-3, Six4-4, Six4-5), and *Six5* (Six5-1) were tested for their ability to knock-down their targets. Two *Six1* shRNAs (Six1-1 and Six1-2) and three *Six4* shRNAs (Six4-1, Six4-4, Six4-5) showed significant knock-down of their targets, normalized to GAPD levels and an shRNA targeting *LacZ* (N=3-6). **B)** shRNAs targeting *Six1* block fold induction F/R luciferase (SAG/veh) in SL2 cells. shRNAs targeting *Six4* have no effect on F/R luciferase values in response to SAG, normalized to GAPD levels and an shRNA targeting *LacZ* (N=3). **C)** shRNAs targeting *Six1* reduce Six1 protein levels. **D)** Western blot quantification of Six1 protein in unstimulated (veh) cells, normalized to actin levels and an shRNA targeting *LacZ* (N=3-6). Z-test, *p<0.01; error bars = SEM.

We next verified that *Six1* shRNAs block endogenous *Gli1* gene induction following pathway activation. Two independent shRNAs targeting *Six1* block the induction of *Gli1* mRNA and Gli1 protein following SAG stimulation by qRT-PCR and western blot (Figure 3.5a-c). Notably, *Six1* knock-down and *Eya1* knock-down block SAG-induced *Gli1* induction to similar extents. In addition, knocking down *Eya1* and *Six1* simultaneously in SL2 cells does not produce a greater effect than knocking-down either gene alone (data not shown). Together, these data are consistent with a model whereby Eya1 works in concert with its co-factor Six1 to regulate Hh pathway activation in SL2 cells.

Eya1 and Six1 Act in the Hh Signaling Pathway Between Smo and Sufu

Genetic epistasis experiments reveal the sequential order of elements within a signaling pathway from ligand reception to gene induction. To help uncover the molecular mechanism by which Eya1 and Six1 regulate Hh signaling, we investigated where along the pathway they influence pathway activation.

At the top of the Hh signaling pathway, Hh ligands bind Ptch1, which relieves inhibition of Smo, resulting in pathway activation. As shown previously, Eya1 and Six1 are necessary for Shh and SAG-mediated induction of the pathway. Because SAG is a Smo agonist, activating the pathway downstream of Hh binding to Ptch1 and downstream of Ptch1 disinhibition of Smo, Eya1 and Six1 are not necessary for ligand reception or Smo activation and must act below the level of Smo in the pathway.

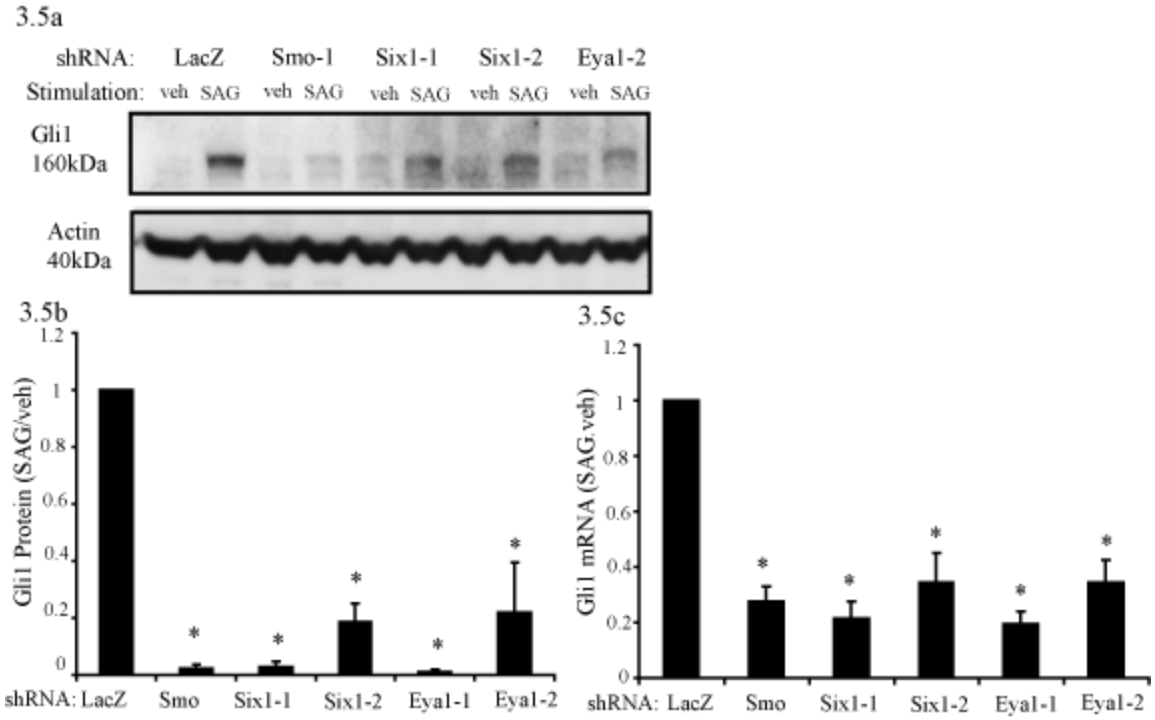

Figure 3.5 Six1 regulates Hh signal transduction. A) shRNAs targeting *Six1* block Gli1 protein induction by SAG stimulation. **B)** Western blot quantification of Gli1 protein induction (SAG/veh), normalized to actin levels and an shRNA targeting *LacZ* (N=3-6). **C)** shRNAs targeting *Six1* block *Gli1* mRNA induction (SAG/veh), normalized to GAPD levels and an shRNA targeting *LacZ* (N=4-5). Z-test, *p<0.01; error bars = SEM.

The primary cilia is a microtubule-based organelle essential for Hh signaling and is needed for Smo activation *in vivo* (Corbit et al. 2005; reviewed in Ruat et al. 2012). In cultured cells, mutations in genes important for cilia development and maintenance result in Hh signaling deficits (Ocbina & Anderson 2008). In addition, previous RNAi screens for Hh pathway regulators have identified genes that disrupt Hh signal transduction through disrupting primary cilia (Evangelista et al. 2008). For these reasons, it is important to test for an effect of Eya1 on cilogenesis. Staining for γ-tubulin, which marks basal bodies at the base of cilia, and for acetylated-α-tubulin, which marks the ciliary axoneme, we conclude that *Eya1*$^{-/-}$ cells along the neural tube of E10.5 embryos develop cilia (Figure 3.6). Therefore, *Eya1* is not necessary for cilogenesis.

Sufu is a negative regulator of the Hh signaling pathway downstream of Smo activation. Sufu can bind all three Gli transcription factors (Humke et al. 2010; Pearse et al. 1999) and inhibits the Hh pathway by simultaneously keeping Gli activators from the nucleus and promoting the formation of GliR. Loss of Sufu is sufficient for ligand-independent activation of the pathway (Cooper et al. 2005). To test if Eya1 and Six1 are acting at or downstream of Sufu, we activated the Hh pathway by knocking-down *Sufu* in SL2 cells by RNAi. We then asked whether *Eya1* and *Six1* knock-down could reduce the heightened pathway activation in these cells. If Eya1 and Six1 are acting at the level of or downstream of Sufu, we would expect to see a decrease in elevated *Gli1* expression. If, however, Eya1 and Six1 exert their influence on the pathway upstream of Sufu, we would expect to see no effect of *Eya1* and *Six1* shRNAs on heighted levels of *Gli1* expression.

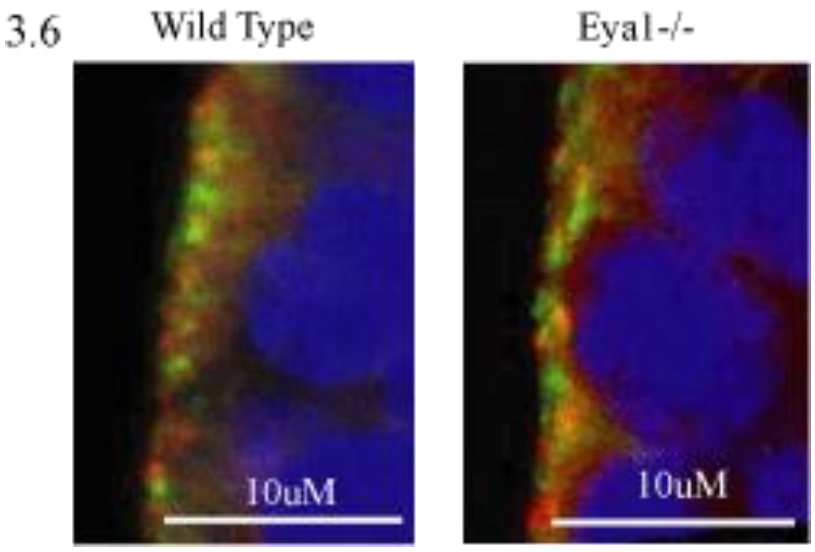

Figure 3.6 *Eya1*$^{-/-}$ neural tube ventricles are ciliated. E10.5 wild type and *Eya1*$^{-/-}$ neural tube stained with γ-tubulin (red) to mark basal bodies at the base of cilia and acetylated-α-tubulin (green) to mark ciliary axoneme. Nuclei are marked by DAPI (blue). Primary cilia project into the ventricle of the neural tube (Chamerlain et al. 2008). The proximity of γ-tubulin and acetylated-α-tubulin in the ventricles indicate the presence of primary cilia.

We generated a stable SL2 cell line with *Sufu* knock-down by infecting SL2 cells with lentivirus encoding *Sufu* shRNA and selecting for infection. *Sufu* knock-down (*Sufu* KD) cells have reduced Sufu protein levels (Figure 3.7a). As expected, *Sufu* KD cells demonstrate elevated basal levels of Hh pathway activation indicated by increased levels of Gli1 protein in the absence of Shh or SAG stimulation (Figure 3.7a, lanes 1 and 5). Upon SAG stimulation, levels of Gli1 are increased further (Figure 3.7b, lanes 1 and 2).

Eya1 and *Six1* shRNAs fail to reduce elevated basal levels of *Gli1* in unstimulated cells by western blot and qRT-PCR, demonstrating that Eya1 and Six1 are not required for pathway activation downstream of Sufu (Figure 3.7c-d). However, Eya1 is still required for SAG-dependent pathway activation (Figure 3.7b). These data strongly suggest that Eya1 and Six1 function upstream or at the level of Sufu to regulate Hh signaling activity.

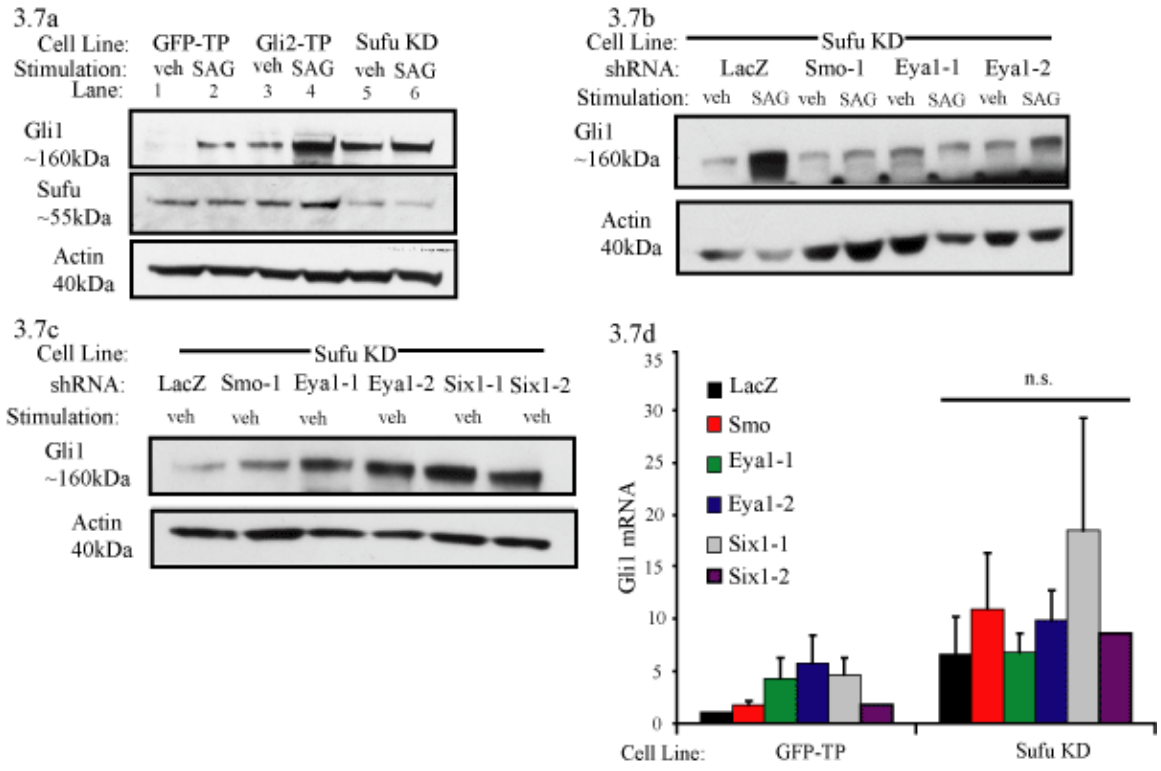

Figure 3.7 Eya1 and Six1 act in the Hh signaling pathway upstream of Sufu. A) Stable cell lines with *Sufu* knock-down (Sufu KD) or Gli2 overexpression (Gli2-TP) have elevated levels of Gli1 protein in unstimulated (veh) cells relative to veh cells stably overexpressing GFP (GFP-TP; see lanes 1, 3, 5). Sufu KD cells have lower levels of Sufu protein. **B)** *Eya1* and *Six1* shRNAs block SAG-dependent Gli1 induction in Sufu KD cells. **C)** In Sufu KD cells (veh), *Eya1* and *Six1* shRNAs do not reduce heightened Gli1 protein levels. **D)** *Eya1* and *Six1* shRNAs do not reduce heighted basal *Gli1* mRNA in Sufu KD cells relative to GFP-TP cells by qRT-PCR, normalized to GAPD levels and an shRNA targeting *LacZ* in the GFP-TP cell line (N=1-5). By Student's t-test, there is no significant (n.s.) difference in *Gli1* expression among the knock-down conditions of the Sufu KD cell line; error bars = SEM.

Gli2 is the primary transcriptional activator mediating the output of Hh signaling and *Gli2* overexpression is sufficient for ligand-independent activation of the pathway (Grachtchouk et al. 2000). To check if Eya1 and Six1 are necessary for Gli2-mediated gene transcription in response to Hh pathway stimulation, we asked whether *Eya1* and *Six1* knock-down block pathway activation in cells with *Gli2* overexpression.

To test this, we generated stable cell lines overexpressing *Gli2* or *GFP* by transfecting SL2 cells with transposons carrying *Gli2* and *GFP* (Gli2 TP cells) or GFP alone (GFP TP). Gli2 TP and GFP TP cells express GFP, confirming TP are present (Figure 3.8a). Gli2 TP cells also have elevated levels of Gli2 protein (Figure 3.8a). Importantly, Gli2 TP cells show elevated basal levels of Gli1 as compared to cells overexpressing GFP alone (Figure 3.7a, lanes 1 and 3). *Eya1* and *Six1* shRNAs do not reduce the increased basal levels of Gli1 by western blot or qRT-PCR (Figure 3.8b-c). These data show that Eya1 and Six1 function upstream of Gli2 activity to regulate Hh signaling activity, consistent with our model that Eya1 and Six1 impact Hh signaling between Smo and Sufu.

As Eya1 and Six1 are co-transcriptional activators, we felt it was important to test whether they function as part of a bigger transcriptional complex with Gli1 or Gli2. While we were able to replicate previous reports of Eya1 and Six1 forming a complex *in vitro*, co-transfecting *Eya1* and *Six1* constructs alone or together with either *Gli1* or *Gli2* constructs failed to demonstrate binding between Eya1/Six1 and Gli transcription factors in 293T cells (data not shown).

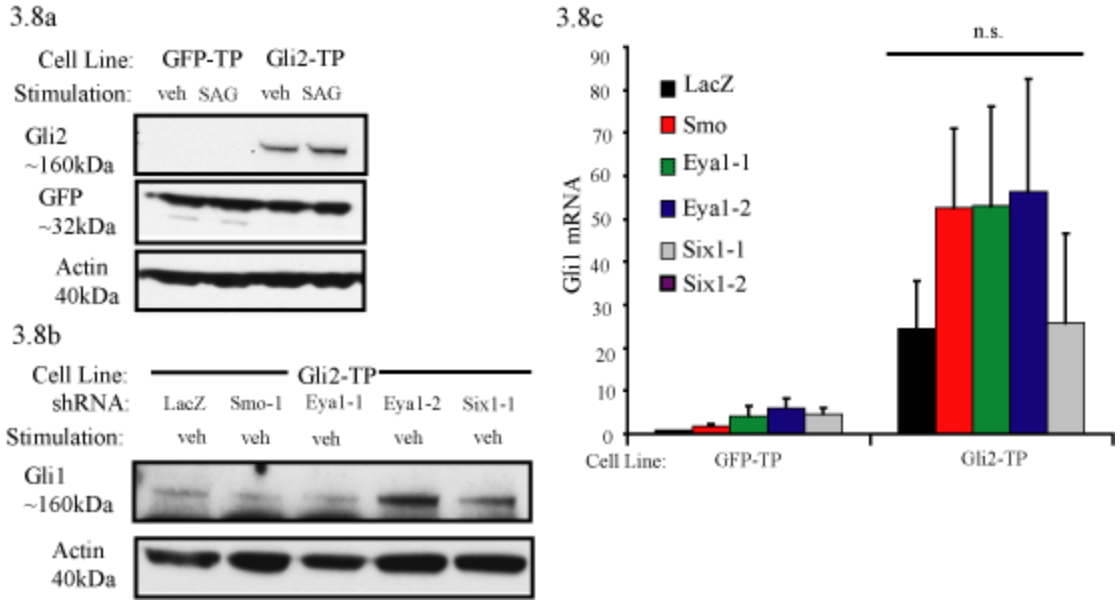

Figure 3.8 Eya1 and Six1 act in the Hh signaling pathway upstream of Gli2A. A) Gli2-TP cells overexpress Gli2; GFP-TP and Gli2-TP cells express GFP. **B)** *Eya1* and *Six1* shRNA do not reduce heightened Gli1 protein levels in unstimulated (veh) Gli2-TP cells. **C)** shRNAs targeting *Eya1* or *Six1* do not reduce heighted *Gli1* mRNA in Gli2-TP cells relative to GFP-TP cells by qRT-PCR, normalized to GAPD levels and an shRNA targeting *LacZ* in the GFP-TP cell line (N=1-5). By Student's t-test, there is no significant (n.s.) difference in *Gli1* expression among the knock-down conditions in the Gli2-TP cell line; error bars = SEM.

Eya1 is not Required for SAG-Induced Gli3R Inhibition

In the absence of Hh stimulation, full-length Gli3 is proteolytically processed into an 83kDa amino terminal fragment, Gli3R, which is the primary transcriptional repressor of the pathway (Wang et al. 2000). Hh stimulation is important to promote Gli2-mediated gene activation as well as to inhibit Gli3R-mediated gene repression. Eya1 is required for Shh and SAG-induced GliA activity. To investigate whether Eya1 is necessary for SAG-induced inhibition of Gli3R, we examined Gli3 processing after *Eya1* knock-down in SL2 cells.

As expected, knock-down of *Smo* prevents the ability of SAG to inhibit Gli3R formation. Interestingly, we find SAG is able to inhibit Gli3R formation following *Eya1* knock-down (Figure 3.9a-b). These data suggest that Eya1 is required specifically for GliA function and not for the inhibition of Gli3R formation. A similar dissociation between Gli2 and Gli3 regulation was also observed after knock-down of *Nrp1* and *Nrp2* (Hillman 2010) and has been reported in *Arl13b* mutants (Caspary et al. 2007). As much is still unknown about Gli transcription factor regulation, the discovery of factors that uncouple their regulation may provide valuable mechanistic insight.

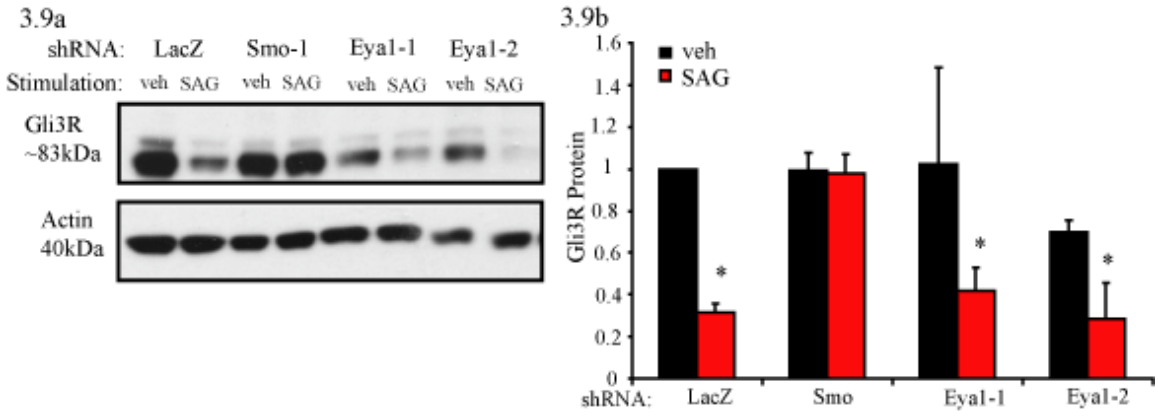

Figure 3.9 Eya1 is not required for SAG-mediated Gli3R inhibition. A) SAG stimulation inhibits Gli3R formation. *Smo* knock-down blocks the inhibition of Gli3R formation whereas *Eya1* knock-down does not. **B)** Western blot quantification of Gli3R, normalized to actin levels and an shRNA targeting *LacZ* in the unstimulated (veh) condition (N=3). Z-test, *p<0.01, error bars = SEM.

Eya1 and Six1 Regulate Positive Regulators of Hh Signaling, *Nrp1 and Nrp2*

There are very few known factors acting in the Hh signaling pathway between Smo and Sufu. Nrp1 and Nrp2, however, are reported positive regulators of Hh signaling downstream of Smo and upstream of Sufu (Hillman et al. 2011). Additionally, in agreement with our data, Nrp1 and Nrp2 appear to be necessary for GliA activity but not for the inhibition of Gli3R formation (Hillman 2010).

Given the similarity between these data and our own, we hypothesized that Eya1 and Six1 regulate Hh signaling through regulating *Nrp* expression. In fact, we find knock-down of *Eya1* and *Six1* result in reduced *Nrp1* and *Nrp2* expression by western blot and qRT-PCR (Figure 3.10). These data suggest Eya1 and Six1 regulate Hh signaling at least partially through the regulation *Nrp1* and *Nrp2* expression.

Figure 3.10 Eya1 and Six1 regulate *Nrp* expression. A) shRNAs targeting *Eya1* and *Six1* reduce Nrp1 and Nrp2 protein levels. **B)** Western blot quantification of Nrp1 in unstimulated (veh) conditions; normalized to actin levels and an shRNA targeting *LacZ* (N=1 or 4). **C)** Western blot quantification of Nrp2 in unstimulated (veh) conditions; normalized to actin levels and an shRNA targeting *LacZ* (N=3). **D)** shRNAs targeting *Eya1* and *Six1* reduce *Nrp1* mRNA, normalized to GAPD levels and an shRNA targeting *LacZ* (N=3-6). **E)** shRNAs targeting *Eya1* and *Six1* reduce *Nrp2* mRNA, normalized to GAPD levels and an shRNA targeting *LacZ* (N=2-5). Z-test, *$p<0.01$; error bars = SEM.

Figure 3.10 (continued):

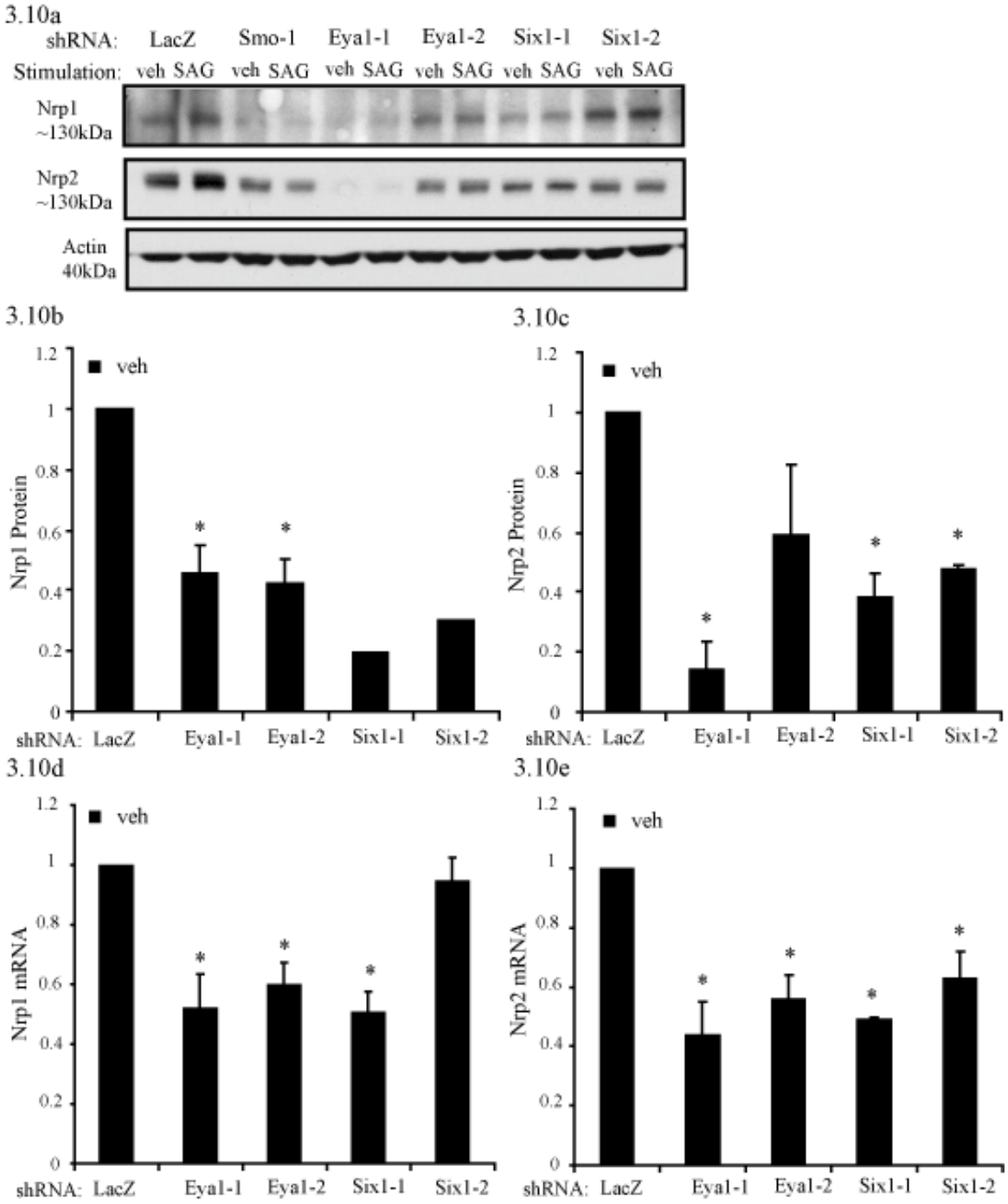

Eya1 May Contribute to MB Cell Growth

Eya1 is specifically up-regulated in the subtype of human MB that requires Shh signaling for survival (Kool et al. 2008; Northcott et al. 2011; Thompson et al. 2006). Given our data that Eya1 is required for maximal Hh signaling activation in SL2 cells, we asked whether Eya1 might also be required for survival in MB cells. Our lab has generated MB cell lines which retain Hh dependence *in vitro* (unpublished data). These cells are derived from the MB tumors of *Ptch1*$^{+/-}$ mice and are sensitive to Smo inhibitors, showing a decrease in Hh pathway activity shortly before dying (data not shown). Using this cell line, we measured the effect of *Smo* and *Eya1* shRNA on cell survival using an MTS assay, a measure of cellular metabolic activity which reflects the number of viable cells in a 96-well dish. These MTS assays provide evidence that *Smo* shRNA and *Eya1* shRNA significantly decrease the number of viable cells as compared to *LacZ* shRNA (Figure 3.11a). Strikingly, the effect on cell survival of a shRNA targeting *Eya1* is similar to that of *Smo* knock-down.

Several cellular mechanisms regulate cell death and survival and it is possible that Eya1 is necessary for MB survival through a mechanism independent of Hh signaling. To support our hypothesis that *Eya1* knock-down kills MB cells as a result of lowering Hh pathway activation, we conducted qRT-PCR for *Gli1* after *Smo* and *Eya1* knock-down. While we did detect a decrease in *Gli1* mRNA levels following *Smo* and *Eya1* knock-down, these decreases were not significantly different from the negative control (Figure 3.11b). These preliminary data raise the intriguing possibility that Eya1 may be important for MB cell survival.

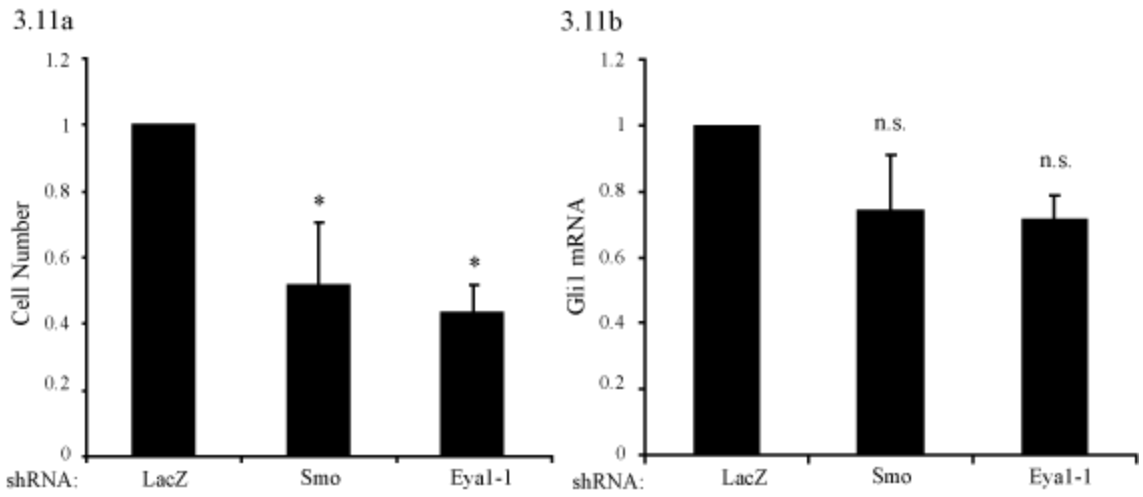

Figure 3.11 Eya1 may be important for MB cell survival. A) shRNAs targeting *Eya1* reduce the number of viable MB21 cells; normalized to LacZ (N=3). **B)** *Smo* and *Eya1* shRNA trend toward reducing *Gli1* mRNA in MB21 cells, normalized to GAPD levels and an shRNA targeting *LacZ* (N=4-5). Z-test, *p<0.01, not significant (n.s.); error bars = SEM.

Discussion

In this chapter we have demonstrated that Eya1 is needed for maximal response to Hh signaling *in vitro*. We have demonstrated the importance of Eya1 using multiple endogenous readouts of Hh-dependent gene transcription in SL2 cells, showing *Eya1* knock-down blocks the induction of multiple Hh response genes at the mRNA level and blocks Gli1 protein induction. In addition, an Eya1 co-factor, Six1 is also needed for maximal response to Hh signaling *in vitro*. These proteins, apparently acting as co-transcription factors, regulate the expression of Hh regulators, *Nrp1* and *Nrp2*, providing a mechanism by which Eya1 and Six1 exert their effect. According to our model, *Eya1* and *Six1* knock-down reduce *Nrp1* and *Nrp2* levels, impairing the ability of a cell to respond to Hh pathway stimulation.

Furthermore, we show Eya1 and Six1 act between Smo and Sufu within the Hh signaling pathway. These results are exciting because little is known about how Smo activation regulates Sufu activity and newly identified components between these two key players in the pathway are of great interest. Interestingly, while shRNAs targeting *Eya1* and *Six1* block SAG-induced gene induction, they do not block SAG-induced inhibition of Gli3R formation. These data suggest that Eya1 and Six1 are specifically needed to regulate Gli activator species, presumably mediated by Gli2, but are not involved in regulating Gli3R formation. This finding is notable as one of the few examples, along with *Nrp1+2* knock-down, of a pathway perturbation that disrupts Gli-mediated gene activation without also altering Gli-mediated gene repression.

Dissociation of Gli2 and Gli3 Following Pathway Activation

Primary cilia are required for Hh signal transduction, both for the activity of Gli activator forms as well as for generating Gli3R. Primary cilia depend on IFT proteins. As such, specific IFT protein mutants that lack cilia and are unresponsive to Hh ligands due to a lack of Gli transcriptional regulation (Houde et al. 2006; Huangfu et al. 2003; Liu et al. 2005; May et al. 2005; Tran et al. 2008). Mutants for *Arl13b*, however, display a loss of Gli2A modulation with normal Gli3R processing, uncoupling the regulation of these Gli proteins (Caspary et al. 2007). Arl13b is a small GTPase localized along the length of the cilia and mutants have shorter cilia. Caspary and colleagues (2007) suggest a model in which the creation of "high-level activator" Gli species and the release of these species to the nucleus require full-length cilia whereas Gli3 processing can occur normally in shortened *Arl13b* mutant cilia. While our data show cilia are present in embryonic *Eya1*$^{-/-}$ neural tubes, we cannot rule out the possibility that there are subtle differences in cilia length or function between *Eya1*$^{-/-}$ and wild type animals, which may account for the requirement of Eya1 for SAG-induced Gli2-mediated transcriptional activity but not for SAG-induced inhibition of Gli3R formation.

While it is clear that mutations resulting in altered cilia structure can affect processing of Gli proteins, Gli processing also requires proteins that do not play a role in cilia development. We propose a model in which Eya1 and Six1 are required specifically for Gli2 activation through *Nrp* gene regulation and hypothesize this is independent of ciliary structure.

Eya1 and MB

Activated Hh signaling causes cancer and positive regulators of the pathway serve as therapeutic targets. A subtype of MB caused by over-active Hh signaling is dependent on Hh signaling for survival. Our initial findings that *Eya1* shRNA induce MB cell death to a similar extent as *Smo* shRNA are very exciting. We show MB cells are dependent on Eya1 for survival and present the possibility that Eya1 could serve as a new therapeutic target.

One likely explanation for a weak effect on *Gli1* mRNA is poor knock-down of target mRNA by shRNA in these cells. Knock-down in MB cells is much less efficient in MB21 cells as compared to SL2 cells. In the MB21 cells, *Smo* shRNA and *Eya1* shRNA only provide around 50% knock-down compared to 87% and 79% in SL2 cells, respectively (data not shown).

While published data of *Eya1* up-regulation in human Shh-subtype of MB and our own data showing Eya1 is required for MB cell survival are promising, to pursue the role of Eya1 in MB, additional experiments are necessary.

Methods

Lentiviral Production

RNAi was achieved using lentivirus-delivered shRNA. shRNA constructs were provided by the Broad Institute RNAi Consortium as glycerol stocks in pLKO.1 vectors. Glycerol stocks were streaked on ampicillin-selective plates and a single colony was picked and grown in a culture of LB medium containing 50-100ug/ml ampicillin. DNA was prepared from bacterial cultures and purified using an EndoFree Plasmid Purification kit (Qiagen).

293T packaging cells were plated in 6cm tissue culture plates at 1.3-1.5x10^5 cells/ml (x6ml per plate) in "293T Growth Medium" (DMEM, 10% FBS, 1unit/ml penicillin, and 1ug/ml streptomycin). Cells were incubated for 1-2 days (37 °C, 5% CO_2), or until ~70-90% confluent. 293T cells in 6cm dishes were transfected with a mixture of shRNA-pLKO.1 vector (1ug), packaging plasmid (pCMV-dR8.9; 900ng), and envelope plasmid (VSV-G/pMD2.G; 100ng) using Fugene6 reagent (Promega; 6ul) following manufacturer's instructions. Cells were incubated for 18-20 hours and media was replaced with 6ml 293T Growth Medium. 24 hours later, media was collected and stored at 4°C. 24 hours later, a second collection of media was added to the first collection. After the final harvest, media containing virus was spun at 1250rpm for 5 minutes to pellet any packaging cells that were collected during harvesting. Virus was stored at -80°C. When virus was produced for use with MB21 cells, virus was collected in MB21 growth media (DMEM/F12, 1x B27 Supplement (Gibco # 17504044), 1unit/ml penicillin, and 1ug/ml streptomycin and streptomycin).

SL2-Derived Stable Cell Lines

To generate stable *Sufu* knock-down SL2 cells, SL2 cells were infected with lentivirus encoding shRNA targeting *Sufu*. Cells were selected for successful infection with 4ug/ml puromycin and were maintained in puromycin.

To generate SL2 cells stably overexpressing *GFP* and *Gli2*, SL2 cells were transfected in 10cm dishes using Fugene 6 (36ul). Cells were transfected with mouse *PiggyBac transposase* (6ug) and *transposon* (3ug) encoding *GFP* alone or *Gli2* and *GFP*. These constructs were generated by Xuesong Zhao in the Segal lab (unpublished data). Cells were selected for successful transfection with 4ug/ml puromycin and maintained in puromycin.

To generate SL2 cells stably overexpressing *Eya1*, the coding region of *Eya1* and an HA-tagged *Eya1* were cloned into a pLX303 lentiviral expression vector. pLX303 expressing *tdTomato* was provided by Xuesong Zhao (Segal Lab) as a negative control. Cells were infected with lentivirus encoding these expression vectors. Cells were selected for successful infection with 8ug/ml blastacin and maintained in blastacin.

To generate SL2 cells stably overexpressing *Nrp1*, cells were transfected using Lipofectatmine LTX & Plus Reagent (Invitrogen #15338100) according to manufacturer's protocol for "Transfecting Plasmid DNA into NIH3T3 Cells". *Pinco-mNrp1* was acquired from Addgene (#21937), deposited by Guido Serini (Valdembri et al. 2009).

293T Co-Transfection for Eya1 Protein Knock-Down

$1.2x10^5$ 293T cells were plated in 12-well dishes in 293T growth media. Two days later, cells were 70-90% confluent and were transfected using Fugene6 (3ul) and a mixture of two DNA constructs: an expression plasmid (1ug) and an shRNA (1ug). 18 hours later, the media was changed. 72 hours after transfection, cells were collected for protein.

Quantitative Real-Time PCR (qRT-PCR)

$6x10^4$ SL2 cells were plated with virus in 12-well tissue culture plates in SL2 growth media (DMEM, 10% calf serum, 1unit/ml penicillin, 1ug/ml streptomycin, 0.4mg/ml G418, and 0.15mg/ml zeocin); 10-30% of the total volume/well consisted of media containing virus. 24 hours after plating the media containing virus was changed with media containing 4ug/ml puromycin to select for infection. 48 hours after selection, cells were ~60-90% confluent and were stimulated with 300ng SAG (Enzo Life Sciences; in equal parts water and DMSO) or an equal volume of veh (equal parts water and DMSO). 48 hours after stimulation, RNA was collected from cells using TriZOL Reagent (Ambion #15596) following manufacturer's protocol for RNA Isolation. When RNA was collected to test for target knock-down by shRNA, cells were not stimulated and were collected 3-4 days after selection or until ~100% confluent.

Following TriZOL extraction, genomic DNA was degraded by treating RNA with DNase (New England Biolabs #M0303S) for 15-30min at 37°C, DNAse was inactivated using DNAse Inactivator and the concentration of RNA was determined using a NanoDrop Products Spectrophotometer. 2ug of RNA was reverse-transcribed into cDNA using the High Capacity cDNA Reverse Transcription Kit (Life Technologies, #4368813)

following manufacturer's protocol (100ul final volume). qRT-PCR reactions were run using TaqMan Universal PCR Master Mix (Applied Biosystems #4324018) with TaqMan Gene Expression assay PCR probes (11.25ul Master Mix, 1.25ul probe, 2.5ul cDNA in 25ul total volume). The PCR program: 50°C for 2 minutes, 95°C for 10 minutes, then 40 cycles of 15 seconds at 95°C followed by one minute at 60°C. Applied Biosystems gene expression assays used: *Eya1* Mm00438796_m1, *Smo* Mm01162710_m1, *Gli1* Mm00494645_m1, *Ptch1* Mm00436026_m1, *Gli2* Mm01293117_m1, *c-fos* Mm00487425_m1, *H2AX* Mm00515990_s1, *Dach2* Mm00473899_m1, *Six1* Mm00808212_m1, *Six2* Mm00807058_m1, *Six4* Mm00803396_m1, *Six5* Mm01305439_g1, *Eya3* Mm00438810_m1, *Eya4* Mm00438832_m1, *Math1* Mm01181529_s1, *Gas1* Mm01700206_g1, *Nrp1* Mm00435371_m1, Nrp2 Mm00803099_m1.

qRT-PCR experiments were run using an Eppendorf ep mastercycler realplex machine, which tracks the fluorescent signal of the reporter dye and reports the cycle at which the dye signal crosses an arbitrarily threshold, the C(T) value. At the C(T) value, the PCR is in an exponential phase of amplification and the initial amount of cDNA bound by the reporter dye is determined by calculating $2^{-C(T)}$.

Each sample was run in triplicate and triplicate values were averaged. Each probe was normalized to GAPD as a control for initial total amount of cDNA. Within each experiment, samples were normalized to LacZ levels (our negative control). Normalized values were then averaged across experiments. The standard error of the mean (S.E.M.) was also determined as a measure of variability. Statistical significance was determined by using a z-test relative to one in Microsoft Office Excel.

Western Blot

$1.1x10^5$ SL2 cells were plated with virus in 6-well tissue culture plates in SL2 growth media; 10-30% of the total volume/well consisted of media containing virus. 24 hours after plating the media containing virus was changed with media containing 4ug/ml puromycin to select for infection. 48 hours after selection, cells were stimulated with 300ng SAG or an equal volume of veh. 48-72 hours after stimulation, protein was collected from cells in modified RIPA buffer (50mM NaTris pH 7.4, 150mM NaCl, 1% v/v NP-40, 0.25% NaDeoxycholate, 1mM DTT, 10mM NaF, 1mM activated NaVanadate, 1mM PMSF, protease inhibitor cocktail). Lysate was stored at -80°C or run directly in a western blot. The protein concentration of each sample was determined using Bio-Rad Protein Assay Dye Reagent Concentrate (Bio-Rad #500-0006) and a BSA protein standard. Equal amounts of protein were prepared with 10x NuPAGE sample reducing agent (Invitrogen #NP0004) and 4x NuPAGE Sample Buffer (Invitrogen #NP0007), boiled for 5 minutes, and run at 115 volts in 4-12% or 10% Novex Bis-Tris pre-cast gels (#NP0321BOX, NP0323BOX, NP0301BOX). Protein was transferred to a membrane at 30 volts for 2-3 hours. Membranes were blocked in TBST with 5% nonfat dehydrated milk for 1 hour at room temperature and incubated over-night at 4°C in antibodies in milk. Membranes were washed with TBST 3x 5 minutes at room temperature, incubated in secondary antibody (1:5000) for 1 hour at room temperature in block, washed with TBST 3x 10 minutes at room temperature, and developed on film using an ECL western blotting substrate (GE Healthcare #RPN2106; Thermo Scientific #34075). Antibodies: Eya1 (Aviva Systems Biology #ARP32434), HA (Millipore #05-

904), Actin (Cell Signaling #4968), Gli1 (Cell Signaling #2534), Anti-Phosphotyrosine clone 4G10 (Millipore #05-321), H2AX (Cell Signaling #2595, #5438, #2577), Six1 (Abcam #ab84329, #ab86028), Nrp1 (R&D Systems #AF566), Nrp2 (Cell Signaling #3366), Sufu (Cell Signaling #2520S), Gli2 (Aviva Systems Biology #ARP31885), GFP (Abcam #ab6556), Gli3 (R&D Systems #AF3690).

For western blot quantification, film was scanned using Epson perfection V750 pro scanner and Epson scan software. Background-subtracted band density was measured in ImageJ. Each lane was normalized to actin as a loading control for initial total amounts of protein. Within each experiment, samples were normalized to LacZ levels (our negative control). Normalized values were then averaged across experiments. Statistical significance was determined by using a z-test relative to one in Microsoft Office Excel.

MB21 MTS Assay

MB21 cells were maintained as neurosphere cultures in MB21 growth media. Neurospheres were dissociated using Accutase (Sigma Aldrich #A6964) following manufacturer's protocol. $50x10^3$ cells were plated in 96-well tissue culture plates with 20% virus by volume. Within the same plate, serial dilutions of MB21 cells were plated as a standard curve. The next day, half the media was carefully removed and replaced with media containing 1ug/ml puromycin (0.5ug/ml final concentration). 4 days later (5 days after infection), cells were assayed using CellTiter96 Aqueous One Solution Cell Proliferation Assay (Promega #G3580) following manufacturer's protocol. The standard curve was included to ensure that the color development was in a linear range. Within

each experiment, samples were normalized to LacZ levels (our negative control). Normalized values were then averaged across experiments. Statistical significance was determined by using a z-test relative to one in Microsoft Office Excel.

For qRT-PCR, $1x10^6$ dissociated cells were plated in 6-well tissue culture dishes and virus was added the following day. Two days after viral addition, cells were resuspended in media containing 0.5ug/ml puromycin. Three days after selection (5 days after infection), cells were collected and RNA was isolated following the protocol described above for SL2 cells.

Cilia staining and imagining and analysis

E10.5 embryos were collected in cold PBS and fixed overnight in 4% PFA in Sorenson's buffer at 4°C (0.0532M Na2HPO4, 0.0133M KH2PO4, pH 7.4, DEPC treated). Embryos were equilibrated serially at 4°C in 10%, 20%, and 30% sucrose in Sorenson's buffer overnight or until tissue sank. Embryos were embedded in Tissue Freezing Medium (Triangle Biomedical Sciences, Inc. #TFM-5) and sectioned at a thickness of 10uM using a Leica cryostat and collected on Fisherbrand Superfrost Plus Microscope Slides (Fisher Scientific #12-550-15).

Sections were dried at room temperature for 30-60 minutes and then blocked and permeabilized in a 10% NGS and 0.1% Triton-X100 in PBS for 1hour. Tissue was incubated overnight at 4°C with primary antibody in blocking solution. Rabbit (rb) anti-γ-tubulin (1:250, Sigma Aldrich #T5192) was used to mark the basal body of the cilia and mouse (ms) anti-acetylated-α-tubulin (1:250, Invitrogen #322700) was used to mark the cilia axoneme. After primary antibody incubation, tissue was washed 3 times for 5

minutes in PBST. Secondary antibodies (1:500, anti-ms Alexa-488 and anti-rb Alexa-546, Invitrogen) were applied in block for one hour at room temperature. Secondary antibody was then removed and tissue was washed 3 times for 5 minutes in PBST. DAPI (5ug/ml in PBS) was applied for 1 minute and slides were washed with PBS once for 5 minutes. Tissue was mounted with Immu-Mount (Thermo Scientific #9990412).

Sections were imaged using a Leica confocal microscope and images were acquired with the Leica Microsystems Application Suite (24.1 build 6384). Images were processed and analyzed using ImageJ software and Adobe Photoshop.

Author Contribution:

I independently carried out experiments for Figures 3.1-3.5, 3.10. Dr. Pencheng Zhou conducted experiments for Figure 3.6. I independently conducted the experiments for Figure 3.7 and 3.8 using transposon constructs developed by Dr. Xuesong Zhao. Maria Pazyra Murphy ran one western blot contributing to Figure 3.9; I conducted the rest of the experiments for that figure. I conducted the experiments for Figure 3.11 with cells developed by Dr. Tatyana Ponomaryov in collaboration with Xuesong Zhao.

CHAPTER 4: *IN VIVO* EVIDENCE FOR THE IMPORTANCE OF EYA1 IN HH SIGNALING

Introduction

In the previous chapters we demonstrate Eya1 is a positive regulator of Hh signaling and regulates *Nrp* expression. Our finding that *Eya1* is important for Shh-dependent MB survival suggests functional relevance for Eya1 in a biological system. Based on these data *in vitro*, we next investigated a role of Eya1 in Hh signaling *in vivo.*

We obtained *Eya1*$^{-/-}$ mice (Xu et al. 1999) and focused our attention on the developing cerebellum, a region where Shh is known to be a potent mitogen in stimulating the proliferation of granule cell precursors (GCPs; Dahmane & Ruiz i Altaba 1999; Wallace 1999; Wechsler-Reya & Scott 1999). In addition, we surveyed several other locations where Shh and Eya1 are important for development, including the embryonic spinal cord, otic vesicle, and lung. In these systems, we find *Eya1*$^{-/-}$ mice display reduced Hh signaling *in vivo*, *Eya1*$^{-/-}$ mice present phenotypes resembling Shh loss-of-function, and *Eya1*$^{-/-}$ mice have reduced levels of *Nrp* expression. Furthermore, we find there is a genetic interaction between Eya1 and Hh signaling, demonstrated using compound *Eya1/Ptch1* heterozygous mice (Goodrich et al. 1997). Notably the contribution of Eya1 to Hh signaling varies among the regions analyzed. Together, these data show our *in vitro* results predict a role for Eya1 in Hh signaling *in vivo*.

Results:

Eya1 Contributes to Cerebellar Proliferation

Shh, produced by Purkinje cells of the cerebellum, has long been appreciated as a crucial factor stimulating GCP proliferation in the developing external granule cell layer

(Dahmane & Ruiz i Altaba 1999; Wallace 1999; Wechsler-Reya & Scott 1999). When Hh signaling is constitutively activated in GCPs, these cells can give rise to MB (Lee et al. 2009; Hatton et al. 2008). Given the significance of Eya1 in MB cell proliferation demonstrated in Chapter 3, we examined GCP proliferation in the E18.5 *Eya1*$^{-/-}$ external granule cell layer. There we find a dramatic reduction in proliferation as assessed by Phospho-Histone H3 (PH3) staining (Figure 4.1a-b). This phenotype is strikingly similar to a loss-of-Shh phenotype and consistent with a functional importance for Eya1 in Hh signaling *in vivo* and in tumorigenesis.

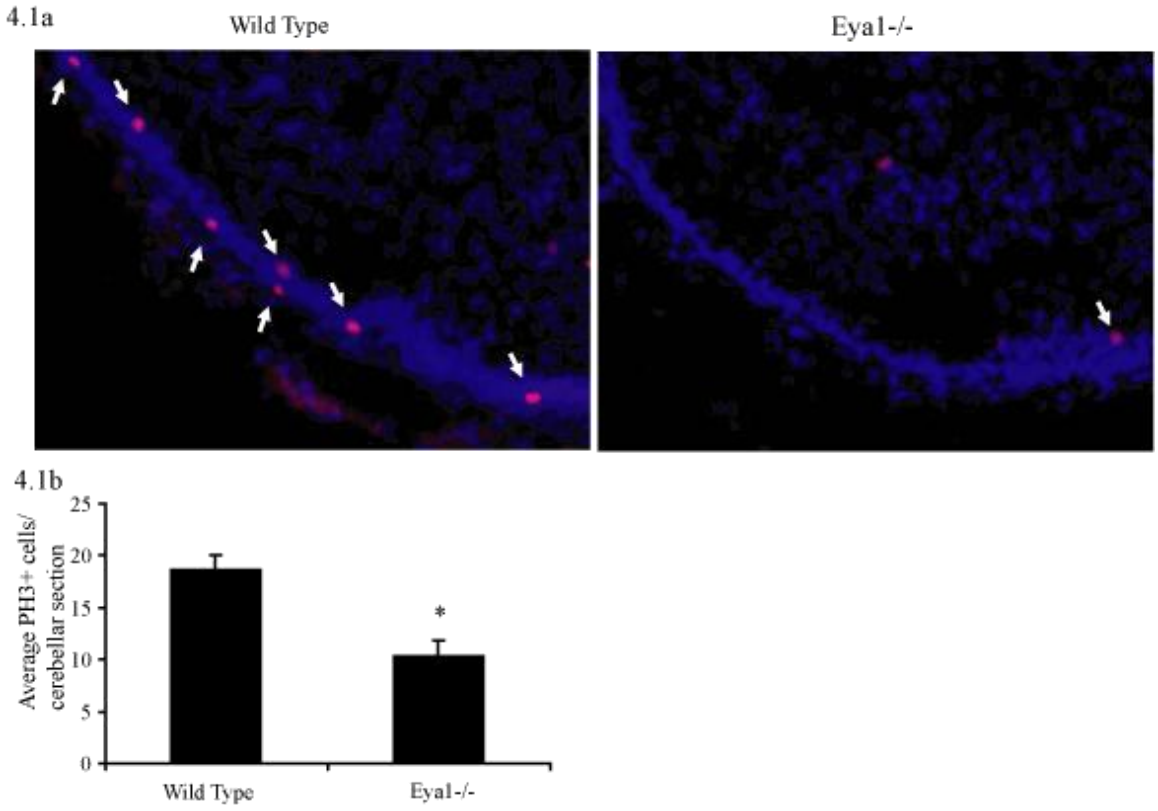

Figure 4.1 Eya1 contributes to E18.5 cerebellar proliferation. A) *Eya1*$^{-/-}$ E18.5 cerebella display reduced proliferation as assayed by PH3 immunohistochemistry. Nuclei are stained with DAPI (blue). White arrows indicate PH3-positive cells (red). **B)** Quantification of average PH3-positive cells per cerebellum (N=24 cerebellar sections from three wild type mice and N=36 cerebellar sections from three litter-matched *Eya1*$^{-/-}$ mice, each pair was taken from a unique litter). Student's t-ttest, *p<0.01; error bars = SEM.

Eya1 and Hh Signaling Interact in Otic Vesicle Development

Cerebellar development has many similarities to the development of the auditory system. For this reason, we next investigated potential *in vivo* phenotypes in the *Eya1*$^{-/-}$ otic vesicle. Additionally, expression data and phenotypic analysis in the literature suggest a possible interaction between Hh and Eya pathways in otic vesicle development. *Eya1* and *Six1* are expressed in Shh responsive cells in the otic vesicle (Ozaki et al. 2004; Zheng et al. 2003) and *Eya1*$^{-/-}$, *Six1*$^{-/-}$, and *Shh*$^{-/-}$ mutants have similar otic vesicle phenotypes at E10.5 (Xu et al. 1999; Zou et al. 2006; Zheng et al. 2003; Ozaki et al. 2004).

By *in situ* hybridization, we find a reduction in Gli1 expression in *Eya1*$^{-/-}$ otic vesicles at E10.5 (Figure 4.2a). These data suggest loss of *Eya1* results in reduced Hh signaling and indicate that Eya1 is required for maximal Hh signaling *in vivo*.

Eya1$^{-/-}$ otic vesicles display increased cell death by TUNEL staining (Xu et al. 1999; Zou et al. 2006) and we find that this phenotype is present in heterozygous *Eya*$^{+/-}$ otic vesicles as well (Figure 4.2b-c). *Shh*$^{-/-}$ otic vesicles also show increased cell death (Bok et al. 2007). To test for a genetic interaction, we genetically amplified the Hh signaling pathway in *Eya*$^{+/-}$ mice by crossing them to animals heterozygous for *Ptch1*. The apoptotic phenotype observed in *Eya1*$^{+/-}$ mice is reversed in *Eya1*$^{+/-}$*/Ptch1*$^{+/-}$ double-heterozygote otic vesicles, further demonstrating a functional relationship and a novel genetic interaction between these two pathways *in vivo* (Figure 4.2b-c).

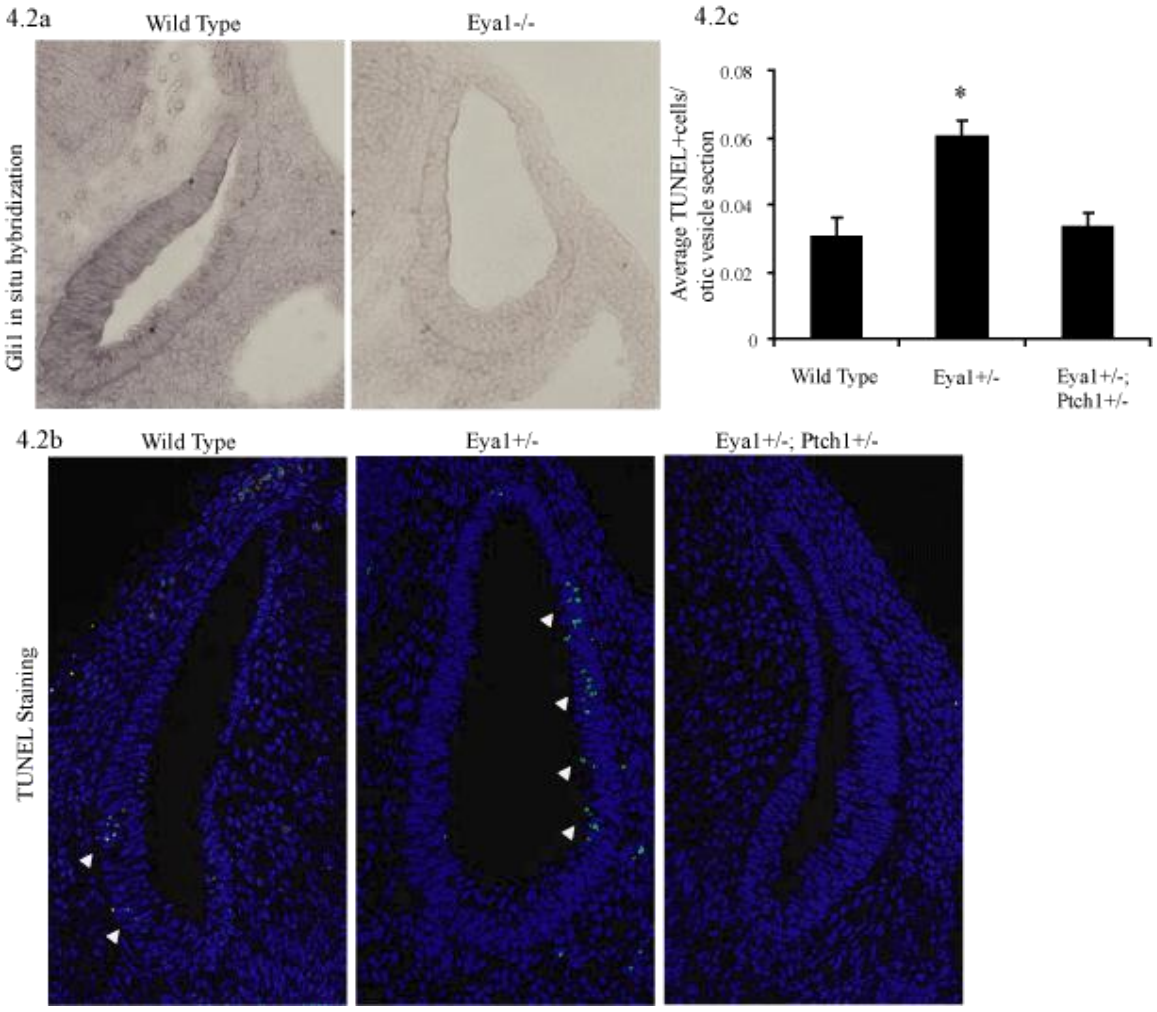

Figure 4.2 Eya1 and Shh signaling interact in the developing otic vesicle. 4.1 *Eya1*$^{-/-}$ otic vesicles at E10.5 have reduced *Gli1* expression by *in situ* hybridization. **4.2** E10.5 *Eya*$^{+/-}$ otic vesicles have increased apoptosis as assessed by TUNEL staining (green), nuclei are stained by DAPI (blue). Genetically increasing levels of Shh signaling by crossing *Eya*$^{+/-}$ mice to *Ptch1*$^{+/-}$ mice (*Eya*$^{+/-}$;*Ptch1*$^{+/-}$) reverses this phenotype. **4.3** Quantification of average TUNEL-positive cells normalized to the number of nuclei per otic vesicle (N=19 otic vesicle sections from two wild type mice and N=19 otic vesicle sections from two litter-matched *Eya1*$^{-/-}$ mice, each pair was taken from a unique litter). Student's t-test, *$p<0.01$; error bars = SEM.

Dorsal-Ventral Neural Tube Patterning Appears Normal in *Eya1*$^{-/-}$ Mice

Shh is a well established morphogen in the developing vertebrate neural tube, acting in a concentration-dependent manner to induce cell fate along the dorsal-ventral axis (Dessaud et al. 2008, Jessell 2000; Ribes & Briscoe 2009). Continuing to survey the *Eya1*$^{-/-}$ embryo for Shh-related phenotypes, we examined the *Eya1*$^{-/-}$ neural tube at E10.5 and found that ventral cell fates are appropriately acquired (Figure 4.3). These data suggest that the role of Eya1 in Hh signaling is specialized to some, but not all, developmental functions of Shh signaling.

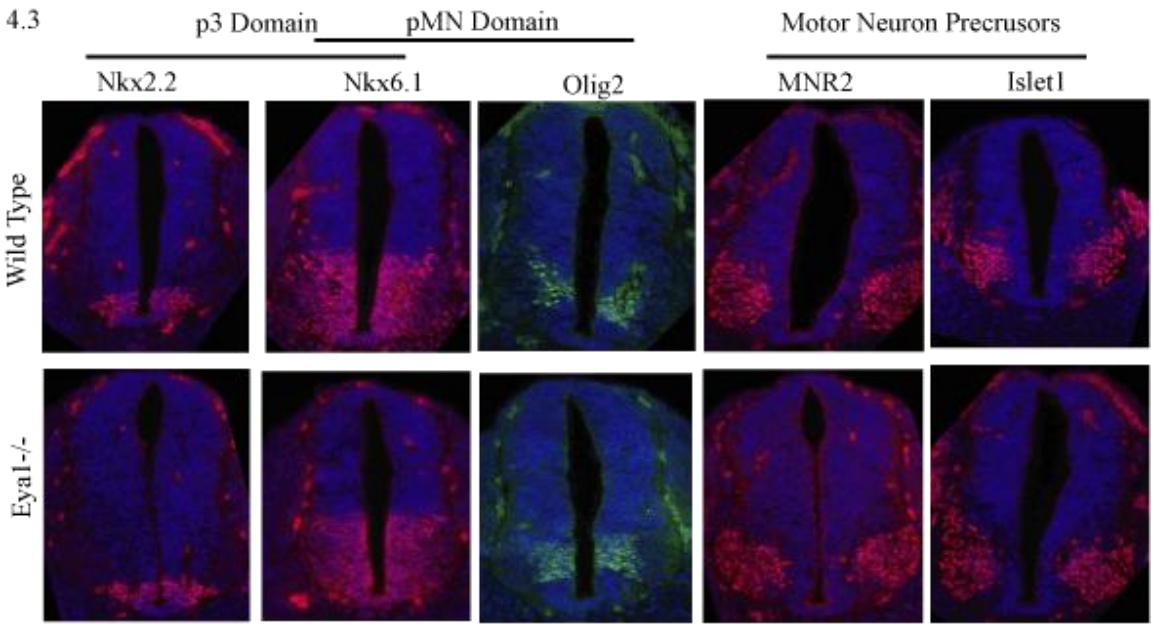

Figure 4.3 Ventral cell types of the neural tube appear properly patterned in *Eya*$^{-/-}$ mice at E10.5. The most ventral spinal cord progenitor domains are termed pMN and p3. The pMN domain gives rise to somatic motor neurons and the p3 domain generates V3 interneurons. Cells in the p3 region are Nkx2.2- and Nkx6.1-positive (both shown in red). Cells in the pMN region are Nkx6.1- and Olig2-positive (Olig2 shown in green). Motor neuron identify is specified in MNR2-psoitive domain and motor neuron precursors are Islet1-positive (both shown in red). These ventral domains appear to be correctly specified in *Eya1*$^{-/-}$ neural tubes.

Eya1 Regulates *Nrp1* Expression *in vivo*

Eya1, *Six1*, *Nrp1*, and *Nrp2* are all expressed in lung tissue during development and have a role in regulating branching (El-Hashash et al. 2011a; El-Hashash et al. 2011b; Ito et al. 2000; Kagoshima et al. 2001). To test the biological relevance of our *in vitro* finding that Eya1 regulates *Nrp1* expression, we looked by western blot at Nrp1 levels in *Eya1*$^{-/-}$ mouse embryos and find reduced Nrp1 protein levels in *Eya1*$^{-/-}$ lung tissue by western blot (Figure 4.4a-b). These data demonstrate that Eya1 regulation of *Nrp* gene expression is generalizable and biologically relevant. Interestingly, we find Gli1 protein is increased *Eya1*$^{-/-}$ lung tissue, indicating Hh signaling is increased (data not shown). While these data do not agree with our findings that Eya1 is a positive regulator of Hh signaling, they are consistent with previous reports that the *Eya1*$^{-/-}$ lung resembles Hh gain-of-function phenotypes; this could be due to a complex network involving Fgf signaling in the lung (El-Hashash et al. 2011b; Bellusci et al. 1997; Chuang et al. 2003).

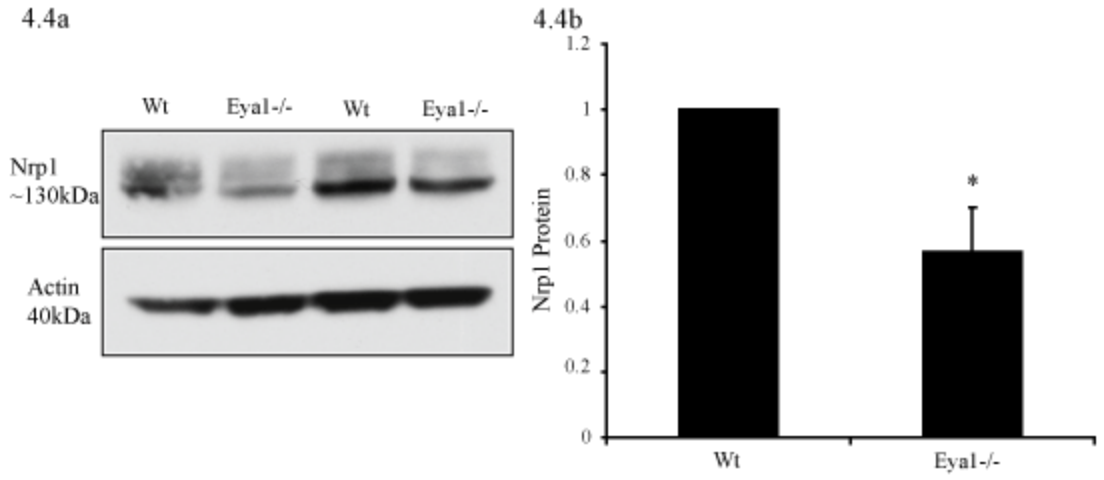

Figure 4.4 Eya1 regulates *Nrp1* expression in lung. **A)** Nrp1 protein levels are reduced in *Eya1*$^{-/-}$ lung tissue at E18.5 by western blot. **B)** Western blot quantification of Nrp1; normalized to actin and wild type tissue (N=2 lung samples from two wild type (wt) mice and N=2 lung samples from litter-matched *Eya1*$^{-/-}$ mice, each pair was taken from a unique litter). Student's t-test; *$p<0.01$; error bars = SEM.

Discussion

Examining regions of the developing mouse where Shh and Eya1 are known to be important factors, we identify significance for Eya1 in Hh signaling and *Nrp* gene regulation *in vivo.*

Reduced proliferation in E18.5 *Eya1*$^{-/-}$ cerebella and reduced *Gli1* expression in E10.5 otic vesicles provide evidence that Eya1 is required for maximal Hh pathway activation *in vivo*. In addition, reduced GCP proliferation is consistent with our previous observation that Eya1 is important for MB survival. The similarity of the *Eya1*$^{-/-}$ cerebellar proliferative phenotype to loss-of Shh signaling phenotypes (Corrales et al. 2004; Spassky et al. 2008) and the discovery that increased Hh signaling reverses an Eya loss-of-function phenotype, support an interaction between these pathways. Finally, our data in the embryonic lung show *Eya1* is necessary for maximal *Nrp* expression *in vivo*.

It will be interesting to know if Eya1 regulates Hh signaling through regulating *Nrp* gene expression in the cerebellum and the otic vesicle. In addition to regulating *Nrp,* Eya1 could be acting to regulate other genes relevant to Hh signaling. One candidate gene to examine would be *Atoh1,* also known as *Math1*. *Atoh1* is necessary for Shh-dependent proliferation in the cerebellum (Ben-Arie et al. 1997; Flora et al. 2009) a well as MB development (Briggs et al. 2008; Flora et al. 2009). *Atoh1* is also known to be regulated by Eya1 and Six1 in controlling hair cell differentiation (Ahmed et al. 2012; Zou et al. 2008).

As mentioned in Chapter 3, areas in development of overlap between *Nrp* expression and Hh signaling include the spinal cord, limb bud, and yolk sac. Future studies looking for Nrp and Hh related phenotypes in the limb bud and yolk sac of *Eya1*$^{-/-}$

embryos would be of interest as potential sites where all three proteins could be working together in development. Eya1 and Six1 are also involved in renalgenesis and myogenesis as evidenced by phenotypes in BOR/BO patients. Future studies examining potential links between Eya1, Nrp, and Shh in these areas of development could also provide information about how these pathways interact as well as therapeutic insight.

Methods

Mice

The mice used in this study have been described previously. *Eya1*$^{-/-}$ mice have a targeted deletion in the Eya1 gene from 305bp upstream of exon 10 to 1,068bp downstream of exon 13 in the conserved ED domain, replaced with pkg-neo (Xu et al. 1999). *Eya1* mice were genotyped by PCR using primers 5'CAG ATT TTC TGT CTG GCT CC (common forward), 5'GTC GTC TGA TGA AAC ATC ATC TAT (wild type reverse), and 5'AAG GGC CAG CTC ATT CCT CCC ACT (neo reverse). These mice were obtained from Dr. Pin-Xian Xu, Mt Sinai School of Medicine. *Ptch*$^{+/-}$ mice were generated by homologous recombination whereby part of *ptc* exon 1 and all of exon 2 were replaced with a *lacZ* and a neomycin resistant gene (Goodrich et al. 1997). *Ptch1* mice were genotyped by PCR using a master mix of the follow primers 5'CTG CGG CAA GTT TTT GGT TG, 5'AGG GCT TCT CGT TGG CTA CAA G, 5'TGG GGT GGG ATT AGA TAA ATG CC, 5'TGT CTG TGT GTG CTC GTG AAT CAC. This strain was obtained from Jackson Laboratory (strain name STOCK*Ptch1*^{tmsMps}/J; stock number 003081). Mice used in this study were maintained on *C57B16/J* or mixed backgrounds. Aging of embryos was determined by designating the morning of the day a vaginal plug was detected as E0.5. Pregnant females were anesthetized with isoflurane before decapitation. Embryos were dissected from pregnant females in cold PBS.

Immunohistochemistry

E18.5 embryos were decapitated for cerebellar staining. Heads were fixed overnight in 4% paraformaldehyde at 4°C. Fixed brains were dissected from the skull

and equilibrated sequentially in 15% and 30% sucrose overnight at 4°C. Cryopreserved brains were embedded and sectioned as described in Chapter 3. For Phospho-Histone H3 detection, sections were dried at room temperature for 30-60 minutes, rehydrated with PBS twice for 5 minutes and then underwent antigen retrieval in Tris-EDTA antigen retrieval solution (0.005M Tris, 0.001M EDTA) then blocked and permeabilized (3% NGS, 5% BSA, 0.3% Triton-X100 in PBS) for 1hour. Tissue was incubated overnight at 4°C with antibody in (3% NGS and 0.3% Triton in PBS). Cells in M-phase of the cell cycle were detected using mouse anti-Phospho-Histone H3 (Ser10; 1:250, Cell Signaling #9706). Primary antibody was washed, secondary antibody was applied, and cells were mounted as described in Chapter 3. Phospho-Histone H3-positive cells were detected by immunofluorescence on a Nikon Eclipse E800 microscope with Nikon camera using NIS Elements imaging software (64 bit 3.22.13 Build 730). Positive cells were manually counted. Sections were collected from three pairs of mutant and wild type animals and each pair was collected from a unique litter. The average number of Phospho-Histone H3-positive cells per cerebellum and the standard error of the mean were calculated in Microsoft excel.

E10.5 tissue for detecting spinal cord markers was prepared and stained as described in Chapter 3 for cilia staining. Tissue was imaged as described for Phospho-Histone H3 staining. Antibodies used: Olig2 (1:10,000 gift from Dr. Chuck Stiles, Dana Farber Cancer Institute). Islet1 (40.2D6-c), MNR2 (81.5C10), and Nkx2.2 (74.5A5) were developed by Dr. Thomas M Jessell and Susan Brenner-Morton and were obtained from the Developmental Studies Hybridoma Bank. Nkx6.1 (F55A10) was developed by Ole D. Madsen and obtained from the Developmental Studies Hybridoma Bank. All

antibodies and hybridomas from the Developmental Studies Hybridoma Banks were used at a concentration of 3ug/ul and were developed under the auspices of NICHD and maintained by the University of Iowa, Department of Biology, Iowa City, IA 42242.

Terminal deoxynucleotidyl transferase-mediated biotinylated UTP nick-end labeling (TUNEL)

The detection of apoptotic cells within the otic vesicle was conducted using DeadEnd™ Fluorometic TUNEL system staining (Progema, G3250). E10.5 tissue was prepared and cryosectioned as described in Chapter 3. TUNEL-positive cells were imaged using a Nikon Eclipse TI inverted microscope. To produce an image of the entire otic vesicle, the scanning feature of NIS elements was used to stitch a series of sequential images. The percent of TUNEL-positive cells was calculated using NIS elements software to manually count TUNEL-positive cells and the number DAPI-stained nuclei. The number of TUNEL-positive cells was normalized to the number of DAPI-stained nuclei in each otic vesicle. Sections were collected from two pairs of mutant and wild type animals and each pair was collected from a unique litter. The average number of TUNEL-positive cells per otic vesicle and the standard error of the mean were calculated in Microsoft excel.

***In Situ* Hybridization**

In situ hybridization probes were linearized from DNA vectors by PCR using a T7 and T3 or SP6 primer and TAQ polymerase. Antisense riboprobes were polymerized and labeled with digoxigenin (DIG) from 5ug of DNA. The resulting RNA probes were

treated with DNAse and purified using the RNeasy Mini Kit from Qigaen (#74014) and diluted in Hybridization buffer (50% formamide, 5x SSC, 0.2mg/ml yeast tRNA, 100ug/ml Heparin, 1x Denhart's Solution, 0.1% Tween, 0.1% Chaps, 5mM EDTA) at a concentration of 1-2ug/ml and stored at -20°C. The *Gli1 in situ* probe was a gift from Dr. Clifford Tabin at Harvard Medical School, who received the probe from Dr. Alexandra Joyner, currently at Memorial Sloan-Kettering Cancer Center.

Slides were dried at 30°C for 2 hours then at 50°C for 15 minutes before fixation with RNAse-free 4% paraformaldehyde for 20 minutes at room temperature. Slides were treated with 10ug/ml proteinase K for 8-11 minutes at room temperature, fixed again in 4% paraformaldehype for 15 minutes, treated with 0.1M RNase-free triethanolamine-HCl with 0.25% acetic anhydride for 10 minutes, and pre-hybridized in hybridization buffer at 65°C for 1-4 hours. Slides were then incubated with *in situ* probe overnight at 65°C. After hybridization, slides were washed with 2x SSC and 0.2x SSC at 65°C and with PBT (2mg/ml BSA, 0.1% Triton X-100, PBS). Slides were blocked (10% heat inactivated lamb serum in PBT) for one hour at room temperature and incubated with anti-DIG antibody conjugated to alkaline phosphatase in block overnight at 4°C (1:2000, Roche #011093274910). Slides were washed three times in PBT for 30 minutes at room temperature, treated with alkaline-phosphatase buffer twice for 5 minutes at room tempterature (100mM Tris pH 9.5, 50mM MgCl2, 100mM NaCl, 0.1% Tween-20), and developed at 37°C using BM Purple AP Substrate (Roche, #14492400) until signal was visible. Slides were then washed in PBS, post-fixed with 4% paraformaldehype for more than 15 minutes at room temperature, and mounted using 70-100% glycerol. Signal was

imaged using a Nikon Eclipse E800 microscope with Nikon camera using NIS Elements imaging software (64bit 3.22.13 Build 730).

Western Blot

Lung tissue was collected from E18.5 embryos and manually homogenized in modified RIPA buffer (50mM NaTris pH 7.4, 150mM NaCl, 1% v/v NP-40, 0.25% NaDeoxycholate, 1mM DTT, 10mM NaF, 1mM activated NaVanadate, 1mM PMSF, protease inhibitor cocktail). Lysate was stored at -80°C or run directly in a western blot as described in Chapter 3. Antibodies: Actin (Cell Signaling #4968), Nrp1 (R&D Systems #AF566).

Author Contribution:

Maria Pazyra Murphy sectioned, stained, and quantified phospho-histone H3 staining in Figure 4.1; I acquired the images shown. I conducted experiments shown in Figure 4.2; Maria Pazyra Murphy quantified TUNEL positive cells. I independently carried out experiments for Figures 4.3-4.4.

CHAPTER 5: DISCUSSION

In this study, we conducted an RNAi screen to identify novel phosphatases in the Hh signaling pathway. Among the many phosphatases identified in the screen, we chose to focus our studies on Eya1, a tyrosine phosphatase and transcriptional co-activator, because it is known to be differentially regulated in a subtype of MB dependent on Hh signaling. We verify that SL2 cells require Eya1 for maximal response to Hh pathway activation using multiple pathway readouts.

As a phosphatase, Eya1 is best characterized for its activity dephosphorylating a tyrosine residue on H2AX, a histone family member known to promote DNA repair in response to double-stranded DNA breakages. Before its phosphatase activity was recognized, however, Eya1 was being studied as a co-transcriptional factor that acts in cooperation with members of the RDGN in multiple developmental contexts. To understand the mechanism by which Eya1 regulates Hh signal transduction, we tested the possibilities that Eya1 acts as a phosphatase and as a transcriptional co-activator to regulate Hh signaling. We examined modulation of tyrosine phosphorylation in SL2 cells following *Eya1* knock-down and/or Hh pathway stimulation. We also applied shRNAs targeting other components of the RDGN to SL2 cells to determine if other members of the network are required for Hh signal transduction. While Eya1-mediated H2AX tyrosine dephosphorylation does not appear to be linked to Hh signaling activity, we found that Six1, an Eya1 co-factor from the RDGN, is specifically required for Hh signaling *in vitro*, suggesting Eya1 and Six1 are acting together to regulate Hh signal transduction. In support of the significance for Six1 in Hh signaling, the *Drosophila*

homolog, *So*, was identified in a genome-wide RNAi screen for new components of the Hh signaling pathway (Nybakken et al. 2005).

For further insight into the mechanism by which Eya1 and Six1 regulate Hh signaling, we conducted several experiments designed to place Eya1 and Six1 within the Hh signaling pathway. Because shRNAs targeting *Eya1* and *Six1* block Hh responsiveness to direct Smo activation, we know these proteins are required downstream of ligand reception and Smo activation. Furthermore, the presence of cilia in the *Eya1*$^{-/-}$ neural tube shows Eya1 is not necessary for cilia formation. The inability of shRNAs targeting *Eya1* or *Six1* to suppress heightened levels of *Gli1* mRNA and protein found in cells with *Sufu* knock-down, indicates that Eya1 and Six1 act upstream of Sufu inhibition. Furthermore, the inability of *Eya1* and *Six1* shRNAs to suppress heightened levels of *Gli1* in cells with *Gli2* overexpression, demonstrates that Eya1 and Six1 are not required for Gli2 transcriptional activity. Interestingly, while *Eya1* and *Six1* shRNA block SAG-induced gene activation, they do not block SAG-induced inhibition of Gli3R formation. These data suggest that Eya1 and Six1 are specifically needed for Smo-dependent regulation of GliA, presumably mediated by Gli2, but are not involved in the regulation of Gli3R formation.

There are very few identified factors that function in the Hh pathway between Smo and Sufu. Recently, Nrp1 and Nrp2, were identified as positive Hh regulators in the pathway downstream of Smo and upstream or at the level of Sufu (Hillman et al. 2011). Interestingly, RNAi targeting *Nrp* also interfered with Gli transcriptional activation without prohibiting Gli3R inhibition (Hillman et al. 2011). Furthermore, a published ChIP-on-chip experiment showed Six1 binds directly to the promoter region for *Nrp1*

(Liu et al. 2010). In light of these data, we hypothesized that Eya1 and Six1 regulate Hh signaling via the transcriptional regulation of *Nrp1* and *Nrp2*. Our data demonstrating a reduction in *Nrp* expression following *Eya1* or *Six1* knock-down in SL2 cells and a decrease in Nrp1 protein in *Eya1*$^{-/-}$ lung *in vivo* both support this model.

Finally, we present evidence identifying a role for Eya1 in Hh signaling *in vivo*. A striking reduction in granule cell proliferation in E18.5 *Eya1*$^{-/-}$ cerebella and reduced *Gli1* expression in E10.5 otic vesicles provide evidence that Eya1 is required for maximal Hh pathway activation *in vivo*. The similarity of the *Eya1*$^{-/-}$ cerebellar proliferative phenotype to loss-of Shh signaling phenotypes (Corrales et al. 2004; Spassky et al. 2008) and the discovery of a genetic interaction between Eya1 and Ptch1 mutations in the otic vesicle are indicative of a role for Eya1 in the Hh pathway.

Where in the Hh Pathway Do Eya1 and Nrp Regulate Signaling?

The mechanistic insights that Eya1 regulates Hh signaling between Smo and Sufu and is needed for transcriptional activity mediated by GliA in response to Hh signaling but not for the inhibitory effects of GliR, allow us to hypothesize more specifically about where within the Hh pathway Eya1 is necessary for signaling.

In the absence of Hh ligand, Sufu forms a complex with Gli proteins at the base of the cilia where Gli proteins also interact with the motor protein Kif7. Full-length Gli is hyperphosphorylated and processed to GliR or is rapidly degraded (reviewed in Ryan & Chiang 2012). Upon Hh binding, three events occur to inhibit GliR formation and promote GliA activity: 1) Sufu, Gli, and Kif7 traffic to the tip of the cilia, 2) these three proteins dissociate and GliA traffics from the cilia, and 3) GliA enters the nucleus where it promotes transcription (reviewed in Ryan & Chiang 2012).

From our studies and those of Hillman et al. (2011), we know that Eya1 and Nrps are not required for the assembly of primary cilia and that Gli2 does not require Nrp to translocate to the tip of the cilia upon Hh pathway stimulation. Once translocated to the cilia, full-length Gli appears to be protected from phosphorylation and GliR formation is therefore inhibited. We also know that GliA does not require Eya1 to enter the nucleus or activate gene transcription as overexpressed Gli2 induces *Gli1* following *Eya1* knock-down. Therefore, we propose that Eya1 is necessary for the disassembly of GliA protein complexes in the primary cilia and/or for the trafficking of GliA from the cilia. A requirement of Eya1 for either of these processes is consistent with a role for Eya1 acting between Smo and Sufu to promote GliA activity in response to Hh signaling without having a role in the regulation GliR formation. This is also consistent with our observations that overexpressed Gli2 is able to induce *Gli1* transcription following *Eya1* knock-down as overexpressed Gli2 does not require cilia to activate gene transcription (Han et al. 2009). Future experiments examining Sufu-Gli complexes and Gli2 trafficking before and after pathway stimulation, with and without *Eya1* knock-down, would be of great interest to test the role of Eya1 in these processes.

A Molecular Mechanism of Eya1 Function in Hh Signaling

Eya1 is known to function both as a phosphatase and as a co-transcriptional factor (reviewed in Tadjuidje & Hegde 2012; Jemc & Rebay 2007). While the gene was included as a target in our screen for its phosphatase activity, we believe Eya1 transcriptional activator activity is involved in regulating Hh signal transduction. We propose Eya1 functions with Six1 to regulate Hh signal transduction through regulation of *Nrp* gene expression (Figure 5.1a).

5.1

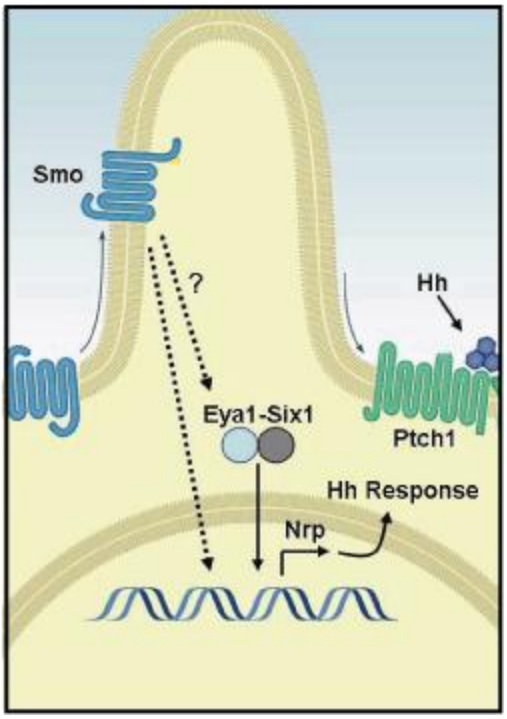

Figure 5.1 Molecular mechanism of Eya1 function in Hh signal transduction. We propose a model wherein an Eya1-Six1 transcriptional activator complex regulates *Nrp* expression. Dashed arrows indicate the possibility that Eya1-Six1 regulate Hh-induced *Nrp* gene induction in addition to regulating basal levels of *Nrp* expression. Nrp promotes a response to Hh pathway activation. Adapted from (Ryan & Chiang 2012).

Eya1 and Six1 are well established transcriptional co-factors in a variety of developmental contexts (reviewed in Tadjuidje & Hegde 2012; Jemc & Rebay 2007). Our findings that knock-down of *Eya1* and *Six1* have similar effects on *Gli1* induction suggests to us that these proteins are working together to regulate Hh-responsiveness in SL2 cells. Simultaneous knock-down of *Eya1* and *Six1* does not enhance the effect blocking *Gli1* induction, consistent with this model. In addition, we observe overexpressed Eya1 and Six1 form a complex in SL2 cells as assessed by nuclear translocation (data not shown). That knock-down of *Eya1* and *Six1* have similar effects on *Nrp* gene induction suggests they are working together to regulate *Nrp* expression. Consistent with our model that Six1 directly regulates *Nrp* expression, Six1 has been shown to directly bind to the *Nrp1* promoter region in mouse cell culture (Liu et al. 2010).

Of course, transcriptional activation activity of Eya1 with Six1 does not rule out the possibility that Eya1 is also acting as a phosphatase in regulating gene expression. Mutations in *Eya1* that disrupt the protein's phosphatase activity also impair the *in vivo* function and transactivation activities of Eya-Six complexes (Rayapureddi et al. 2003; Tootle et al. 2003; Buller et al. 2001; Mutsuddi et al. 2005). The extent to which Eya1 phosphatase activity influences its activity as co-transcription factor, however, remains unclear.

Nrp1 expression is induced by Hh signaling and is required for maximal response to Hh signaling (Hillman et al. 2011). In addition, *Nrp1* overexpression increases maximal Hh target gene activation (Hillman et al. 2011). Thus far, our data are consistent with a model wherein Eya1-Six1 regulate Hh-induced *Nrp* gene induction in

addition to regulating basal levels of Nrp expression. Further studies will be needed to test this model more specifically (Figure 5.1).

A Molecular Mechanism of Nrp Function in Hh Signaling

In some ways, the mechanism we propose above begs the question: How does Nrp regulate Hh signaling? Nrps are transmembrane proteins. The Nrp extracellular domain has been shown to bind ligands and facilitate the transduction of ligand signaling in cooperation with a co-receptor (reviewed in Pellet-Many et al. 2008; Parker et al. 2012). The Nrp intracellular domain contains three critical C-terminal amino acids that constitute a PDZ domain-binding motif, allowing Nrps to bind to PDZ domain proteins such as GIPC (Cai & Reed 1999). In addition to serving as a co-receptor in complexes where its partner transduces signaling, this PDZ domain-binding motif may provide a mechanism for Nrp to directly transduce intracellular signaling. We consider two models by which Nrp may be regulating the Hh signaling pathway. First, Nrp could be serving as a receptor for an extracellular signal which influences Hh signaling (Figure 5.2a). Second, the intracellular PDZ domain of Nrp could serve as a scaffold for cytoplasmic components of the Hh signaling pathway (Figure 5.2b).

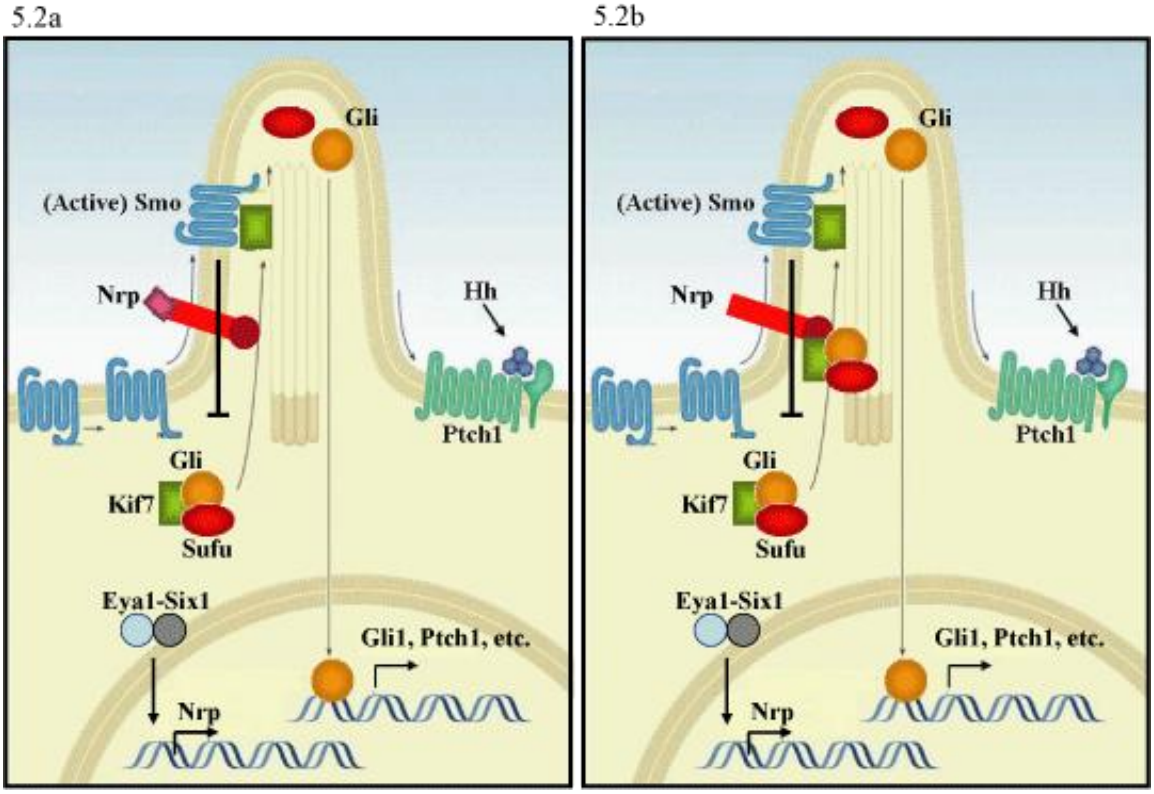

Figure 5.2 Molecular mechanisms of Nrp function in Hh signal transduction. A) Nrps serve as a receptor for an extracellular signal that engages in cross-talk with active Hh signaling to promote Hh-induced gene expression. This signaling function may or may not involve a Nrp co-receptor (not pictured). **B)** The intracellular Nrp PDZ domain serves as a scaffold for cytoplasmic components of Hh signaling, such as Sufu, Kif7, or Gli proteins in a way to promote Hh response gene expression. Adapted from (Ryan & Chiang 2012).

The first model, that Nrp is a cell-surface receptor for an extracellular signal that engages in cross-talk with Hh signaling, was tested by Hillman and colleagues (2011). Nrps are well-characterized receptors for Sema3 ligands to promote growth cone collapse (Chen et al. 1997; Giger et al. 1998; Kolodkin et al. 1997) and for VEGF ligands in vasculogenesis (Kawasaki et al. 1999; Soker et al. 1998; Takashima et al. 2002). Hillman and colleagues applied Sema3A or Sema3F to SL2 cells in combination with recombinant Shh ligand and, across multiple concentrations of Shh, did not observe modulation of Hh signaling with Sema3s (2011). Similarly, they did not observe cross-talk between Shh and VEGF164 and were unable to detect expression of the Nrp co-receptor VEGF-R2 in NIH3T3 fibroblasts (Hillman et al. 2011). Therefore, it is unlikely that a Sema3- or VEGF-mediated signal is responsible for the regulation of Hh signal transduction by Nrps. Nrps are cell surface receptors that interact with multiple ligands (reviewed in Neufeld & Kessler 2008), however, and it is possible that Nrps bind an untested/unidentified ligand or convey information from cell-cell interactions that cross-talk with Hh signaling. PlGF may be a candidate ligand to test as it has been reported to signal through Nrp1 to promote MB cell survival (Snuderl et al. 2013).

A model whereby Nrp functions as a co-receptor for Hh ligands and regulates the pathway by influencing the Hh receptor by Ptch1, is appealing but seems highly unlikely given our data presented in this study. This model is analogous to known functions of Nrp as a co-receptor for Sema3 and VEGF ligands (reviewed in Pellet-Many et al. 2008; Parker et al. 2012). Additionally, there is much precedent in the Hh literature for Hh-binding proteins at the cell surface that regulate pathway activity. Examples include the co-receptors Ihog/Cdo, Boi/Boc, Gas1 (reviewed in Beachy et al. 2012), and Hhip

(Chuang & Mcmahon 1999) and, like Nrp, many of these co-receptors are also transcriptionally regulated by Hh signaling (Hillman et al. 2011; reviewed in Ribes & Briscoe 2009). Our data and the data presented by Hillman and colleagues (2011), however, clearly show the effect of Eya1, Six1, and Nrp to be downstream of Hh signal reception and Smo activation. Therefore, we feel confident we can rule out this model as a plausible mechanism.

A third possibility, and one we favor, is that the intracellular PDZ domain of Nrp serves as a scaffold to localize cytoplasmic components of the Hh signaling pathway. Subcellular localization is an important regulatory mechanism in Hh signaling. Many core components of the pathway including Ptch1, Smo, and Gli proteins are carefully localized and trafficked within the cell corresponding to pathway activation (Corbit et al. 2005; Ding et al. 1999; Humke et al. 2010; Kogerman et al. 1999; Rohatgi et al. 2007). Sufu and Kif7 are pathway components thought to function at least in part by regulating the subcellular localization of Gli proteins. This third model postulates that Nrp could also be an important scaffolding protein via protein interactions with its PDZ domain.

To test these models, Nrp structure-function experiments would be helpful. Chimeric Nrp1 receptors have been used to demonstrate structural features that confer binding to Sema3A or VEGF165 (Gu et al. 2002). Similarly, one could test the abilities of full-length *Nrp*, *Nrp* mutants lacking each of the individual extracellular domains, and a *Nrp* mutant lacking the PDZ-interaction domain to regulate Hh signaling (Valdembri et al. 2009). These data would provide insight into the contributions of the extracellular and intracellular portions of the Nrp protein to Hh signal transduction. If extracellular structural elements of Nrp are required, it would suggest Nrp influences Hh signaling by

conveying ligand-based stimuli. If the extracellular portions of Nrp appear dispensable while the intracellular portion appears important for Hh signaling, this would support a mechanism whereby Nrp regulates Hh signaling as a scaffold for cytoplasmic factors.

Eya1 and Hh in Development

Phenotypic analysis of *Eya1*$^{-/-}$ embryos shows that the contribution of Eya1 to Shh signaling varies among developmental regions analyzed. Among many other functions, Hh signaling is crucial for limb specification, cerebellar proliferation, and neural tube patterning. *Eya1*$^{-/-}$ embryos have normal digit specification (Xu et al. 1999) and we find no defect in neural tube patterning. However there is a striking cerebellar proliferative defect in *Eya1*$^{-/-}$ mice. These *in vivo* data are consistent with our findings *in vitro* that Eya1 specifically regulates GliA in response to Shh without perturbing GliR inhibition. Phenotypes of mice mutant for the *Gli* transcription factors have demonstrated that some functions of Shh are heavily dependent on Shh-induced GliA activity while other functions rely on Hh signaling to inhibit GliR (reviewed in Hui & Angers 2011). The role of Shh in digit patterning relies more heavily on Gli3 as *Gli3* mutants exhibit polydactyly while there is no *Gli2* or *Gli1* mutant limb phenotype (reviewed in Bénazet & Zeller 2009). Conversely, cerebellar proliferation is primarily stimulated through the activities of GliA as *Gli2* mutants exhibit a severe proliferative defect while the EGL of *Gli3* mutants resemble that of wild type animals (Corrales et al. 2004). In the spinal cord, both Gli2 and Gli3 appear to be important for patterning cell fate (reviewed in Hui & Angers 2011). Our finding that *Eya1*$^{-/-}$ cerebella have a proliferation phenotype resembling Shh loss-of-function while limb and neural tube

patterning remain intact suggest Eya1 is necessary for the development of regions with a strong reliance on GliA in response to Hh without perturbing GliR inhibition.

Eya1, Nrp, and Hh in Cancer

Many human cancers have active Hh signaling and aberrant Hh signaling can cause cancer (reviewed in Marini et al. 2011). Several promising small molecule inhibitors of Smo have been developed and are in clinical trial to treat MB and BCC (reviewed in Cohen 2012). The identification of additional druggable targets in the Hh signaling pathway is of great interest. GCPs are thought to be the cell of origin for MB (reviewed in Gilbertson & Ellison 2008). Therefore, the ability of Hh signaling to initiate MB is consistent with its role stimulating the proliferation of GCPs in normal development (reviewed in Manoranjan et al. 2012). Published microarray data that *Eya1* is specifically up-regulated in the Shh-subtype of MB, along with our findings that *Eya1* knock-down reduces viability in a MB cell line, and with our observation that GCP proliferation is greatly reduced in the developing cerebellum of the $Eya1^{-/-}$ mutant embryo, suggest that targeting Eya1 may provide a novel strategy for limiting the growth of MB.

Overexpression of EYA proteins has been reported in many human cancers (reviewed in Tadjuidje & Hegde 2012). EYA1 overexpression has been found in Wilms' tumor (Li et al. 2002) and EBV-negative gastric cancer (Matsusaka et al. 2011). Overexpression of EYA2 is reported in epithelial ovarian cancer (Zhang et al. 2005) and breast cancer (Farabaugh et al. 2012). In these cancers, EYA2 expression correlates with poor prognosis. EYA4 is overexpressed in malignant peripheral nerve sheath tumors (MPNST; Miller et al. 2010), colon and colorectal cancers (Kim et al. 2011; Osborn et al.

2006), as well as esophageal adenocarcinoma (Zou et al. 2005). Inhibition of Eya4 expression in MPNST cells results in necrosis, suggesting Eya4 promotes tumor cell survival (Miller et al. 2010). Furthermore, Pandey et al., (2010) show that over-expression of EYA1, EYA2, or EYA3 in breast cancer cells results in increased proliferation, migration, invasion, and transformation. *In vivo*, silencing EYA3 expression reduces metastasis (Pandey et al. 2010).

The molecular mechanisms by which Eya proteins contribute to these cancers is unknown although Pandey et al., (2010) show that the promotion of migration, invasion, and transformation by overexpressed Eya requires phosphatase activity. In addition, misregulation of EYA expression in cancer is often accompanied by misregulation of SIX and DACH gene expression, suggesting that RDGN proteins may be working together to promote tumorigenesis in the adult (reviewed in Tadjuidje & Hegde 2012).

Unlike most transcription factors, Eya1 has enzymatic activity which makes it an attractive druggable target. Inhibiting the phosphatase activity of Eya proteins may sufficiently disrupt relevant Eya transactivation activities as these functions appear to be linked. Although it has traditionally been difficult to specifically inhibit phosphatases, Eya proteins belong to the HAD family of phosphatases, which have an uncommon catalytic domain. The rare biochemical properties of Eya phosphatase activity may provide an opportunity to identify specific Eya phosphatase inhibitors (Krueger et al. 2013). Recently, specific Eya2 phosphatase inhibitors have been identified (Krueger et al. 2013; Park et al. 2012). In addition, the uricosuric agents Benzbromarone and Benzarone are potent Eya inhibitors, albeit less selective (Tadjuidje et al. 2012b). Eya1 may be a particularly attractive target to pursue in treating Hh-dependent tumors because, unlike

Smo inhibitors, inhibiting Eya1 will not perturb all Hh signaling activities in patients as Eya1 does not appear to be a universally potent regulator of Hh signaling.

Nrps have also been implicated in the development and progression of human cancer. Nrp expression and function correlate to tumor aggressiveness and metastasis in a variety of tumors (reviewed in Parker et al. 2012). Nrp interactions with VEGF ligands and VEGF receptors to promote angiogenesis provide tumor cells with oxygen and nutrients promoting their growth. Blocking Nrp decreases tumor angiogenesis and growth, particularly when combined with anti-VEGF treatments (reviewed in Bagri et al. 2009; Koch 2012). In addition, various Sema3s, through interactions with Nrps and Plexins, can either promote or inhibit tumor growth by regulating tumor angiogenesis, metastasis, and cell survival (reviewed in Neufeld & Kessler 2008).

Interestingly, a recent study by Snuderl et al. (2013) reports Nrp1 is required for the growth and spread of MB. They report that Nrp1 acts as a receptor for PlGF, which is produced by the cerebellar stroma in response to tumor-derived Shh and signals, to promote tumor cell survival. It will be interesting to examine whether Nrp1 is regulated by Eya in this context.

Scientists have conducted unbiased screens to identify novel factors important in biology for decades. The current understanding of the Hh signaling pathway has certainly benefited from the results of such screens. This study contributes to this rich literature by identifying Eya1 as a novel factor regulating Hh pathway transduction. In addition, by focusing on a phosphatase important in Shh-dependent MB, it is our hope that this information will also contribute to the development of novel, effective cancer therapies.

Bibliography

Abdelhak, S., Kalatzis, V., and Heilig, R. (1997). A human homologue of the Drosophila eyes absent gene underlies branchio-oto-renal (BOR) syndrome and identifies a novel gene family. Nature *15*, 157-164.

Aguilar-Hidalgo, D., Domínguez-Cejudo, M.A, Amore, G., Brockmann, A., Lemos, M.C., Córdoba, A., and Casares, F. (2013). A Hh-driven gene network controls specification, pattern and size of the Drosophila simple eyes. Development *140*, 82–92.

Ahmed, M., Wong, E.Y.M., Sun, J., Xu, J., Wang, F., and Xu, P.X. (2012). Eya1-Six1 interaction is sufficient to induce hair cell fate in the cochlea by activating Atoh1 expression in cooperation with Sox2. Developmental Cell *22*, 377–390.

Azuma, N., Hirakiyama, A., Inoue, T., Asaka, A., and Yamada, M. (2000). Mutations of a human homologue of the Drosophila eyes absent gene (EYA1) detected in patients with congenital cataracts and ocular anterior segment anomalies. Human Molecular Genetics *9*, 363–366.

Bagri, A., Tessier-Lavigne, M., and Watts, R.J. (2009). Neuropilins in tumor biology. Clinical Cancer Research *15*, 1860–1864.

Bai, J., and Montell, D.J. (2002). Eyes Absent, a key repressor of polar cell fate during Drosophila oogenesis. Development *129*, 5377–5388.

Barakat, M.T., Humke, E.W., and Scott, M.P. (2010). Learning from Jekyll to control Hyde: Hedgehog signaling in development and cancer. Trends in Molecular Medicine *16*, 337–348.

Bastida, M.F., and Ros, M.A. (2008). How do we get a perfect complement of digits? Current Opinion in Genetics & Development *18*, 374–380.

Beachy, P., and Hymowitz, S. (2010). Interactions between Hedgehog proteins and their binding partners come into view. Genes & Development *24*, 2001–2012.

Bellusci, S., Furuta, Y., Rush, M.G., Henderson, R., Winnier, G., and Hogan, B.L. (1997). Involvement of Sonic hedgehog (Shh) in mouse embryonic lung growth and morphogenesis. Development *124*, 53–63.

Ben-Arie, N., Bellen, H.J., Armstrong, D.L., McCall, a E., Gordadze, P.R., Guo, Q., Matzuk, M.M., and Zoghbi, H.Y. (1997). Math1 is essential for genesis of cerebellar granule neurons. Nature *390*, 169–172.

Bénazet, J.-D., and Zeller, R. (2009). Vertebrate limb development: moving from classical morphogen gradients to an integrated 4-dimensional patterning system. Cold Spring Harbor Perspectives in Biology *1*, a001339.

Bialojan, C., and Takai, A. (1988). Inhibitory effect of a marine-sponge toxin, okadaic acid, on protein phosphatases. Specificity and kinetics. The Biochemical Journal *256*, 283–290.

Birmingham, A., Selfors, L.M., Forster, T., Wrobel, D., Kennedy, C.J., Shanks, E., Santoyo-Lopez, J., Dunican, D.J., Long, A., Kelleher, D., et al. (2009). Statistical methods for analysis of high-throughput RNA interference screens. Nature Methods *6*, 569–575.

Blanco, J., Seimiya, M., Pauli, T., Reichert, H., and Gehring, W.J. (2009). Wingless and Hedgehog signaling pathways regulate orthodenticle and eyes absent during ocelli development in Drosophila. Developmental Biology *329*, 104–115.

Blume-Jensen, P., and Hunter, T. (2001). Oncogenic kinase signalling. Nature *411*, 355–365.

Bok, J., Dolson, D.K., Hill, P., Rüther, U., Epstein, D.J., and Wu, D.K. (2007). Opposing gradients of Gli repressor and activators mediate Shh signaling along the dorsoventral axis of the inner ear. Development *134*, 1713–1722.

Briggs, K.J., Corcoran-Schwartz, I.M., Zhang, W., Harcke, T., Devereux, W.L., Baylin, S.B., Eberhart, C.G., and Watkins, D.N. (2008). Cooperation between the Hic1 and Ptch1 tumor suppressors in medulloblastoma. Genes & Development *22*, 770–785.

Buller, C., Xu, X., and Marquis, V. (2001). Molecular effects of Eya1 domain mutations causing organ defects in BOR syndrome. Human Molecular Genetics *10*, 2775–2781.

Bumcrot, D.A, Takada, R., and McMahon, A.P. (1995). Proteolytic processing yields two secreted forms of sonic hedgehog. Molecular and Cellular Biology *15*, 2294–2303.

Burke, R., Nellen, D., Bellotto, M., Hafen, E., Senti, K.A., Dickson, B.J., and Basler, K. (1999). Dispatched, a novel sterol-sensing domain protein dedicated to the release of cholesterol-modified hedgehog from signaling cells. Cell *99*, 803–815.

Byrd, N., Becker, S., Maye, P., Narasimhaiah, R., St-Jacques, B., Zhang, X., McMahon, J., McMahon, A., and Grabel, L. (2002). Hedgehog is required for murine yolk sac angiogenesis. Development *129*, 361–372.

Cai, H., and Reed, R.R. (1999). Cloning and characterization of neuropilin-1-interacting protein: a PSD-95/Dlg/ZO-1 domain-containing protein that interacts with the cytoplasmic domain of neuropilin-1. The Journal of Neuroscience *19*, 6519–6527.

Campeau, E., and Gobeil, S. (2011). RNA interference in mammals: behind the screen. Briefings in Functional Genomics *10*, 215–226.

Caspary, T., García-García, M.J., Huangfu, D., Eggenschwiler, J.T., Wyler, M.R., Rakeman, A.S., Alcorn, H.L., and Anderson, K.V. (2002). Mouse Dispatched homolog1 is required for long-range, but not juxtacrine, Hh signaling. Current Biology *12*, 1628–1632.

Caspary, T., Larkins, C.E., and Anderson, K.V. (2007). The graded response to Sonic Hedgehog depends on cilia architecture. Developmental Cell *12*, 767–778.

Chamoun, Z., Mann, R.K., Nellen, D., Von Kessler, D.P., Bellotto, M., Beachy, P.A., and Basler, K. (2001). Skinny hedgehog, an acyltransferase required for palmitoylation and activity of the hedgehog signal. Science *293*, 2080–2084.

Charron, F., Stein, E., Jeong, J., McMahon, A.P., and Tessier-Lavigne, M. (2003). The morphogen sonic hedgehog is an axonal chemoattractant that collaborates with netrin-1 in midline axon guidance. Cell *113*, 11–23.

Chen, Y., and Jiang, J. (2013). Decoding the phosphorylation code in Hedgehog signal transduction. Cell Research *23*, 186–200.

Chen, H., Chédotal, A., He, Z., Goodman, C.S., and Tessier-Lavigne, M. (1997). Neuropilin-2, a novel member of the neuropilin family, is a high affinity receptor for the semaphorins Sema E and Sema IV but not Sema III. Neuron *19*, 547–559.

Chen, H., Bagri, A., Zupicich, J., and Zou, Y. (2000). Neuropilin-2 regulates the development of select cranial and sensory nerves and hippocampal mossy fiber projections. Neuron *25*, 43–56.

Chen, J.K., Taipale, J., Young, K.E., Maiti, T., and Beachy, P.A. (2002). Small molecule modulation of Smoothened activity. Proceedings of the National Academy of Sciences of the United States of America *99*, 14071–14076.

Chen, M., Gao, N., Kawakami, T., and Chuang, P. (2005). Mice Deficient in the Fused Homolog Do Not Exhibit Phenotypes Indicative of Perturbed Hedgehog Signaling during Embryonic Development. Molecular and Cellular Biology *25*, 7042–7053.

Chen, M., Wilson, C., and Li, Y. (2009). Cilium-independent regulation of Gli protein function by Sufu in Hedgehog signaling is evolutionarily conserved. Genes & Devleopment *23* 1910–1928.

Chen, M.-H., Li, Y.-J., Kawakami, T., Xu, S.-M., and Chuang, P.-T. (2004a). Palmitoylation is required for the production of a soluble multimeric Hedgehog protein complex and long-range signaling in vertebrates. Genes & Development *18*, 641–659.

Chen, W., Barak, L.S., Chen, J.K., and Beachy, P.A. (2004b). Activity-Dependent Internalization of Smoothened Mediated by b-Arrestin 2 and GRK2. Science *306*, 2257-2260.

Chen, Y., Gallaher, N., Goodman, R.H., and Smolik, S.M. (1998). Protein kinase A directly regulates the activity and proteolysis of cubitus interruptus. Proceedings of the National Academy of Sciences of the United States of America *95*, 2349–2354.

Chen, Y., Sasai, N., Ma, G., Yue, T., Jia, J., Briscoe, J., and Jiang, J. (2011a). Sonic Hedgehog Dependent Phosphorylation by CK1α and GRK2 Is Required for Ciliary Accumulation and Activation of Smoothened. PLoS Biology *9*, e1001083.

Chen, Y., Yue, S., Xie, L., Pu, X., Jin, T., and Cheng, S.Y. (2011b). Dual Phosphorylation of suppressor of fused (Sufu) by PKA and GSK3beta regulates its stability and localization in the primary cilium. The Journal of Biological Chemistry *286*, 13502–13511.

Cheung, H.O.-L., Zhang, X., Ribeiro, A., Mo, R., Makino, S., Puviindran, V., Law, K.K.L., Briscoe, J., and Hui, C.-C. (2009). The kinesin protein Kif7 is a critical regulator of Gli transcription factors in mammalian hedgehog signaling. Science Signaling *2*, ra29.

Chiang, C., Litingtung, Y., Lee, E., Young, K.E., Corden, J.L., Westphal, H., and Beachy, P.A. (1996). Cyclopia and defective axial patterning in mice lacking Sonic hedgehog gene function. Nature *383*, 407-413.

Chiang, C., Litingtung, Y., Harris, M.P., Simandl, B.K., Li, Y., Beachy, P.A., and Fallon, J.F. (2001). Manifestation of the limb prepattern: limb development in the absence of sonic hedgehog function. Developmental Biology *236*, 421–435.

Chuang, P., and Mcmahon, A.P. (1999). Vertebrate Hedgehog signalling modulated by induction of a Hedgehog-binding protein. Nature *397*, 617–621.

Chuang, P.-T., Kawcak, T., and McMahon, A.P. (2003). Feedback control of mammalian Hedgehog signaling by the Hedgehog-binding protein, Hip1, modulates Fgf signaling during branching morphogenesis of the lung. Genes & Development *17*, 342–347.

Cohen, D.J. (2012). Targeting the hedgehog pathway: role in cancer and clinical implications of its inhibition. Hematology/oncology Clinics of North America *26*, 565–88, viii.

Cohen, M.M. (2010). Hedgehog signaling update. American Journal of Medical Genetics. Part A *152A*, 1875–1914.

Cohen, P. (2002). Protein kinases--the major drug targets of the twenty-first century? Nature Reviews Drug Discovery *1*, 309–315.

Cook, P.J., Ju, B.G., Telese, F., Wang, X., Glass, C.K., and Rosenfeld, M.G. (2009). Tyrosine dephosphorylation of H2AX modulates apoptosis and survival decisions. Nature *458*, 591–596.

Cooper, A.F., Yu, K.P., Brueckner, M., Brailey, L.L., Johnson, L., McGrath, J.M., and Bale, A.E. (2005). Cardiac and CNS defects in a mouse with targeted disruption of suppressor of fused. Development *132*, 4407–4417.

Corbit, K.C., Aanstad, P., Singla, V., Norman, A.R., Stainier, D.Y.R., and Reiter, J.F. (2005). Vertebrate Smoothened functions at the primary cilium. Nature *437*, 1018–1021.

Corrales, J.D., Rocco, G.L., Blaess, S., Guo, Q., and Joyner, A.L. (2004). Spatial pattern of sonic hedgehog signaling through Gli genes during cerebellum development. Development *131*, 5581–5590.

Dahmane, N., and Ruiz i Altaba, A. (1999). Sonic hedgehog regulates the growth and patterning of the cerebellum. Development *126*, 3089–3100.

Denef, N., Neubu, D., Perez, L., and Cohen, S.M. (2000). Hedgehog Induces Opposite Changes in Turnover and Subcellular Localization of Patched and Smoothened. Cell *102*, 521–531.

Dessaud, E., McMahon, A.P., and Briscoe, J. (2008). Pattern formation in the vertebrate neural tube: a sonic hedgehog morphogen-regulated transcriptional network. Development *135*, 2489–2503.

Dickey, J.S., Redon, C.E., Nakamura, A.J., Baird, B.J., Sedelnikova, O.A., and Bonner, W.M. (2008). γH2AX and cancer. Nature Reviews Cancer *8*, 957-967.

Ding, Q., Fukami, S.I., Meng, X., Nishizaki, Y., Zhang, X., Sasaki, H., Dlugosz, A., Nakafuku, M., and Hui, C.C. (1999). Mouse suppressor of fused is a negative regulator of sonic hedgehog signaling and alters the subcellular distribution of Gli1. Current Biology *9*, 1119–1122.

Echeverri, C.J., and Perrimon, N. (2006). High-throughput RNAi screening in cultured cells: a user's guide. Nature Reviews Genetics *7*, 373–384.

El-Hashash, A.H., Turcatel, G., Al Alam, D., Buckley, S., Tokumitsu, H., Bellusci, S., and Warburton, D. (2011a). Eya1 controls cell polarity, spindle orientation, cell fate and Notch signaling in distal embryonic lung epithelium. Development *138*, 1395–1407.

El-Hashash, A.H.K., Al Alam, D., Turcatel, G., Bellusci, S., and Warburton, D. (2011b). Eyes absent 1 (Eya1) is a critical coordinator of epithelial, mesenchymal and vascular morphogenesis in the mammalian lung. Developmental Biology *350*, 112–126.

Embry, A., Glick, J., Linder, M., and Casey, P. (2004). Reciprocal signaling between the transcriptional co-factor Eya2 and specific members of the Gαi family. Molecular Pharmacology *66*, 1325–1331.

Endoh-Yamagami, S., Evangelista, M., Wilson, D., Wen, X., Theunissen, J.-W., Phamluong, K., Davis, M., Scales, S.J., Solloway, M.J., De Sauvage, F.J., et al. (2009). The mammalian Cos2 homolog Kif7 plays an essential role in modulating Hh signal transduction during development. Current Biology *19*, 1320–1326.

Epstein, E.H. (2008). Basal cell carcinomas: attack of the hedgehog. Nature Reviews Cancer *8*, 743–754.

Evangelista, M., Lim, T.Y., Lee, J., Parker, L., Ashique, A., Peterson, A.S., Ye, W., Davis, D.P., and De Sauvage, F.J. (2008). Kinome siRNA screen identifies regulators of ciliogenesis and hedgehog signal transduction. Science Signaling *1*, ra7.

Fan, X., Brass, L.F., Poncz, M., Spitz, F., Maire, P., and Manning, D.R. (2000). The alpha subunits of Gz and Gi interact with the eyes absent transcription co-factor Eya2, preventing its interaction with the six class of homeodomain-containing proteins. The Journal of Biological Chemistry *275*, 32129–32134.

Farabaugh, S.M., Micalizzi, D.S., Jedlicka, P., Zhao, R., and Ford, H.L. (2012). Eya2 is required to mediate the pro-metastatic functions of Six1 via the induction of TGF-β signaling, epithelial-mesenchymal transition, and cancer stem cell properties. Oncogene *31*, 552–562.

Farrington, S.M., Belaoussoff, M., and Baron, M.H. (1997). Winged-helix, Hedgehog and Bmp genes are differentially expressed in distinct cell layers of the murine yolk sac. Mechanisms of Development *62*, 197–211.

Flora, A., Klisch, T.J., Schuster, G., and Zoghbi, H.Y. (2009). Deletion of Atoh1 disrupts Sonic Hedgehog signaling in the developing cerebellum and prevents medulloblastoma. Science *326*, 1424–1427.

Giger, R.J., Urquhart, E.R., Gillespie, S.K., Levengood, D.V., Ginty, D.D., and Kolodkin, A.L. (1998). Neuropilin-2 is a receptor for semaphorin IV: insight into the structural basis of receptor function and specificity. Neuron *21*, 1079–1092.

Giger, R.J., Cloutier, J.F., Sahay, A., Prinjha, R.K., Levengood, D.V., Moore, S.E., Pickering, S., Simmons, D., Rastan, S., Walsh, F.S., et al. (2000). Neuropilin-2 is required in vivo for selective axon guidance responses to secreted semaphorins. Neuron *25*, 29–41.

Gilbertson, R.J., and Ellison, D.W. (2008). The origins of medulloblastoma subtypes. Annual Review of Pathology *3*, 341–365.

Gluzman-Poltorak, Z., Cohen, T., Shibuya, M., and Neufeld, G. (2001). Vascular endothelial growth factor receptor-1 and neuropilin-2 form complexes. The Journal of Biological Chemistry *276*, 18688–18694.

Goetz, S.C., and Anderson, K.V. (2010). The primary cilium: a signalling centre during vertebrate development. Nature Reviews. Genetics *11*, 331–344.

Goodrich, L.V. (1997). Altered Neural Cell Fates and Medulloblastoma in Mouse patched Mutants. Science *277*, 1109–1113.

Goodrich, L.V., Johnson, R.L., Milenkovic, L., McMahon, J.A., and Scott, M.P. (1996). Conservation of the hedgehog/patched signaling pathway from flies to mice: induction of a mouse patched gene by Hedgehog. Genes & Development *10*, 301–312.

Grachtchouk, M., Mo, R., Yu, S., Zhang, X., Sasaki, H., Hui, C.C., and Dlugosz, A.A. (2000). Basal cell carcinomas in mice overexpressing Gli2 in skin. Nature Genetics *24*, 216–217.

Gu, C., Limberg, B.J., Whitaker, G.B., Perman, B., Leahy, D.J., Rosenbaum, J.S., Ginty, D.D., and Kolodkin, A.L. (2002). Characterization of neuropilin-1 structural features that confer binding to semaphorin 3A and vascular endothelial growth factor 165. The Journal of Biological Chemistry *277*, 18069–18076.

Gu, C., Yoshida, Y., Livet, J., Reimert, D. V, Mann, F., Merte, J., Henderson, C.E., Jessell, T.M., Kolodkin, A.L., and Ginty, D.D. (2005). Semaphorin 3E and plexin-D1 control vascular pattern independently of neuropilins. Science *307*, 265–268.

Hahn, H., Wicking, C., Zaphiropoulous, P.G., Gailani, M.R., Shanley, S., Chidambaram, A., Vorechovsky, I., Holmberg, E., Unden, a B., Gillies, S., et al. (1996). Mutations of the human homolog of Drosophila patched in the nevoid basal cell carcinoma syndrome. Cell *85*, 841–851.

Han, Y.-G., Kim, H.J., Dlugosz, A. a, Ellison, D.W., Gilbertson, R.J., and Alvarez-Buylla, A. (2009). Dual and opposing roles of primary cilia in medulloblastoma development. Nature Medicine *15*, 1062–1065.

Hatton, B.A., Villavicencio, E.H., Tsuchiya, K.D., Pritchard, J.I., Ditzler, S., Pullar, B., Hansen, S., Knoblaugh, S.E., Lee, D., Eberhart, C.G., et al. (2008). The Smo/Smo model: hedgehog-induced medulloblastoma with 90% incidence and leptomeningeal spread. Cancer Research *68*, 1768–1776.

He, Z., and Tessier-Lavigne, M. (1997). Neuropilin is a receptor for the axonal chemorepellent Semaphorin III. Cell *90*, 739–751.

Hillman, R.T. (2010). Neuropilins Are Positive Regulators of Hedgehog Signal Transduction. Stanford Univeristy.

Hillman, R.T., Feng, B.Y., Ni, J., Woo, W.-M., Milenkovic, L., Hayden Gephart, M.G., Teruel, M.N., Oro, A.E., Chen, J.K., and Scott, M.P. (2011). Neuropilins are positive regulators of Hedgehog signal transduction. Genes & Development *25*, 2333–2346.

Hooper, J., and Scott, M. (2005). Communicating with hedgehogs. Nature Reveiw Molecular Cellular Biology *6*, 18–20.

Hoskins, B.E., Cramer, C.H., Silvius, D., Zou, D., Raymond, R.M., Orten, D.J., Kimberling, W.J., Smith, R.J.H., Weil, D., Petit, C., et al. (2007). Transcription factor SIX5 is mutated in patients with branchio-oto-renal syndrome. American Journal of Human Genetics *80*, 800–804.

Houde, C., Dickinson, R.J., Houtzager, V.M., Cullum, R., Montpetit, R., Metzler, M., Simpson, E.M., Roy, S., Hayden, M.R., Hoodless, P.A., et al. (2006). Hippi is essential for node cilia assembly and Sonic hedgehog signaling. Developmental Biology *300*, 523–533.

Huangfu, D., Liu, A., Rakeman, A.S., and Murcia, N.S. Niswander L., Anderson K.V. (2003). Hedgehog signalling in the mouse requires intraflagellar transport proteins. Nature *426*, 83–87.

Hui, C.-C., and Angers, S. (2011). Gli proteins in development and disease. Annual Review of Cell and Developmental Biology *27*, 513–537.

Hui, C.-C., and Joyner, A. (1993). A mouse model of Greig cephalo–polysyndactyly syndrome: the extra–toesJ mutation contains an intragenic deletion of the Gli3 gene. Nature Genetics *3*, 241-246.

Humke, E.W., Dorn, K.V., Milenkovic, L., Scott, M.P., and Rohatgi, R. (2010). The output of Hedgehog signaling is controlled by the dynamic association between Suppressor of Fused and the Gli proteins. Genes & Development *24*, 670–682.

Ingham, P.W., and Mcmahon, A.P. (2001). Principles Hedgehog signaling in animal development: paradigms and principles. Genes & Development *15*, 3059–3087.

Ingham, P.W., Nakano, Y., and Seger, C. (2011). Mechanisms and functions of Hedgehog signalling across the metazoa. Nature Reviews Genetics *12*, 393–406.

Ito, T., Kagoshima, M., Sasaki, Y., Li, C., Udaka, N., Kitsukawa, T., Fujisawa, H., Taniguchi, M., Yagi, T., Kitamura, H., et al. (2000). Repulsive axon guidance molecule Sema3A inhibits branching morphogenesis of fetal mouse lung. Mechanisms of Development *97*, 35–45.

Jacob, L.S., Wu, X., Dodge, M.E., Fan, C.-W., Kulak, O., Chen, B., Tang, W., Wang, B., Amatruda, J.F., and Lum, L. (2011). Genome-Wide RNAi Screen Reveals Disease-Associated Genes That Are Common to Hedgehog and Wnt Signaling. Science Signaling *4*, ra4–ra4.

Jean, D., Bernier, G., and Gruss, P. (1999). Six6 (Optx2) is a novel murine Six3-related homeobox gene that demarcates the presumptive pituitary/hypothalamic axis and the ventral optic stalk. Mechanisms of Development *84*, 31–40.

Jemc, J., and Rebay, I. (2007). The eyes absent family of phosphotyrosine phosphatases: properties and roles in developmental regulation of transcription. Annual Review of Biochemistry *76*, 513–538.

Jessell, T.M. (2000). Neuronal specification in the spinal cord: inductive signals and transcriptional codes. Nature Reviews Genetics *1*, 20–29.

Jia, H., Liu, Y., Yan, W., and Jia, J. (2009). PP4 and PP2A regulate Hedgehog signaling by controlling Smo and Ci phosphorylation. Development *136*, 307–316.

Jia, J., Amanai, K., Wang, G., Tang, J., Wang, B., and Jiang, J. (2002). Shaggy/GSK3 antagonizes Hedgehog signalling by regulating Cubitus interruptus. Nature *416*, 548–552.

Jia, J., Tong, C., Wang, B., Luo, L., and Jiang, J. (2004). Hedgehog signalling activity of Smoothened requires phosphorylation by protein kinase A and casein kinase I. Nature *432*, 1045–1050.

Jiang, J., and Struhl, G. (1998). Regulation of the Hedgehog and Wingless signalling pathways by the F-box/WD40-repeat protein Slimb. Nature *391*, 493–496.

Jin, Z., Mei, W., Strack, S., Jia, J., and Yang, J. (2011). The antagonistic action of B56-containing protein phosphatase 2As and casein kinase 2 controls the phosphorylation and Gli turnover function of Daz interacting protein 1. The Journal of Biological Chemistry *286*, 36171–36179.

Johansen, F.E., and Prywes, R. (1994). Two pathways for serum regulation of the c-fos serum response element require specific sequence elements and a minimal domain of serum response factor. Molecular and Cellular Biology *14*, 5920–5928.

Johnson, R., Rothman, A., Xie, J., Goodrich, L.V., Bare, J., Bonifas, J., Quinn, A., Myers, R., Cox, D., Epstein, E.H., et al. (1996). Human homolog of patched, a candidate gene for the basal cell nevus syndrome. Science *274*, 1668–1671.

Kagoshima, M., Ito, T., Kitamura, H., and Goshima, Y. (2001). Diverse gene expression and function of semaphorins in developing lung: positive and negative regulatory roles of semaphorins in lung branching morphogenesis. Genes to Cells *6*, 559–571.

Kawakami, T., Kawcak, T., Li, Y.-J., Zhang, W., Hu, Y., and Chuang, P.-T. (2002). Mouse dispatched mutants fail to distribute hedgehog proteins and are defective in hedgehog signaling. Development *129*, 5753–5765.

Kawasaki, T., Kitsukawa, T., Bekku, Y., Matsuda, Y., Sanbo, M., Yagi, T., and Fujisawa, H. (1999). A requirement for neuropilin-1 in embryonic vessel formation. Development *126*, 4895–4902.

Kim, J., Kato, M., and Beachy, P.A. (2009). Gli2 trafficking links Hedgehog-dependent activation of Smoothened in the primary cilium to transcriptional activation in the nucleus. Proceedings of the National Academy of Sciences of the United States of America *106*, 21666–21671.

Kim, J.H., Do, H.J., Wang, W.H., Macháty, Z., Han, Y.M., Day, B.N., and Prather, R.S. (1999). A protein tyrosine phosphatase inhibitor, sodium orthovanadate, causes parthenogenetic activation of pig oocytes via an increase in protein tyrosine kinase activity. Biology of Reproduction *61*, 900–905.

Kim, Y.-H., Lee, H.C., Kim, S.-Y., Yeom, Y. Il, Ryu, K.J., Min, B.-H., Kim, D.-H., Son, H.J., Rhee, P.-L., Kim, J.J., et al. (2011). Epigenomic analysis of aberrantly methylated genes in colorectal cancer identifies genes commonly affected by epigenetic alterations. Annals of Surgical Oncology *18*, 2338–2347.

Kitsukawa, T., Shimono, A., Kawakami, A., Kondoh, H., and Fujisawa, H. (1995). Overexpression of a membrane protein, neuropilin, in chimeric mice causes anomalies in the cardiovascular system, nervous system and limbs. Development *121*, 4309–4318.

Kobayashi, M., Nishikawa, K., Suzuki, T., and Yamamoto, M. (2001). The homeobox protein Six3 interacts with the Groucho corepressor and acts as a transcriptional repressor in eye and forebrain formation. Developmental Biology *232*, 315–326.

Koch, S. (2012). Neuropilin signalling in angiogenesis. Biochemical Society Transactions *40*, 20–25.

Kochhar, A., Fischer, S.M., Kimberling, W.J., and Smith, R.J.H. (2007). Branchio-Oto-Renal Syndrome. *1678*, 1671–1678.

Kogerman, P., Grimm, T., Kogerman, L., Krause, D., Undén, a B., Sandstedt, B., Toftgård, R., and Zaphiropoulos, P.G. (1999). Mammalian suppressor-of-fused modulates nuclear-cytoplasmic shuttling of Gli-1. Nature Cell Biology *1*, 312–319.

Kolodkin, a L., Levengood, D. V, Rowe, E.G., Tai, Y.T., Giger, R.J., and Ginty, D.D. (1997). Neuropilin is a semaphorin III receptor. Cell *90*, 753–762.

Kool, M., Koster, J., Bunt, J., Hasselt, N.E., Lakeman, A., Van Sluis, P., Troost, D., Meeteren, N.S., Caron, H.N., Cloos, J., et al. (2008). Integrated genomics identifies five medulloblastoma subtypes with distinct genetic profiles, pathway signatures and clinicopathological features. PloS One *3*, e3088.

Kovacs, J.J., Whalen, E.J., Liu, R., Xiao, K., Kim, J., Chen, M., Wang, J., Chen, W., and Lefkowitz, R.J. (2008). Beta-arrestin-mediated localization of smoothened to the primary cilium. Science *320*, 1777–1781.

Krauss, S., Foerster, J., Schneider, R., and Schweiger, S. (2008). Protein phosphatase 2A and rapamycin regulate the nuclear localization and activity of the transcription factor GLI3. Cancer Research *68*, 4658–4665.

Krishnan, N., Jeong, D.G., Jung, S.-K., Ryu, S.E., Xiao, A., Allis, C.D., Kim, S.J., and Tonks, N.K. (2009). Dephosphorylation of the C-terminal tyrosyl residue of the DNA damage-related histone H2A.X is mediated by the protein phosphatase eyes absent. The Journal of Biological Chemistry *284*, 16066–16070.

Krueger, A.B., Dehdashti, S.J., Southall, N., Marugan, J.J., Ferrer, M., Li, X., Ford, H.L., Zheng, W., and Zhao, R. (2013). Identification of a selective small-molecule inhibitor series targeting the eyes absent 2 (Eya2) phosphatase activity. Journal of Biomolecular Screening *18*, 85–96.

Lauth, M., Bergström, A., Shimokawa, T., and Toftgård, R. (2007). Inhibition of GLI-mediated transcription and tumor cell growth by small-molecule antagonists. Proceedings of the National Academy of Sciences of the United States of America *104*, 8455–8460.

Lauth, M., Bergström, A., Shimokawa, T., Tostar, U., Jin, Q., Fendrich, V., Guerra, C., Barbacid, M., and Toftgård, R. (2010). DYRK1B-dependent autocrine-to-paracrine shift of Hedgehog signaling by mutant RAS. Nature Structural & Molecular Biology *17*, 718–725.

Leary, S.E.S., and Olson, J.M. (2012). The molecular classification of medulloblastoma: driving the next generation clinical trials. Current Opinion in Pediatrics *24*, 33–39.

Lee, J., Ekker, S.C., Von Kessler, D.P., Porter, J. a, Sun, B.I., and Beachy, P.A. (1994). Autoproteolysis in hedgehog protein biogenesis. Science *266*, 1528–1537.

Lee, Y., Miller, H.L., Jensen, P., Hernan, R., Connelly, M., Wetmore, C., Zindy, F., Roussel, M.F., Curran, T., Gilbertson, R.J., et al. (2003). A Molecular Fingerprint for Medulloblastoma. Cancer Research *63*, 5428–5437.

Li, C.-M., Guo, M., Borczuk, A., Powell, C.A., Wei, M., Thaker, H.M., Friedman, R., Klein, U., and Tycko, B. (2002). Gene expression in Wilms' tumor mimics the earliest committed stage in the metanephric mesenchymal-epithelial transition. The American Journal of Pathology *160*, 2181–2190.

Li, X., Oghi, K. a, Zhang, J., Krones, A., Bush, K.T., Glass, C.K., Nigam, S.K., Aggarwal, A.K., Maas, R., Rose, D.W., et al. (2003). Eya protein phosphatase activity regulates Six1-Dach-Eya transcriptional effects in mammalian organogenesis. Nature *426*, 247–254.

Li, Y., Zhang, H., Litingtung, Y., and Chiang, C. (2006). Cholesterol modification restricts the spread of Shh gradient in the limb bud. Proceedings of the National Academy of Sciences of the United States of America *103*, 6548–6553.

Liem, K.F., He, M., Ocbina, P.J.R., and Anderson, K.V. (2009). Mouse Kif7/Costal2 is a cilia-associated protein that regulates Sonic hedgehog signaling. Proceedings of the National Academy of Sciences of the United States of America *106*, 13377–13382.

Litingtung, Y., Dahn, R.D., Li, Y., and Fallon, J.F. (2002). Shh and Gli3 are dispensable for limb skeleton formation but regulate digit number and identity. Nature *14*, 979–983.

Liu, A., Wang, B., and Niswander, L.A. (2005). Mouse intraflagellar transport proteins regulate both the activator and repressor functions of Gli transcription factors. Development *132*, 3103–3111.

Liu, Y., Chu, A., Chakroun, I., Islam, U., and Blais, A. (2010). Cooperation between myogenic regulatory factors and SIX family transcription factors is important for myoblast differentiation. Nucleic Acids Research *38*, 6857–6871.

Lopez-Rios, J., Tessmar, K., Loosli, F., Wittbrodt, J., and Bovolenta, P. (2003). Six3 and Six6 activity is modulated by members of the groucho family. Development *130*, 185–195.

Lum, L., Yao, S., Mozer, B., Rovescalli, A., Von Kessler, D., Nirenberg, M., and Beachy, P.A. (2003). Identification of Hedgehog pathway components by RNAi in Drosophila cultured cells. Science *299*, 2039–2045.

Manoranjan, B., Venugopal, C., McFarlane, N., Doble, B.W., Dunn, S.E., Scheinemann, K., and Singh, S.K. (2012). Medulloblastoma stem cells: where development and cancer cross pathways. Pediatric Research *71*, 516–522.

Mao, J., Maye, P., Kogerman, P., Tejedor, F.J., Toftgard, R., Xie, W., Wu, G., and Wu, D. (2002). Regulation of Gli1 transcriptional activity in the nucleus by Dyrk1. The Journal of Biological Chemistry *277*, 35156–35161.

Marini, K.D., Payne, B.J., Watkins, D.N., and Martelotto, L.G. (2011). Mechanisms of Hedgehog signalling in cancer. Growth Factors *29*, 221–234.

Matsusaka, K., Kaneda, A., Nagae, G., Ushiku, T., Kikuchi, Y., Hino, R., Uozaki, H., Seto, Y., Takada, K., Aburatani, H., et al. (2011). Classification of Epstein-Barr virus-positive gastric cancers by definition of DNA methylation epigenotypes. Cancer Research *71*, 7187–7197.

May, S.R., Ashique, A.M., Karlen, M., Wang, B., Shen, Y., Zarbalis, K., Reiter, J., Ericson, J., and Peterson, A.S. (2005). Loss of the retrograde motor for IFT disrupts localization of Smo to cilia and prevents the expression of both activator and repressor functions of Gli. Developmental Biology *287*, 378–389.

Maye, P., Becker, S., Kasameyer, E., Byrd, N., and Grabel, L. (2000). Indian hedgehog signaling in extraembryonic endoderm and ectoderm differentiation in ES embryoid bodies. Mechanisms of Development *94*, 117–132.

Merchant, M., Evangelista, M., Luoh, S., Frantz, G.D., Chalasani, S., Carano, R.A.D., Hoy, M. Van, Ramirez, J., Ogasawara, A.K., Mcfarland, L.M., et al. (2005). Loss of the Serine / Threonine Kinase Fused Results in Postnatal Growth Defects and Lethality Due to Progressive Hydrocephalus. Molecular and Cellular Biology *25*, 7054–7068.

Méthot, N., and Basler, K. (2000). Suppressor of fused opposes hedgehog signal transduction by impeding nuclear accumulation of the activator form of Cubitus interruptus. Development *127*, 4001–4010.

Méthot, N., and Basler, K. (2001). An absolute requirement for Cubitus interruptus in Hedgehog signaling. Development *128*, 733–742.

Miller, S.J., Lan, Z.D., Hardiman, a, Wu, J., Kordich, J.J., Patmore, D.M., Hegde, R.S., Cripe, T.P., Cancelas, J. a, Collins, M.H., et al. (2010). Inhibition of Eyes Absent Homolog 4 expression induces malignant peripheral nerve sheath tumor necrosis. Oncogene *29*, 368–379.

Mutsuddi, M., Chaffee, B., Cassidy, J., Silver, S.J., Tootle, T.L., and Rebay, I. (2005). Using Drosophila to decipher how mutations associated with human branchio-oto-renal syndrome and optical defects compromise the protein tyrosine phosphatase and transcriptional functions of eyes absent. Genetics *170*, 687–695.

Neufeld, G., and Kessler, O. (2008). The semaphorins: versatile regulators of tumour progression and tumour angiogenesis. Nature Reviews Cancer *8*, 632–645.

Northcott, P.A., Korshunov, A., Witt, H., Hielscher, T., Eberhart, C.G., Mack, S., Bouffet, E., Clifford, S.C., Hawkins, C.E., French, P., et al. (2011). Medulloblastoma comprises four distinct molecular variants. Journal of Clinical Oncology *29*, 1408–1414.

Northcott, P.A., Jones, D.T.W., Kool, M., Robinson, G.W., Gilbertson, R.J., Cho, Y.-J., Pomeroy, S.L., Korshunov, A., Lichter, P., Taylor, M.D., et al. (2012). Medulloblastomics: the end of the beginning. Nature Reviews Cancer *12*, 818–834.

Nusslein-Volhard, C., and Wieschaus, E. (1980). Mutations affecting segment number and polarity in Drosophila. Nature *287*, 795–801.

Nybakken, K., Vokes, S.A., Lin, T.-Y., McMahon, A.P., and Perrimon, N. (2005). A genome-wide RNA interference screen in Drosophila melanogaster cells for new components of the Hh signaling pathway. Nature Genetics *37*, 1323–1332.

Ocbina, P.J.R., and Anderson, K.V. (2008). Intraflagellar transport, cilia, and mammalian Hedgehog signaling: analysis in mouse embryonic fibroblasts. Developmental Dynamics *237*, 2030–2038.

Ohto, H., Kamada, S., Tago, K., Tominaga, S.I., Ozaki, H., Sato, S., and Kawakami, K. (1999). Cooperation of six and eya in activation of their target genes through nuclear translocation of Eya. Molecular and Cellular Biology *19*, 6815–6824.

Okabe, Y., Sano, T., and Nagata, S. (2009). Regulation of the innate immune response by threonine-phosphatase of Eyes absent. Nature *460*, 520–524.

Osborn, N.K., Zou, H., Molina, J.R., Lesche, R., Lewin, J., Lofton-Day, C., Klatt, K.K., Harrington, J.J., Burgart, L.J., and Ahlquist, D.A. (2006). Aberrant methylation of the eyes absent 4 gene in ulcerative colitis-associated dysplasia. Clinical Gastroenterology and Hepatology *4*, 212–218.

Ozaki, H., Nakamura, K., Funahashi, J., Ikeda, K., Yamada, G., Tokano, H., Okamura, H., Kitamura, K., Muto, S., Kotaki, H., et al. (2004). Six1 controls patterning of the mouse otic vesicle. Development *131*, 551–562.

Pan, Y., and Wang, B. (2007). A novel protein-processing domain in Gli2 and Gli3 differentially blocks complete protein degradation by the proteasome. The Journal of Biological Chemistry *282*, 10846–10852.

Pan, Y., Bai, C., Joyner, A., and Wang, B. (2006). Sonic hedgehog signaling regulates Gli2 transcriptional activity by suppressing its processing and degradation. Molecular and Cellular Biology *26*, 3365–3377.

Pan, Y., Wang, C., and Wang, B. (2009). Phosphorylation of Gli2 by protein kinase A is required for Gli2 processing and degradation and the Sonic Hedgehog-regulated mouse development. Developmental Biology *326*, 177–189.

Pandey, R.N., Rani, R., Yeo, E.-J., Spencer, M., Hu, S., Lang, R. a, and Hegde, R.S. (2010). The Eyes Absent phosphatase-transactivator proteins promote proliferation, transformation, migration, and invasion of tumor cells. Oncogene *29*, 3715–3722.

Pappu, K.S., and Mardon, G. (2004). Genetic control of retinal specification and determination in Drosophila. The International Journal of Developmental Biology *48*, 913–924.

Pappu, K.S., Chen, R., Middlebrooks, B., and Mardon, G. (2003). Mechanism of hedgehog signaling during Drosophila eye development. Development *130*, 3053–3062.

Park, H., Ryu, S., and Kim, S. (2012). Structure-based de novo design of Eya2 phosphatase inhibitors. Journal of Molecular Graphics and Modelling *38*, 382–388.

Parker, M.W., Guo, H.-F., Li, X., Linkugel, A.D., and Vander Kooi, C.W. (2012). Function of members of the neuropilin family as essential pleiotropic cell surface receptors. Biochemistry *51*, 9437–9446.

Parra, L.M., and Zou, Y. (2010). Sonic hedgehog induces response of commissural axons to Semaphorin repulsion during midline crossing. Nature Neuroscience *13*, 29–35.

Pauli, T., Seimiya, M., Blanco, J., and Gehring, W.J. (2005). Identification of functional sine oculis motifs in the autoregulatory element of its own gene, in the eyeless enhancer and in the signalling gene hedgehog. Development *132*, 2771–2782.

Pearse, R. V, Collier, L.S., Scott, M.P., and Tabin, C.J. (1999). Vertebrate homologs of Drosophila suppressor of fused interact with the gli family of transcriptional regulators. Developmental Biology *212*, 323–336.

Pellet-Many, C., Frankel, P., Jia, H., and Zachary, I. (2008). Neuropilins: structure, function and role in disease. The Biochemical Journal *411*, 211–226.

Pepicelli, C. V, Lewis, P.M., and McMahon, A.P. (1998). Sonic hedgehog regulates branching morphogenesis in the mammalian lung. Current Biology *8*, 1083–1086.

Pepinsky, R.B., Zeng, C., Wen, D., Rayhorn, P., Baker, D.P., Williams, K.P., Bixler, S.A., Ambrose, C.M., Garber, E. a, Miatkowski, K., et al. (1998). Identification of a palmitic acid-modified form of human Sonic hedgehog. The Journal of Biological Chemistry *273*, 14037–14045.

Porter, J.A., Young, K.E., and Beachy, P.A. (1996). Cholesterol modification of hedgehog signaling proteins in animal development. Science *274*, 255–259.

Price, M.A, and Kalderon, D. (1999). Proteolysis of cubitus interruptus in Drosophila requires phosphorylation by protein kinase A. Development *126*, 4331–4339.

Price, M.A., and Kalderon, D. (2002). Proteolysis of the Hedgehog signaling effector Cubitus interruptus requires phosphorylation by Glycogen Synthase Kinase 3 and Casein Kinase 1. Cell *108*, 823–835.

Qin, J., Lin, Y., Norman, R.X., Ko, H.W., and Eggenschwiler, J.T. (2011). Intraflagellar transport protein 122 antagonizes Sonic Hedgehog signaling and controls ciliary localization of pathway components. Proceedings of the National Academy of Sciences of the United States of America *108*, 1456–1461.

Rayapureddi, J.P., Kattamuri, C., Steinmetz, B.D., Frankfort, B.J., Ostrin, E.J., Mardon, G., and Hegde, R.S. (2003). Eyes absent represents a class of protein tyrosine phosphatases. Nature *426*, 295–298.

Rebay, I., Silver, S.J., and Tootle, T.L. (2005). New vision from Eyes absent: transcription factors as enzymes. Trends in Genetics *21*, 163–171.

Reifenberger, J., Wolter, M., Knobbe, C.B., Köhler, B., Schönicke, A., Scharwächter, C., Kumar, K., Blaschke, B., Ruzicka, T., and Reifenberger, G. (2005). Somatic mutations in the PTCH, SMOH, SUFUH and TP53 genes in sporadic basal cell carcinomas. The British Journal of Dermatology *152*, 43–51.

Ribes, V., and Briscoe, J. (2009). Establishing and interpreting graded Sonic Hedgehog signaling during vertebrate neural tube patterning: the role of negative feedback. Cold Spring Harbor Perspectives in Biology *1*, a002014.

Robbins, D.J., Fei, D.L., and Riobo, N.A. (2012). The Hedgehog signal transduction network. Science Signaling *5*, re6.

Rohatgi, R., Milenkovic, L., and Scott, M.P. (2007). Patched1 regulates hedgehog signaling at the primary cilium. Science *317*, 372–376.

Ruat, M., Roudaut, H., Ferent, J., and Traiffort, E. (2012). Hedgehog trafficking, cilia and brain functions. Differentiation *83*, S97–104.

Rudin, C.M., Hann, C.L., Laterra, J., Yauch, R.L., Callahan, C.A., Fu, L., Holcomb, T., Stinson, J., Gould, S.E., Coleman, B., et al. (2009). Treatment of medulloblastoma with hedgehog pathway inhibitor GDC-0449. The New England Journal of Medicine *361*, 1173–1178.

Ruf, R.G., Xu, P.-X., Silvius, D., Otto, E.A., Beekmann, F., Muerb, U.T., Kumar, S., Neuhaus, T.J., Kemper, M.J., Raymond, R.M., et al. (2004). SIX1 mutations cause branchio-oto-renal syndrome by disruption of EYA1-SIX1-DNA complexes. Proceedings of the National Academy of Sciences of the United States of America *101*, 8090–8095.

Ryan, K.E., and Chiang, C. (2012). Hedgehog secretion and signal transduction in vertebrates. The Journal of Biological Chemistry *287*, 17905–17913.

Sano, T., and Nagata, S. (2011). Characterization of the threonine-phosphatase of mouse eyes absent 3. FEBS Letters *585*, 2714–2719.

Seo, H.C., Curtiss, J., Mlodzik, M., and Fjose, A. (1999). Six class homeobox genes in drosophila belong to three distinct families and are involved in head development. Mechanisms of Development *83*, 127–139.

Silver, S.J., and Rebay, I. (2005). Signaling circuitries in development: insights from the retinal determination gene network. Development *132*, 3–13.

Silver, S.J., Davies, E.L., Doyon, L., and Rebay, I. (2003). Functional Dissection of Eyes absent Reveals New Modes of Regulation within the Retinal Determination Gene Network Functional Dissection of Eyes absent Reveals New Modes of Regulation within the Retinal Determination Gene Network. Molecular and Cellular Biology *23*, 5989–5999.

Snuderl, M., Batista, A., Kirkpatrick, N.D., Ruiz de Almodovar, C., Riedemann, L., Walsh, E.C., Anolik, R., Huang, Y., Martin, J.D., Kamoun, W., et al. (2013). Targeting Placental Growth Factor/Neuropilin 1 Pathway Inhibits Growth and Spread of Medulloblastoma. Cell *152*, 1065–1076.

Soker, S., Takashima, S., Miao, H.Q., Neufeld, G., and Klagsbrun, M. (1998). Neuropilin-1 is expressed by endothelial and tumor cells as an isoform-specific receptor for vascular endothelial growth factor. Cell *92*, 735–745.

Soker, S., Miao, H., Nomi, M., Takashima, S., and Klagsbrun, M. (2002). VEGF 165 Mediates Formation of Complexes Containing VEGFR-2 and Neuropilin-1 That Enhance VEGF 165 - Receptor Binding. Journal of Cellular Biochemsitry *85*, 357-368.

Spassky, N., Han, Y.-G., Aguilar, A., Strehl, L., Besse, L., Laclef, C., Ros, M.R., Garcia-Verdugo, J.M., and Alvarez-Buylla, A. (2008). Primary cilia are required for cerebellar development and Shh-dependent expansion of progenitor pool. Developmental Biology *317*, 246–259.

Stucki, M. (2009). Histone H2A.X Tyr142 phosphorylation: a novel sWItCH for apoptosis? DNA Repair *8*, 873–876.

Svärd, J., Heby-Henricson, K., Henricson, K.H., Persson-Lek, M., Rozell, B., Lauth, M., Bergström, A., Ericson, J., Toftgård, R., and Teglund, S. (2006). Genetic elimination of Suppressor of fused reveals an essential repressor function in the mammalian Hedgehog signaling pathway. Developmental Cell *10*, 187–197.

Tadjuidje, E., and Hegde, R.S. (2012). The Eyes Absent proteins in development and disease. Cellular and Molecular Life Sciences.

Tadjuidje, E., Wang, T. Sen, Pandey, R.N., Sumanas, S., Lang, R. a, and Hegde, R.S. (2012). The EYA tyrosine phosphatase activity is pro-angiogenic and is inhibited by benzbromarone. PloS One *7*, e34806.

Taipale, J., Chen, J.K., Cooper, M.K., Wang, B., Mann, R.K., Milenkovic, L., Scott, M.P., and Beachy, P.A. (2000). Effects of oncogenic mutations in Smoothened and Patched can be reversed by cyclopamine. Nature *406*, 1005–1009.

Taipale, J., Cooper, M.K., Maiti, T., and Beachy, P.A. (2002). Patched acts catalytically to suppress the activity of Smoothened. Nature *418*, 892–897.

Takahashi, T., Fournier, A., Nakamura, F., Wang, L.H., Murakami, Y., Kalb, R.G., Fujisawa, H., and Strittmatter, S.M. (1999). Plexin-neuropilin-1 complexes form functional semaphorin-3A receptors. Cell *99*, 59–69.

Takashima, S., Kitakaze, M., Asakura, M., Asanuma, H., Sanada, S., Tashiro, F., Niwa, H., Miyazaki Ji, J., Hirota, S., Kitamura, Y., et al. (2002). Targeting of both mouse neuropilin-1 and neuropilin-2 genes severely impairs developmental yolk sac and embryonic angiogenesis. Proceedings of the National Academy of Sciences of the United States of America *99*, 3657–3662.

Tempé, D., Casas, M., Karaz, S., Blanchet-Tournier, M.-F., and Concordet, J.-P. (2006). Multisite protein kinase A and glycogen synthase kinase 3beta phosphorylation leads to Gli3 ubiquitination by SCFbetaTrCP. Molecular and Cellular Biology *26*, 4316–4326.

Thompson, M.C., Fuller, C., Hogg, T.L., Dalton, J., Finkelstein, D., Lau, C.C., Chintagumpala, M., Adesina, A., Ashley, D.M., Kellie, S.J., et al. (2006). Genomics identifies medulloblastoma subgroups that are enriched for specific genetic alterations. Journal of Clinical Oncology *24*, 1924–1931.

Tootle, T.L., Silver, S.J., Davies, E.L., Newman, V., Latek, R.R., Mills, I.A., Selengut, J.D., Parlikar, B.E.W., and Rebay, I. (2003). The transcription factor Eyes absent is a protein tyrosine phosphatase. Nature *426*, 299–302.

Tran, P.V., Haycraft, C.J., Besschetnova, T.Y., Turbe-Doan, A., Stottmann, R.W., Herron, B.J., Chesebro, A.L., Qiu, H., Scherz, P.J., Shah, J.V., et al. (2008). THM1 negatively modulates mouse sonic hedgehog signal transduction and affects retrograde intraflagellar transport in cilia. Nature Genetics *40*, 403–410.

Tukachinsky, H., Lopez, L.V., and Salic, A. (2010). A mechanism for vertebrate Hedgehog signaling: recruitment to cilia and dissociation of SuFu-Gli protein complexes. The Journal of Cell Biology *191*, 415–428.

Valdembri, D., Caswell, P.T., Anderson, K.I., Schwarz, J.P., König, I., Astanina, E., Caccavari, F., Norman, J.C., Humphries, M.J., Bussolino, F., et al. (2009). Neuropilin-1/GIPC1 signaling regulates alpha5beta1 integrin traffic and function in endothelial cells. PLoS Biology *7*, e25.

Varjosalo, M., Li, S.-P., and Taipale, J. (2006). Divergence of hedgehog signal transduction mechanism between Drosophila and mammals. Developmental Cell *10*, 177–186.

Varjosalo, M., Björklund, M., Cheng, F., Syvänen, H., Kivioja, T., Kilpinen, S., Sun, Z., Kallioniemi, O., Stunnenberg, H.G., He, W.-W., et al. (2008). Application of active and kinase-deficient kinome collection for identification of kinases regulating hedgehog signaling. Cell *133*, 537–548.

Wallace, V.A. (1999). Purkinje-cell-derived Sonic hedgehog regulates granule neuron precursor cell proliferation in the developing mouse cerebellum. Current Biology *9*, 445–448.

Wang, B., and Li, Y. (2006). Evidence for the direct involvement of {beta}TrCP in Gli3 protein processing. Proceedings of the National Academy of Sciences of the United States of America *103*, 33–38.

Wang, B., Fallon, J.F., Beachy, P.A., and Hughes, H. (2000). Hedgehog-Regulated Processing of Gli3 Produces an Anterior/Posterior Repressor Gradient in the Developing Vertebrate Limb. Cell *100*, 423–434.

Wang, C., Pan, Y., and Wang, B. (2010). Suppressor of fused and Spop regulate the stability, processing and function of Gli2 and Gli3 full-length activators but not their repressors. Development *137*, 2001–2009.

Wechsler-Reya, R.J., and Scott, M.P. (1999). Control of neuronal precursor proliferation in the cerebellum by Sonic Hedgehog. Neuron *22*, 103–114.

Wen, X., Lai, C.K., Evangelista, M., Hongo, J.-A., De Sauvage, F.J., and Scales, S.J. (2010). Kinetics of hedgehog-dependent full-length Gli3 accumulation in primary cilia and subsequent degradation. Molecular and Cellular Biology *30*, 1910–1922.

Wilson, C.W., and Chuang, P.-T. (2010). Mechanism and evolution of cytosolic Hedgehog signal transduction. Development *137*, 2079–2094.

Xiao, A., Li, H., Shechter, D., Ahn, S.H., Fabrizio, L.A., Erdjument-Bromage, H., Ishibe-Murakami, S., Wang, B., Tempst, P., Hofmann, K., et al. (2009). WSTF regulates the H2A.X DNA damage response via a novel tyrosine kinase activity. Nature *457*, 57–62.

Xiong, W., Dabbouseh, N.M., and Rebay, I. (2009). Interactions with the abelson tyrosine kinase reveal compartmentalization of eyes absent function between nucleus and cytoplasm. Developmental Cell *16*, 271–279.

Xu, P.X., Cheng, J., Epstein, J.A., and Maas, R.L. (1997). Mouse Eya genes are expressed during limb tendon development and encode a transcriptional activation function. Proceedings of the National Academy of Sciences of the United States of America *94*, 11974–11979.

Xu, P.X., Adams, J., Peters, H., Brown, M.C., Heaney, S., and Maas, R. (1999). Eya1-deficient mice lack ears and kidneys and show abnormal apoptosis of organ primordia. Nature Genetics *23*, 113–117.

Xu, P.-X., Zheng, W., Laclef, C., Maire, P., Maas, R.L., Peters, H., and Xu, X. (2002). Eya1 is required for the morphogenesis of mammalian thymus, parathyroid and thyroid. Development *129*, 3033–3044.

Yang, Q., Shen, S.S., Zhou, S., Ni, J., Chen, D., Wang, G., and Li, Y. (2012). STAT3 activation and aberrant ligand-dependent sonic hedgehog signaling in human pulmonary adenocarcinoma. Experimental and Molecular Pathology *93*, 227–236.

Yauch, R.L., Dijkgraaf, G.J.P., Alicke, B., Januario, T., Ahn, C.P., Holcomb, T., Pujara, K., Stinson, J., Callahan, C.A., Tang, T., et al. (2009). Smoothened mutation confers resistance to a Hedgehog pathway inhibitor in medulloblastoma. Science *326*, 572–574.

Yu, J., Carroll, T.J., and McMahon, A.P. (2002). Sonic hedgehog regulates proliferation and differentiation of mesenchymal cells in the mouse metanephric kidney. Development *129*, 5301–5312.

Yuan, L., Moyon, D., Pardanaud, L., Bréant, C., Karkkainen, M.J., Alitalo, K., and Eichmann, A. (2002). Abnormal lymphatic vessel development in neuropilin 2 mutant mice. Development *129*, 4797–4806.

Zeng, X., Goetz, J. a, Suber, L.M., Scott, W.J., Schreiner, C.M., and Robbins, D.J. (2001). A freely diffusible form of Sonic hedgehog mediates long-range signalling. Nature *411*, 716–720.

Zhang, C., Williams, E.H., Guo, Y., Lum, L., and Beachy, P.A. (2004a). Extensive phosphorylation of Smoothened in Hedgehog pathway activation. Proceedings of the National Academy of Sciences of the United States of America *101*, 17900–17907.

Zhang, L., Yang, N., Huang, J., Buckanovich, R.J., Liang, S., Barchetti, A., Vezzani, C., Brien-jenkins, A.O., Wang, J., Ward, M.R., et al. (2005). Transcriptional Coactivator Drosophila Eyes

Absent Homologue 2 Is Up-Regulated in Epithelial Ovarian Cancer and Promotes Tumor Growth Cancer and Promotes Tumor Growth. Cancer Research *65*, 925–932.

Zhang, Y., Knosp, B.M., Maconochie, M., Friedman, R. a, and Smith, R.J.H. (2004b). A comparative study of Eya1 and Eya4 protein function and its implication in branchio-oto-renal syndrome and DFNA10. Journal of the Association for Research in Otolaryngology *5*, 295–304.

Zheng, W., Huang, L., Wei, Z.-B., Silvius, D., Tang, B., and Xu, P.-X. (2003). The role of Six1 in mammalian auditory system development. Development *130*, 3989–4000.

Zhu, A.J., Zheng, L., Suyama, K., and Scott, M.P. (2003). Altered localization of Drosophila Smoothened protein activates Hedgehog signal transduction. Genes & Development *17*, 1240–1252.

Zou, D., Silvius, D., Davenport, J., Grifone, R., Maire, P., and Xu, P.-X. (2006). Patterning of the third pharyngeal pouch into thymus/parathyroid by Six and Eya1. Developmental Biology *293*, 499–512.

Zou, D., Erickson, C., Kim, E.-H., Jin, D., Fritzsch, B., and Xu, P.-X. (2008). Eya1 gene dosage critically affects the development of sensory epithelia in the mammalian inner ear. Human Molecular Genetics *17*, 3340–3356.

Zou, H., Osborn, N.K., Harrington, J.J., Klatt, K.K., Molina, J.R., Burgart, L.J., and Ahlquist, D.A. (2005). Frequent Methylation of Eyes Absent 4 Gene in Barrett's Esophagus and Esophageal Adenocarcinoma. Cancer Epidemiol Biomarkers Prev *14*, 830–834.

Zou, Y., Stoeckli, E., Chen, H., and Tessier-Lavigne, M. (2000). Squeezing axons out of the gray matter: a role for slit and semaphorin proteins from midline and ventral spinal cord. Cell *102*, 363–375.